

Determination of Relative Configuration in Organic Compounds by NMR Spectroscopy and Computational Methods

Giuseppe Bifulco,* Paolo Dambruoso,[§] Luigi Gomez-Paloma,[†] and Raffaele Riccio*

Dipartimento di Scienze Farmaceutiche, University of Salerno, Via Ponte Don Melillo, 84084 Fisciano, Salerno, Italy

Received December 9, 2005

Contents

| | | | |
|--|------|--|------|
| 1. Introduction | 3744 | 4.2. QM-NMR in Structural and Conformational Analysis | 3769 |
| 2. <i>J</i> -Based Configurational Analysis: Scope and Limitations | 3746 | 4.3. Relative Configuration Assignments by Combined MM/QM Approaches | 3770 |
| 2.1. Experimental Measurements of ^{2,3} J _{HC} Couplings | 3749 | 4.4. Conformational and Configurational Analysis via ¹³ C NMR GIAO Chemical Shifts Prediction on MM Geometries | 3770 |
| 2.2. <i>J</i> -Based Configurational Analysis: 1,2- and 1,3-Dihydroxy or -Hydroxymethyl Dimethine Systems | 3750 | 4.5. Stereochemical Analysis of the 3α- and 3β-Hydroxy Metabolites of Tibolone through NMR and Quantum Chemical Investigations | 3772 |
| 2.3. Multiple Conformer Equilibria | 3751 | 4.6. Determination of the Relative Configuration of Flexible Organic Compounds through Boltzmann Weighted GIAO ¹³ C NMR Chemical Shift Calculations | 3773 |
| 2.4. Extension of <i>J</i> -Based Configurational Analysis: Different 1,2 and 1,3 Substitution Patterns | 3753 | 4.7. Quantum Mechanical Calculations of NMR <i>J</i> -Coupling Values: Toward the Automatic Determination of Relative Configuration in Organic Compounds | 3774 |
| 2.4.1. Aminated 1,2- and 1,3-Stereocenters | 3753 | 4.7.1. Quantum Mechanical Calculations of NMR <i>J</i> -Coupling Values: Relative Configuration Assignment of the C23–C33 Reidspongionolide Fragment | 3774 |
| 2.4.2. 1-Amino-2-hydroxy and 1-Amino-3-hydroxy Dimethines | 3754 | 4.7.2. New Combined NMR–Quantum Mechanical Strategy in the Determination of the Relative Configuration of Steroids: Application to Stemmosides C and D | 3775 |
| 2.4.3. 1,2-Dichlorinated and 1-Chloro-2-hydroxy Dimethines | 3755 | 5. Conclusion and Future Perspectives | 3777 |
| 2.4.4. Heterosubstituted Methine-Quaternary Adjacent Stereocenters: 2'-Substituted Taxane Side Chains | 3755 | 6. Addendum | 3777 |
| 2.4.5. Psymberin: All in One! | 3757 | 7. Notes and References | 3777 |
| 2.6. Sapinofuranone A: Toward the Computational Methods | 3758 | | |
| 2.7. Survey of ³ J _{HH} and ^{2,3} J _{HC} Values | 3759 | | |
| 3. Universal NMR Database in Achiral Solvents: Concept and Proof | 3759 | | |
| 3.1. Desertomicin/Oasomicin Class of Natural Products: Databases | 3760 | | |
| 3.2. Applications of the UDB Approach: Caylobolide A, Scyphostatin, and Ritterazine M | 3761 | | |
| 3.3. Extension of the Method: Universal NMR Database in Chiral Solvents | 3763 | | |
| 3.4. Application of the "Extended" UDB Method: Mycolactones and Tetrafrabricin | 3764 | | |
| 3.5. UDB Scope and Limitation: Altromycin B and 2'-Substituted Taxanes | 3764 | | |
| 4. Quantum Mechanical Calculation of NMR Properties in the Configurational Assignment of Organic Molecules | 3767 | | |
| 4.1. Quantum Chemical Calculation of NMR Parameters | 3768 | | |

1. Introduction

Stereochemical features have a profound impact on a variety of molecular properties, such as chemical reactivity and catalytic, biological, and pharmacological activities. In light of the above considerations, full stereochemical knowledge of a given system is of fundamental importance in many different fields, spanning from chemical physics to biochemistry. For this reason, the assignment of the configurational pattern in chiral organic compounds containing more than one stereocenter is undoubtedly a key step of the structure elucidation process. Due to the challenge typically posed by such configurational assignments, the search for new and more effective methods for the stereochemical analysis of complex molecular systems has stimulated great attention within the chemical community, having relevant implications to several distinct research areas, such as natural product chemistry, asymmetric synthesis, medicinal chemistry, chemical biology, and material sciences. Approaches relying on NMR spectroscopy of intact molecules are extremely ap-

* Authors to whom correspondence should be addressed [(G.B.) telephone +39089969741, fax +39089969602; e-mail bifulco@unisa.it; (R.R.) telephone +39089969768, fax +39089969602; e-mail riccio@unisa.it].

[§] Present address: GlaxoSmithKline, Psy CEDD, Medicinal Chemistry Support Department, via Fleming 4, 37135 Verona, Italy.

[†] Deceased, April 5, 2006.



Luigi Gomez-Paloma was born in Naples in 1966 and died on April 5, 2006. He received his Ph.D. degree from the University of Naples in 1994, under the supervision of Prof. L. Minale. He was assistant professor of organic chemistry of the Faculty of Pharmacy of the University of Naples and in 1998 moved to the University of Salerno to become an associate professor at the Department of Pharmaceutical Sciences. He was a research associate in the group of Prof. Nicolau, at the Scripps Research Institute in 1994, and was again invited in 1995, 1996, 1998, and 2002 for short research stays. He was also visiting professor at the Center of Structural Biology of Vanderbilt University, Nashville, TN, under the invitation of Prof. W. J. Chazin in 2001 and visiting professor of the University of San Carlos de Guatemala in 2002. He became a full professor of organic chemistry in 2004. His research activity was focused on the chemistry of marine natural products, the determination of the relative configuration of organic molecules by means of NMR spectroscopy, the solid-phase synthesis of peptidic and polyketido-peptidic compounds, and molecular recognition studies regarding bioactive drugs by means of MS and NMR spectroscopy.



Paolo Dambruoso was born in Putignano (Italy) in 1973. He received the industrial chemistry degree at the University of Bologna in 1999, under the tutorship of Prof. Alfredo Ricci. He worked for two years at CNR Bologna in the group of Dr. A. Battaglia, collaborating with the Indena S.p.A. on the industrial synthesis of taxol and taxane derivatives. Then he moved to the University of Piemonte Orientale in Novara, where he received a Ph.D. degree in science of bioactive compounds in 2005 under the supervision of Prof. G. Appendino. During his Ph.D. training he joined the research group of Prof. Gomez-Paloma in Salerno, focusing his research on the determination of the relative configuration of organic molecules by means of NMR spectroscopy. Later, he was a post-doctoral fellow in the group of Prof. A. Dondoni at the University of Ferrara under the tutorship of Dr. A. Massi. Then he moved to the University of Manchester as a research associate in the group of Dr. D. J. Dixon, where he developed new organocatalytic methodologies. As of January 2007 he is a senior scientist at the Medicinal Chemistry Department of the Psychiatry Centre of Excellence for Drug Discovery, GlaxoSmithKline, Verona, Italy.



Giuseppe Bifulco was born in Naples (Italy) in 1968. He received his Ph.D. degree from the University of Naples in 1996. He was a visiting scientist at the Scripps Research Institute (San Diego, CA) under the supervision of Prof. W. J. Chazin working on calcium-binding proteins (1994–1995, 1996, and 1998) and with Prof. K. C. Nicolau working on the interactions between synthetic dimers of calicheamicin and DNA (1995, 1996, 1998). From 1997 to 1999 he has been a post-doctoral fellow at the University of Salerno in the group of Prof. Riccio; from 1999 to 2005 he was an assistant professor at the University of Salerno. Currently, he is an associate professor at the Department of Pharmaceutical Science of the University of Salerno. He is involved in several research fields: structural characterization of biological active natural organic compounds from marine and terrestrial sources, advanced NMR techniques in organic chemistry; quantum chemical calculations for the determination of the conformation and the configuration of bioactive compounds, and structural studies on drug–DNA interactions. He was awarded, in 2004, with the Italian Chemical Society “G. Ciamician” Medal, a national prize for researchers.

peeling in this context, allowing the sample under investigation to be preserved.



Raffaele Riccio was born in Naples, Italy, in 1948. He obtained his degree (Laurea) in chemistry in 1972 from the University of Naples and in 1973 was appointed as Ricercatore of the Consiglio Nazionale delle Ricerche at the Istituto per la Chimica di Molecole di Interesse Biologico, where he began his research activity in the field of marine natural products. From 1976 to 1977 he spent a year in a postdoctoral position with Paul J. Scheuer at the University of Hawaii. In 1987 he moved to the Faculty of Pharmacy of the University of Naples “Federico II” as associate professor of organic chemistry. In 1995 he moved to the Faculty of Pharmacy of the University of Salerno as a full professor. He was head of the Department of Pharmaceutical Sciences from 1998 to 2000 and dean of the faculty from 2000 to 2004. He has spent research periods with Koji Nakanishi at Columbia University in 1981 and with W. Fenical at the Scripps Institute of Oceanography in 1990. His research activity in the chemistry of natural products and in the field of bioactive organic compounds with antiinflammatory, antiviral, antitumor, and immunomodulant activity is witnessed by more than 180 publications.

The stereochemical analysis of compounds with well-defined conformational properties is presently fairly easy to accomplish, given the wealth of high-resolution NMR

experiments useful in these kinds of studies. Typically, cyclic compounds with three- to six-membered rings display a predictable conformational behavior, thus allowing the knowledge of their configuration to be extracted from simple NMR parameters, such as proton–proton J -coupling values and/or nuclear Overhauser effect intensities. A much more challenging task is the assignment of relative (and hence absolute) configuration in the case of conformationally flexible systems, such as polysubstituted open chains and macrocyclic compounds. Traditionally, this kind of difficulty has been expressed in a sort of NMR stereochemical paradigm: knowledge of the conformational properties of a molecule facilitates the determination of its configuration and, conversely, from the configuration of a given system one may derive its conformation (this is typically the case in the NMR studies of biopolymers). Such a paradigm has to do with the degree of geometrical uncertainty that one must simultaneously deal with by NMR spectroscopy. In fact, one should realize that the assignment of the configuration requires the analysis of two distinct levels of uncertainty, interconnected to each other, one of which is, of course, the configuration itself, whereas the other has to do with the conformational properties of the system under investigation.

The present review is focused on the state-of-art NMR methods currently in use for relative configurational assignment in organic compounds, notably of complex natural products. The critical examination of this material should convey the relevant impact in the resolution of stereochemical problems that are provided by approaches such as the J -based analysis, the Universal NMR Database, and the quantum mechanical calculation of NMR parameters. This review is organized in sections discussing the underlying principles of each approach and a variety of practical cases of increasing complexity. Because we are mainly concerned with recent methods, the literature starting from 1999 to date was carefully and systematically covered, whereas some preliminary results published earlier in the 1990s have also been occasionally cited. On the other hand, all of the NMR methods relying on derivatization with chiral reagents for the assignment of *absolute* configuration are not included in this review; however, the reader interested in this specific subject may consult the recent authoritative review by Riguera and co-workers.¹

2. J -Based Configurational Analysis: Scope and Limitations

The well-known phenomenon of scalar coupling supplies important NMR parameters, the coupling constant (J) values, which have proven to be extremely useful for conformational and stereochemical studies of organic molecules, providing relevant geometric information. In particular, the coupling constants between protons separated by three bonds (${}^3J_{\text{HH}}$) are directly related to their dihedral angles through the Karplus equation.² Additional empirical equations have been formulated that, taking into account the substitution pattern, allow an accurate prediction of J values from dihedral angles and vice versa.³ Likewise, heteronuclear (${}^1\text{H}$ – ${}^{13}\text{C}$) vicinal coupling constants (${}^3J_{\text{HC}}$) follow a Karplus-like relationship and therefore can be used to derive additional angular constraints. The ${}^2J_{\text{HC}}$ values, which involve nuclei not describing a dihedral angle, can still be useful when the α -carbon bears an electronegative substituent, that is, if it is directly attached to oxygen, nitrogen, or halogen atoms. In these cases, the relative magnitude of the two-bond coupling

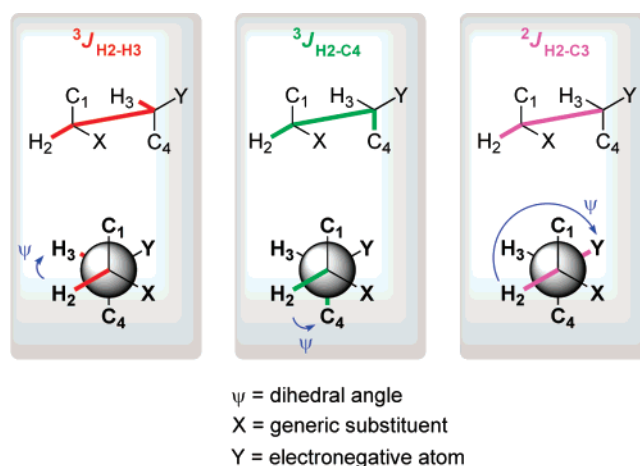


Figure 1. Three- and two-bond homo- and heteronuclear coupling constants.

constant can be related to the dihedral angle between the proton and the electronegative atom bound to the coupled carbon (Figure 1).⁴

The J values depend on the specific substitution pattern of the molecular segment of interest, ranging from 0 to 16 Hz in the case of ${}^3J_{\text{HH}}$, from 0 to 9 Hz for ${}^3J_{\text{HC}}$, and from -6 to 8 Hz for the ${}^2J_{\text{HC}}$ (this subject will be extensively discussed in the following sections). These ranges can be dissected in small, medium, or large categories (Figure 2).

Hence, considering the Newman projection of a given segment, the magnitude of each J can be a priori estimated for all its possible rotamers on the basis of the dihedral angle between the interested nuclei.

The J -based configurational analysis allows the relative configurational assignment of two adjacent (1,2) or alternate (1,3) stereocenters belonging to an acyclic carbon chain. The final configurational assignment stems from an *in depth* conformational analysis of the two- or three-carbon molecular segment of interest accomplished through the comparison of the a priori estimated J values for all their rotamers with the measured couplings on the compound to be assigned. In cases when the molecule contains more than two stereogenic centers, the analysis is conducted considering one molecular fragment at a time. The logic of the method was formalized in an organic and more comprehensive fashion in 1999 by the Murata group,⁵ although preliminary and exploratory applications by the Murata and Yasumoto teams date back to 1995, when they took advantage of this approach to elucidate the diastereomeric relationships of the C27–C29 segment of okadaic acid,⁶ various portions of maitotoxin,^{7–9} the C2–C4 fragment of dysiherbaine,¹⁰ and the acyclic moieties of amphidinol 3.¹¹ A decade after its disclosure to the scientific community, the J -based configurational analysis represents a robust and general method widely used for the relative configuration assignment of polysubstituted acyclic carbon chains, as testified by the large number of papers and reviews^{12–20} reported on this topic.

Capitalizing on the above-mentioned angular dependence of a given spin–spin coupling²¹ (cfr. the Karplus relationship for ${}^3J_{\text{HH}}$ coupling constants^{2,22,23}), the J -based configurational analysis formally considers only staggered rotamers of the two possible relative configurations (*threo* and *erythro*) of the stereopair (Figure 3). Hence, a total of six staggered Newman projections are taken into account, three for each diastereomeric arrangement. In essence, the method relies on unique patterns of spin–spin couplings yielded by each

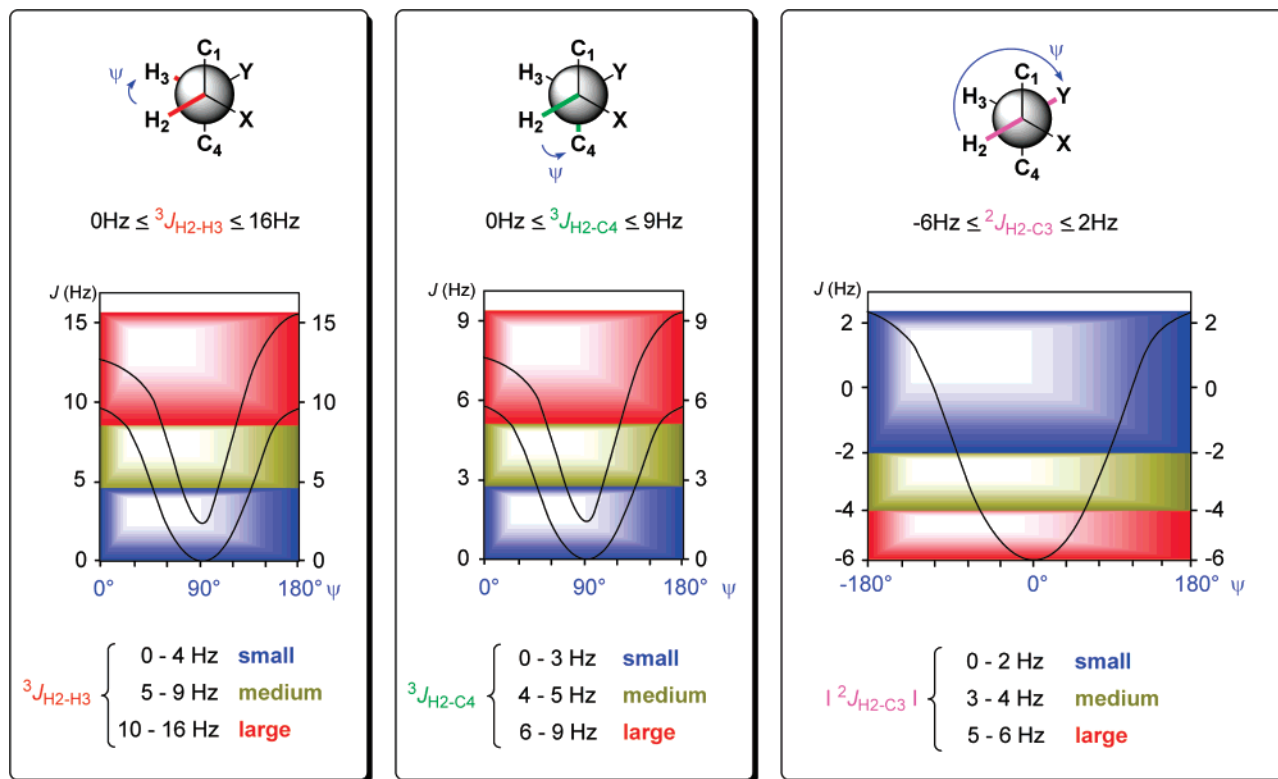


Figure 2. A priori magnitude estimation of J values as a function of dihedral angle ψ (degrees) between interested nuclei. Depending on the nature of X and Y, in the two left panels the two curves report the maximum and minimum expected J values as a function of ψ . In the right panel, the $^2J_{H_2-C_3}$ curve describes the J angular dependence in a 1,2-dioxygenated system.

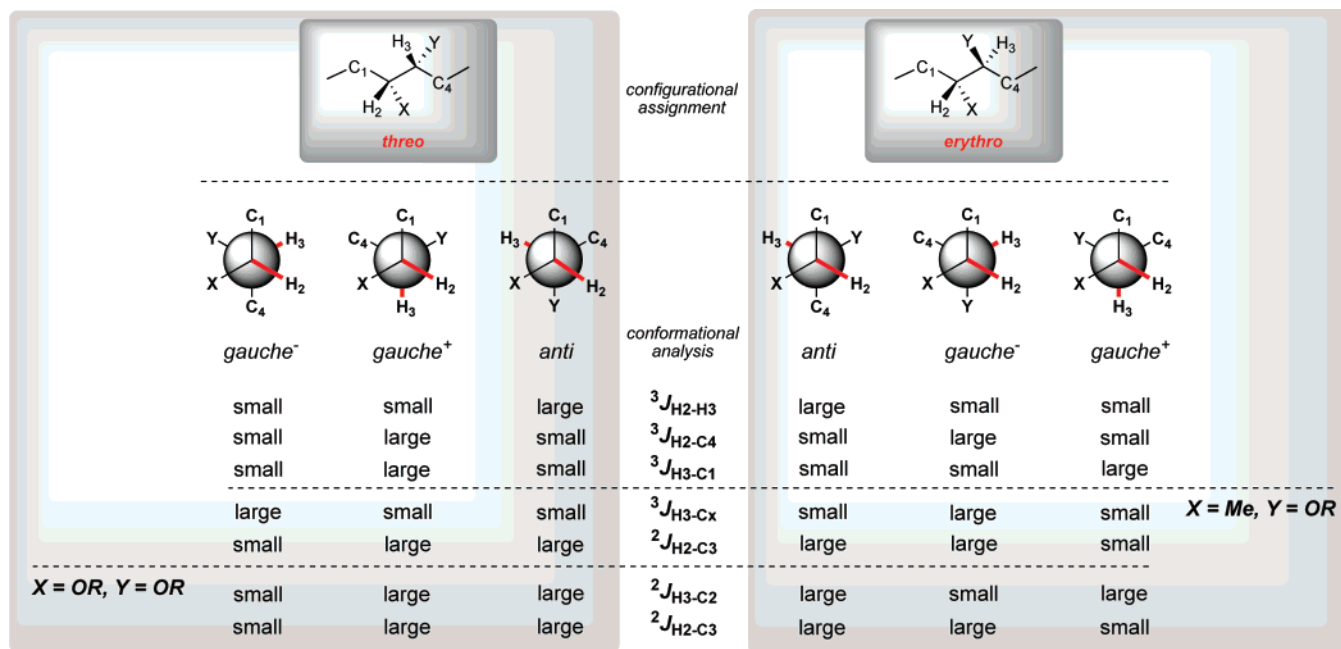


Figure 3. J -based analysis: coupling constants' pattern versus conformational and configurational arrangement in a 1,2-dimethine system.

rotamer, when a complete set of homo- (H,H) and heteronuclear (H,C) $^2,^3J$ values is evaluated. At a semiquantitative level of the estimation of J values, anti rotamers with opposite relative configuration are still indistinguishable, and additional spatial information, typically dipolar effects, are required to discriminate one from the other. In this way, an unequivocal relationship exists between each of the six staggered rotamers and the complete set of all possible $^3J_{HH}$, $^2,^3J_{HC}$, and key ROE/NOE data. Following this principle,

a compound with unassigned relative configuration, the experimental evaluation of the above NMR parameters may allow one to unambiguously identify only one of the six staggered rotamers (conformational analysis) and, consequently, its diastereoisomeric series (configurational assignment).

The analysis can be also extended to methylene-spaced stereopairs⁵ (Figure 4) provided that a stereospecific assignment of the methylene diastereotopic protons may be

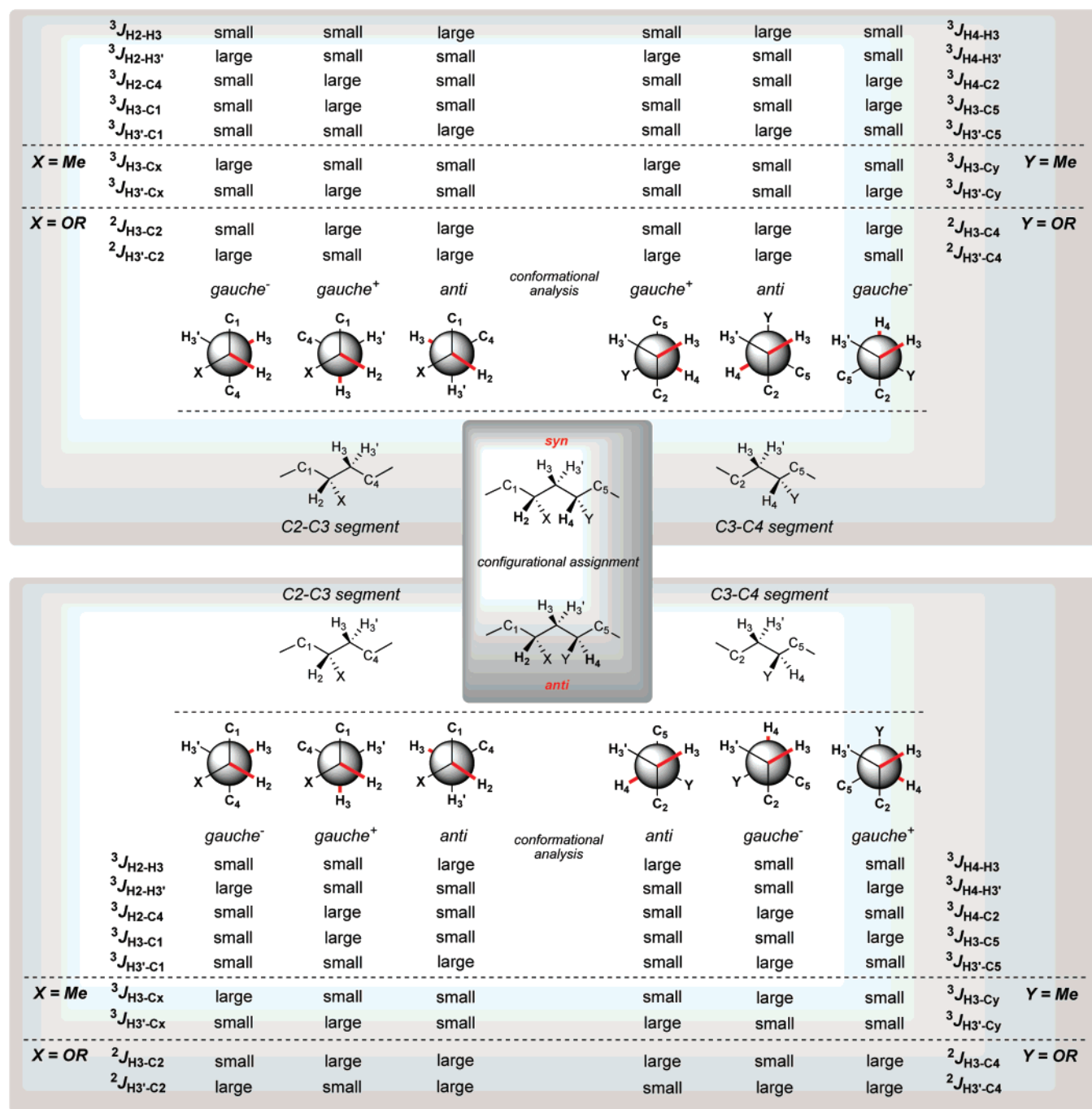


Figure 4. *J*-based analysis: coupling constants' pattern versus conformational and configurational arrangement in a 1,3-dimethine system.

achieved. In this case, the stereorelationships of both stereocenters to the diastereotopic proton pair of the bridging methylene need to be secured following the same logic, which in turn allows their relative configuration to be extracted.

Although the *J*-based configurational analysis has been successfully applied to a wide range of cases, including homo- and heterosubstituted adjacent and alternate stereocenters, some limitations should be mentioned. First of all, this method considers only staggered rotamers. Such a hypothesis is plausible and acceptable for an acyclic carbon chain. In principle, if a given conformer deviates more than 15° from a pure staggered arrangement, the analysis may fail, potentially leading to wrong results.⁶ However, the

semiquantitative version of the method is in a way more tolerant of small deviations. On the other hand, the lack of accurate quantitative information may be critical in various instances, for example, in the cases of C24–C25 and C27–C28 segments of the reidispongolide A fragment.²⁴ Moreover, the range of variability of ${}^{2,3}J_{HX}$ ($X = H$ or C), compressed sometimes in a quite narrow window, strongly depends on the electronegativity of the substituents directly linked to the stereogenic carbons,²¹ adding further variables that need to be duly considered. This can have a strong influence on the possibility of correctly predicting a priori the magnitude of a given coupling. In Figure 5 the effect of different substitution patterns on ${}^2J_{HC}$ is reported for a pair of carbons. For such reason, the sole qualitative evaluation

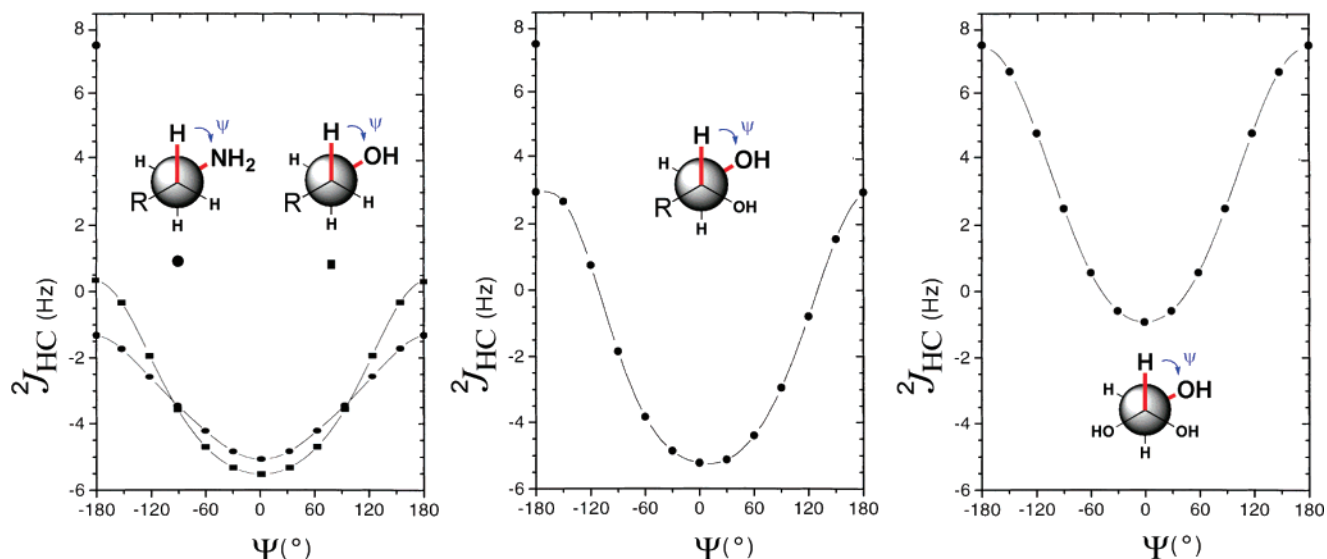


Figure 5. Computed range of variability of ${}^2J_{\text{HC}}$ (hertz) as a function of dihedral angle Ψ (degrees) between interested nuclei in differently functionalized 1,2-dimethine systems (adapted from ref 21).

of ${}^2,3J_{\text{HX}}$ values disregarding effects arising from specific substitution patterns may lead to rough errors in the final assignment.

Finally, a further complication originates from the interpretation of NMR parameters in terms of a single staggered rotamer (the most populated one), neglecting the contribution of the remaining two (or more). As is often the case, the coexistence of more than one significant conformer is also possible. In its original formulation, for the specific case of two equilibrating rotamers, the method would still allow one to reach a conclusion in four of six possible instances.⁵ The efficacy of the analysis is greatly enhanced if a fully quantitative version of the method is applied, better if in combination with J -coupling predictions from first principles (see section 4.7.1.).

A survey on instructive applications of J -based configurational analysis, including challenging cases with multiple conformer equilibria, will follow after a brief account of the NMR experiments used for measuring ${}^2,3J_{\text{HC}}$.

2.1. Experimental Measurements of ${}^2,3J_{\text{HC}}$ Couplings

Whereas the ${}^3J_{\text{HH}}$ values may be straightforwardly extracted by means of homonuclear NMR experiments,^{25,26a} heteronuclear long-range ${}^2,3J_{\text{HC}}$ values have become widely available after the introduction of inverse detection NMR techniques²⁶ and the implementation of pulse-field-gradient (PFG) hardware in commercial NMR spectrometers. These values are determined, in the original method proposed by Murata, by 2D hetero half-filtered TOCSY (HETLOC)²⁷ and phase sensitive HMBC (PS-HMBC)^{28–31} experiments. HSQC-TOCSY spectra have also been used for this purpose.³² Besides the above indicated experiments, a complete survey of heteronuclear correlation experiments for the measurement of heteronuclear coupling constants has been presented by Williamson et al.^{26b}

HETLOC is a two-dimensional homonuclear correlation experiment in which the conventional TOCSY-type peaks are further split in both dimensions by heteronuclear couplings. In particular, a peak in the spectrum corresponding to a long-range coupling between two protons ($\omega_2 = \text{Hx}$ and $\omega_1 = \text{Hy}$) (Figure 6) will show a large ω_1 signal

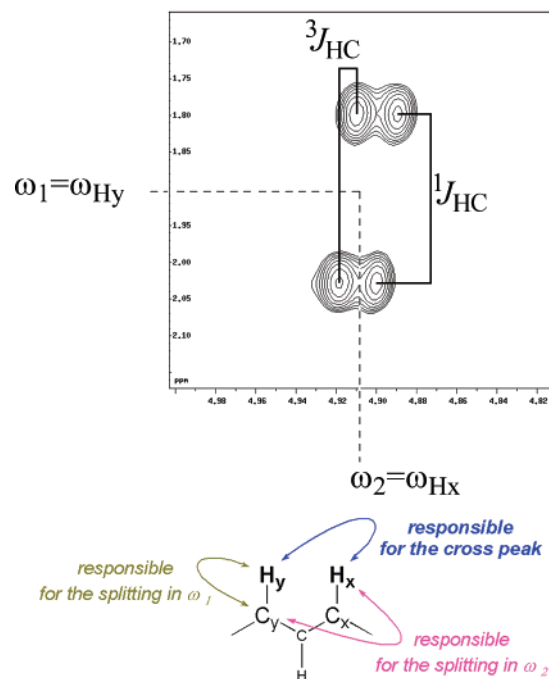


Figure 6. Direct measurement of ${}^2,3J_{\text{HC}}$ coupling constants through analysis of HETLOC cross-peaks.

displacement due to the direct coupling between Hy and Cy (${}^1J_{\text{Hy-Cy}}$), allowing efficient measurement of the small ω_2 peak splitting due to the heteronuclear long-range coupling between proton Hx and Cy (${}^2J_{\text{Hx-Cy}}$ or ${}^3J_{\text{Hx-Cy}}$). The limitation in the HETLOC method lies in the intrinsic nature of the peaks: the two protons must belong to the same spin system and must exhibit a TOCSY correlation peak. For this reason, it is impossible to use this experiment to measure coupling constants between a proton and a quaternary carbon or between a proton and a carbon belonging to a different spin system.

Owing to a relatively low sensitivity, a PFG enhanced version of the HETLOC experiment has been reported.³³ The resonance overlap, another common problem of HETLOC spectra, can be often overcome by spreading 2D signals over larger frequency windows, typically that of ${}^{13}\text{C}$, as in HSQC-

TOCSY, HSQMBC,³⁴ and HMBC spectra. In the PS-HMBC experiment, it is possible to quantitatively analyze the proton–carbon correlations, and from their relative intensity it is possible to extrapolate $^{2,3}J_{\text{HC}}$ values (eq 1)⁵

$$\frac{I_{\text{H-Ca}}}{I_{\text{H-Cb}}} = \frac{\sin^2(^{2,3}J_{\text{H-Ca}}\pi\Delta)}{\sin^2(^{2,3}J_{\text{H-Cb}}\pi\Delta)} \quad (1)$$

where $I_{\text{H-Ca}}$ and $I_{\text{H-Cb}}$ are the volumes of the cross-peaks due to H–Ca and H–Cb couplings, respectively, whereas Δ is the delay of long-range proton–carbon coupling evolution, usually set at 50 ms (corresponding to a maximum J value of 10 Hz). Therefore, a given J value, for instance, $^{2,3}J_{\text{H-Ca}}$, can be obtained by plugging into eq 1 the experimentally determined cross-peak volumes $I_{\text{H-Ca}}$ and $I_{\text{H-Cb}}$ and the $^{2,3}J_{\text{H-Cb}}$ value that needs to be independently measured, for example, by HETLOC spectra.

Because the correlations measured in the PS-HMBC are not read through homonuclear TOCSY correlations, as in the HETLOC spectrum, it is possible to estimate coupling constants between protons and quaternary carbons or between protons and carbons belonging to different spin systems.

More recent pulse sequences added to the repertoire are the HSQMBC³⁴ and J -HMBC.³⁵ In the first, a peak in the spectrum corresponding to a long-range correlation between a proton and a carbon ($\omega_2 = \text{Hx}$ and $\omega_1 = \text{Cy}$) is split, in the ω_1 dimension, by the heteronuclear J -coupling value of interest. The J -HMBC contains the same information of the HSQMBC spectrum with the advantage, especially for compounds displaying crowded spectral regions, of better peak dispersion. In fact, thanks to its sophisticated pulse sequence, an ω_1 splitting larger than the active J -coupling is associated with the peaks of interest. The actual J value is then extracted by applying a mathematical correction to the measured splitting.³⁵

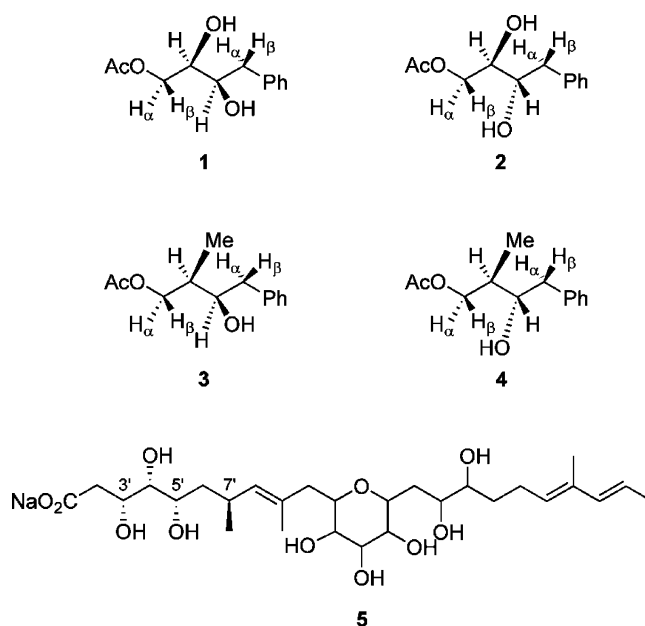
2.2. J -Based Configurational Analysis: 1,2- and 1,3-Dihydroxy or -Hydroxymethyl Dimethine Systems

The J -based configurational analysis was originally introduced by discussing stereoassignments in the stereodefined model compounds **1–4** and in the carboxylic acid **5**, recovered from the LiOH hydrolysate of zooxanthellatoxin (Chart 1).⁵ In this pioneering study, the method was validated for 1,2-dihydroxy (models **1** and **2**) and 1-methyl-2-hydroxy (models **3** and **4**) adjacent stereopairs, and its reliability was probed on the C3'–C7' segment of **5**, including the case of the 1-hydroxy-3-methyl system comprising the two alternate stereogenic centers C5' and C7'.

Given the widespread occurrence of these frameworks in natural products, the J -based configurational analysis was extensively used for the structural elucidation of compounds containing the same or equivalent substitution patterns.^{32,36–60} Among them, simplakidine A³⁸ represents a peculiar study, by virtue of its 1-hydroxy-2-pyridinium system.

As previously mentioned, the reliability of such an analysis strongly depends on the qualitative estimation of the measured $^{2,3}J_{\text{HC}}$ values of unknown compounds. Because their magnitude depends upon the electronegativity of the substituents directly linked to the carbons of interest,²¹ knowledge of their range of variability is required for each specific substitution pattern. This information could be retrieved from the literature or measured in analogous

Chart 1



compounds with known configuration. Alternatively, the values of specific J can be computed as a function of the dihedral angle from empirically derived functions.^{2,3,22,23} For non-, mono-, and dioxygenated⁶¹ carbons of 1,2-dimethine systems, the estimated magnitudes of $^{2,3}J_{\text{HC}}$ values are

Table 1. $^3J_{\text{HH}}$ and $^{2,3}J_{\text{HC}}$ Values (Hertz) for *anti* and *gauche* Orientations in Oxygenated Acyclic Systems

| | | $^3J_{\text{HH}}$ | | | $^3J_{\text{HC}}$ | | | $^2J_{\text{HC}}$ | | | | | |
|---------------|-----------------------|------------------------|----------|----------|-------------------|--|--|------------------------|--|--|--|--|--|
| | | <i>anti</i> | | | <i>anti</i> | | | <i>gauche</i> | | | | | |
| | | <i>gauche</i> | | | <i>gauche</i> | | | <i>anti</i> | | | | | |
| | | X = oxygen or hydrogen | | | | | | Y = oxygen or hydrogen | | | | | |
| | | oxygenation | | | | | | magnitude | | | | | |
| rotamer | $^{2,3}J_{\text{HX}}$ | none | mono | di | estimation | | | | | | | | |
| <i>anti</i> | $^3J_{\text{HH}}$ | 9-12 | 8-11 | 7-10 | large | | | | | | | | |
| <i>gauche</i> | | 2-4 | 1-4 | 0-4 | small | | | | | | | | |
| <i>anti</i> | $^3J_{\text{HC}}$ | 6-8 | 6-8 | 5-7 | large | | | | | | | | |
| <i>gauche</i> | | 1-3 | 1-3 | 1-3 | small | | | | | | | | |
| <i>gauche</i> | $^2J_{\text{HC}}$ | / | -5 to -7 | -4 to -6 | large | | | | | | | | |
| <i>anti</i> | | / | 0 to -2 | 2-0 | small | | | | | | | | |

Table 2. Measured $^3J_{\text{HH}}$ and $^{2,3}J_{\text{HC}}$ with Respect to the C2–C3 Segment in Compound 1^a

| $^{2,3}J_{\text{HX}}$ | nuclei | measured value (Hz) | magnitude estimation |
|-----------------------|--------|------------------------|----------------------|
| $^3J_{\text{HH}}$ | H2-H3 | 2.9 (2.5) ^b | small |
| | H2-C4 | 1 | small |
| $^3J_{\text{HC}}$ | H3-C1 | 2 | small |
| | H3-C2 | 0 | small |
| $^2J_{\text{HC}}$ | H2-C3 | -1 | small |

^a Coupling constants measured in C₅D₅N/CD₃OD (1:1). ^b Measured at -33 °C.

reported in Table 1. For the benefit of readers unacquainted with this approach, its logic can be illustrated by working out the configuration of model compound **1** (Chart 1), as it was still configurationally unassigned. Table 2 reports the measured $^3J_{\text{HH}}$ and $^{2,3}J_{\text{HC}}$ values along with their estimated magnitudes (see Figure 2). The $^3J_{\text{H2-H3}}$ *small* measured value (see also Table 1) fits with all four *gauche* rotamers of the *erythro* and *threo* series (green circle in Figure 7), ruling out *anti* conformers (green cross in Figure 7). The $^3J_{\text{H2-C4}}$ *small* measured value (see Table 1) restricts the analysis to *threo g⁻* and *erythro g⁺* (red circles and crosses), whereas the $^3J_{\text{H3-C1}}$ *small* value, being only compatible with *threo g⁻* (blue circle and cross) allows the assignment (configurational assignment) to be made.

In close analogy with 1,2- and 1,3-dihydroxy and hydroxymethyl systems are 1,2- and 1,3-dialkyl fragments. Stereoassignments on kalkitoxin^{62,63} and spongidepsin^{41,64} represent extensions of the *J*-based methodology to this kind of substitution pattern.

2.3. Multiple Conformer Equilibria

A molecular segment cannot always be represented by a single, highly (>85%) populated, rotamer. In such cases, averaged *J* values are detected, leading to values difficult to

classify, the so-called medium *J* values, a signature for the presence of a fast conformational interconversion (this is not always the case: see section 2.4.2. for a discussion on ascaulitoxin). It is often a valid assumption that the multiple conformer equilibrium can be simply described in terms of staggered interconverting rotamers.⁵ Considering the simplified case of just two equilibrated rotamers, the a priori estimation of *J* magnitudes comes from the weighted mean values of individual *J* as displayed in Figure 8.

As anticipated, the *J*-based configurational analysis should allow the unequivocal assignment of the relative configuration in four of six cases of equilibrated rotamer pairs. Specifically, only the *gauche⁺/gauche⁻* equilibrated rotamers of both *erythro* and *threo* series are spectroscopically indistinguishable. In those cases, conformational analysis can be complicated and a final assignment is hard to reach. The case of C11–C12 segment of amphidinolide **W** (**6**),⁵² a 1,2-dihydroxy dimethine system characterized by multiple conformer equilibrium, can be instructive in this specific context. It is noteworthy that the absolute configuration of the C2 stereocenter of **6** has been recently revised^{52b,c} as reported below. Notwithstanding, the structural revision did not concern the relative configuration of the C11–C12 segment, herein reported and discussed as assigned in the original paper.^{52a}

In particular, the C11–C12 relative configuration was established by examining the measured $^{2,3}J_{\text{HX}}$ values reported in Table 3. In Figure 9 the *medium* magnitude of $^3J_{\text{H11-H12}}$ accounts for a pair of *gauche/anti* equilibrating rotamers (green circle), ruling out the aforementioned *gauche⁺/gauche⁻* equilibrating pair (green cross) for which a *small* $^3J_{\text{H11-H12}}$ may be expected. The *small* values of both $^3J_{\text{H11-C13}}$ (violet circle) and $^3J_{\text{H12-C10}}$ (blue circle) suggest two concurrent *gauche* arrangements of H11–C13 and H12–C10 nuclei. Among the remaining four equilibrating rotamers, only the *gauche⁻/anti* pair of *threo* series fits nicely the spectroscopic data. The *medium* value of $^2J_{\text{H11-C12}}$ adds further strength to this interpretation and hence to the final configurational assignment (red circle).

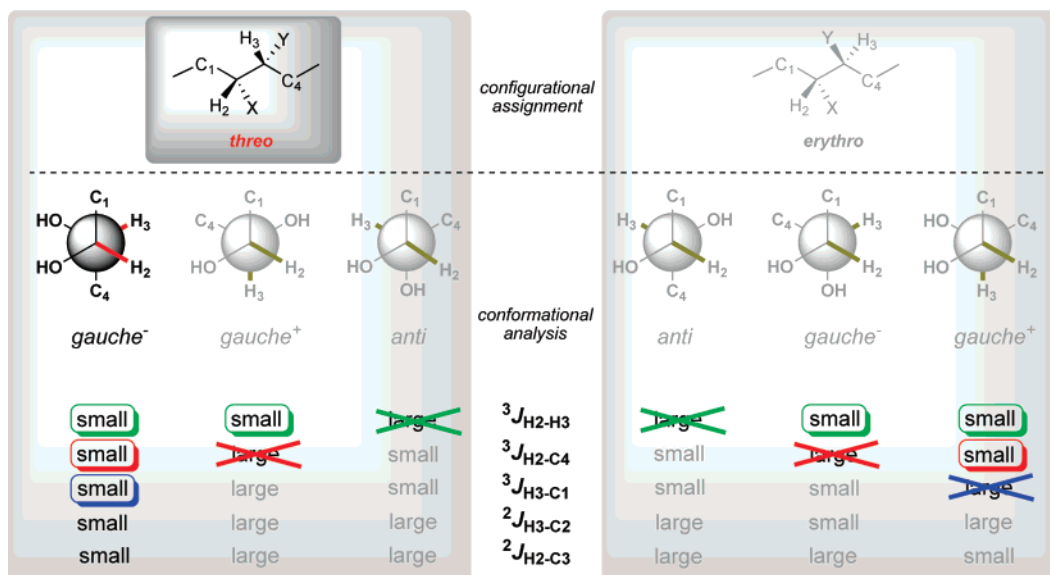


Figure 7. Conformational analysis and configurational assignment in the determination of the relative configuration of the C2–C3 segment in compound **1**.

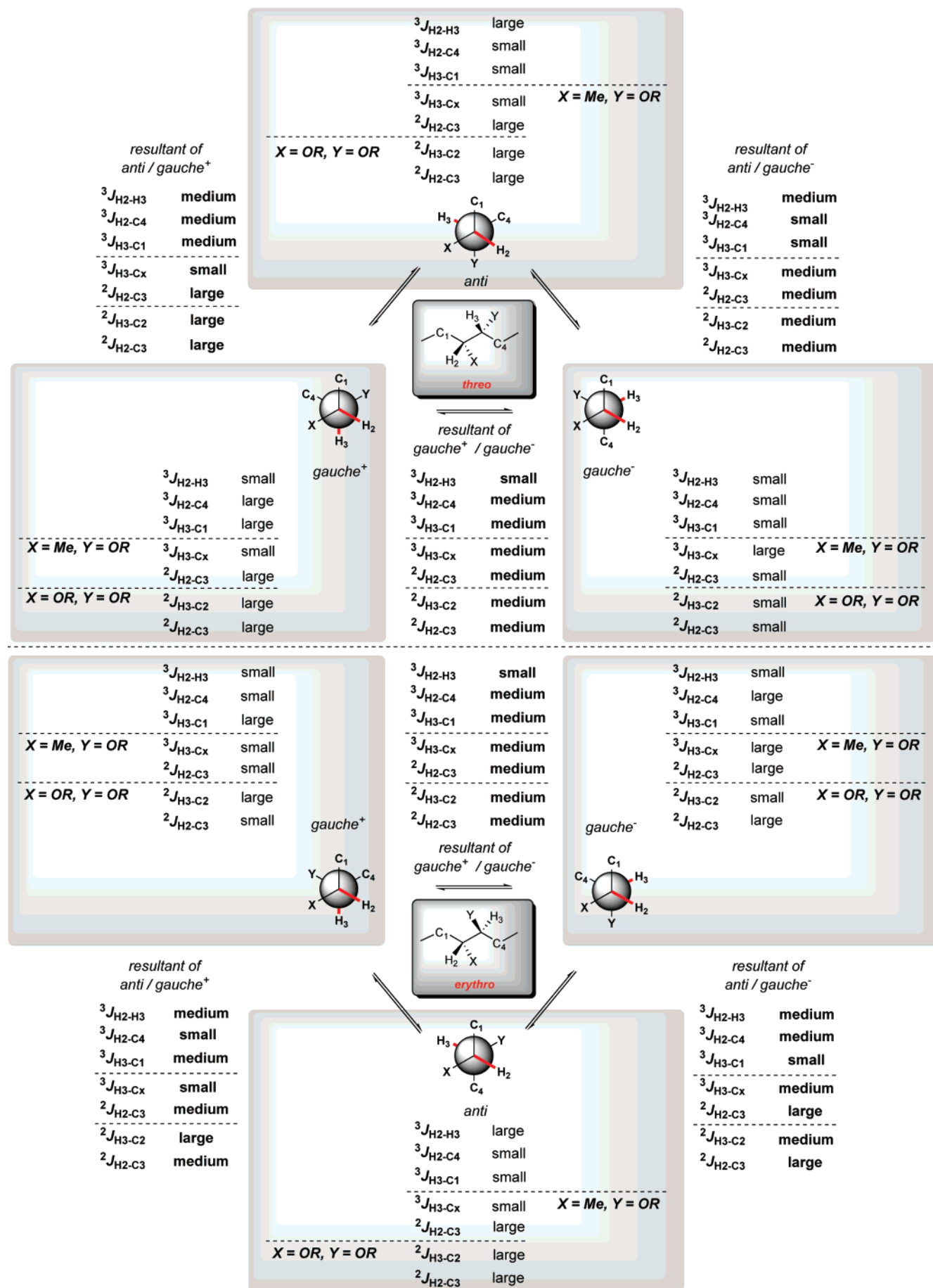
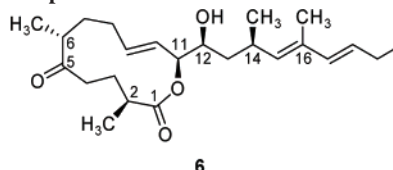


Figure 8. *J*-based analysis: coupling constants' pattern versus conformational and configurational arrangement in a 1,2-dimethine system with equilibrating rotamers.

Table 3. Measured $^3J_{\text{HH}}$ and $^2,^3J_{\text{HC}}$ Relative to the C11–C12 Segment in Compound 6


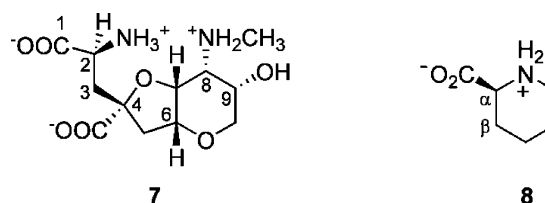
| $^{2,3}J_{\text{HX}}$ | nuclei | measured value (Hz) | magnitude estimation |
|-----------------------|---------|---------------------|----------------------|
| $^3J_{\text{HH}}$ | H11-H12 | 6.5 | medium |
| $^3J_{\text{HC}}$ | H11-C13 | -0 | small |
| | H12-C10 | 2.3 | small |
| $^2J_{\text{HC}}$ | H11-C12 | -2.0 | medium |

2.4. Extension of J -Based Configurational Analysis: Different 1,2 and 1,3 Substitution Patterns

We have previously pointed out that a generalization of the methodology to treat a wider range of substitutions requires great care in the evaluation of the magnitude of homo- and heteronuclear J values. During the past decade a variety of homo- and hetero-substituted 1,2- and 1,3-stereopairs have been studied, providing a solid basis for future assignments of more diverse natural products.

2.4.1. Aminated 1,2- and 1,3-Stereocenters

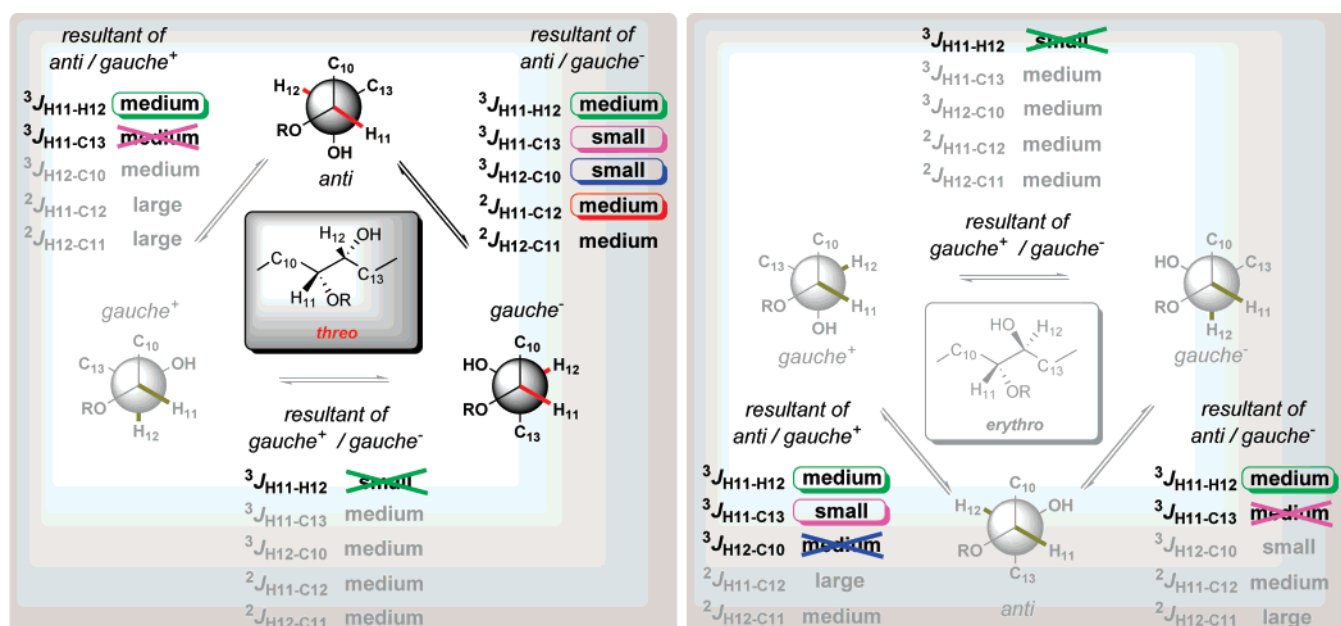
Dysiherbaine 7,¹⁰ a methylene-spaced 1-ammonium-3-quaternary system, represents a more complicated example of the fruitful application of J -based configurational analysis. The relative configuration of the C2–C4 segment was deduced from the stereorelationships of each of C2 and C4 with respect to the pivotal C3 methylene. Whereas C3–C4 could be simply treated like other monooxygenated systems,

Chart 2**Table 4. Comparative Evaluation of Stereorelations in the α - β Segment of Pipecolic Acid and in the C2–C3 Segment of Dysiherbaine**

| $^{2,3}J_{\text{HX}}$ | pipecolic acid 8 | | magnitude estimation | |
|-----------------------|-----------------------------------|----------------|----------------------|------------|
| | nuclei | stereorelation | | value (Hz) |
| $^3J_{\text{HH}}$ | H α -H β_{ax} | <i>anti</i> | 11.6 | large |
| | H α -H β_{eq} | <i>gauche</i> | 3.7 | small |
| $^2J_{\text{HC}}$ | H β_{eq} -C α | <i>anti</i> | -1.8 | small |
| | H β_{ax} -C α | <i>gauche</i> | -4.5 | large |

| $^{2,3}J_{\text{HX}}$ | dysiherbaine 7 | | magnitude estimation | |
|-----------------------|----------------|------------|----------------------|----------------|
| | nuclei | value (Hz) | | stereorelation |
| $^3J_{\text{HH}}$ | H3b-H2 | 11.5 | <i>anti</i> | large |
| | H3a-H2 | 2.5 | <i>gauche</i> | small |
| $^2J_{\text{HC}}$ | H3a-C2 | -2.5 | <i>anti</i> | small |
| | H3b-C2 | -4.5 | <i>gauche</i> | large |

the study of the C2–C3 pair required a preliminary validation analysis of the full set of $^{2,3}J_{\text{HX}}$ values for a reference compound. To this end pipecolic acid 8 (Chart 2) was chosen, and the comparison of J values in the real (dysiherbaine) and model (pipecolic acid) system is shown in Table 4 along

**Figure 9. Conformational analysis and final assignment in the determination of the relative configuration of the C11–C12 segment in compound 6.**

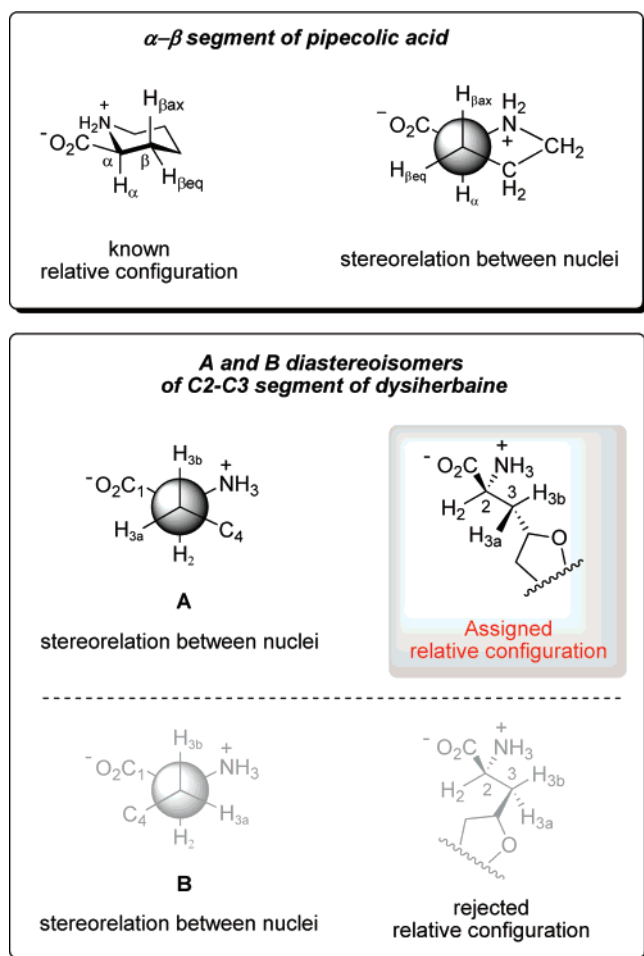


Figure 10. Relative configuration assignment of the C2–C3 segment in dysiherbaine: (top) stereorelations in the α - β segment of pipercolic acid (known configuration); (bottom) same stereorelations in the two possible configurations of dysiherbaine.

with the stereorelations between relevant nuclei in both compounds.

On this ground, rotamer A of dysiherbaine (see Figure 10) was selected and the related configuration assigned. Configurational analysis on halipeptins A **9** and B **10**^{65,66} and taveuniamide E **11**⁶⁷ (Chart 3) represent additional case studies of polyfunctionalized aminated systems.

2.4.2. 1-Amino-2-hydroxy and 1-Amino-3-hydroxy Dimethines

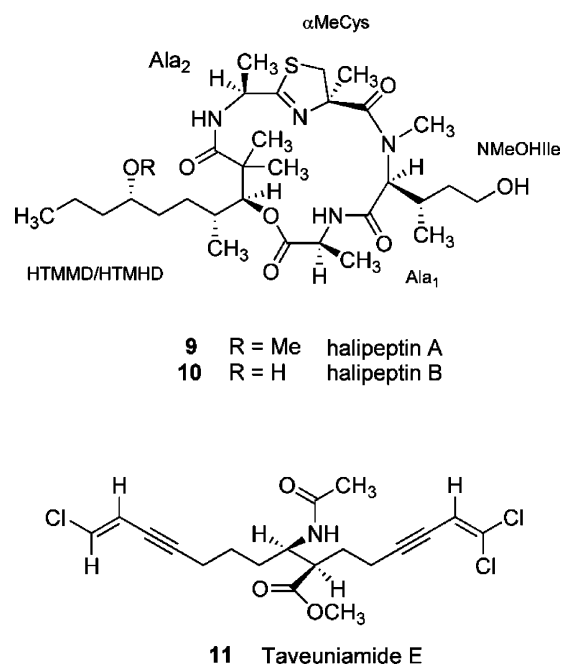
The effect of two adjacent or alternate stereocenters bearing two different electronegative substituents was first analyzed in the configurational assignment of the C2–C7 fragment of ascaulitoxin **12**,⁶⁸ which presents 1,2- and 1,3-aminoalcoholic frameworks.

Reliable curves describing the angular dependence of $^2J_{\text{HC}}$ couplings in nitrogen-containing frameworks have been obtained by ab initio methods.²¹ These curves are qualitatively similar to those of oxygenated systems (Figure 5), even if the $^2J_{\text{HC}}$ values of aminated systems (Table 5) fall in a tighter interval.

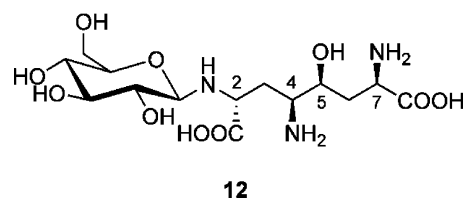
Table 6 reports the measured $^{2,3}J_{\text{HX}}$ values along with dominant rotamers and relative configuration of C4–C5 and C5–C7 in ascaulitoxin.

Of interest are also the $^3J_{\text{HH}}$ values of the C2–C4 segment. All observed values were in the 7–9 Hz range, suggesting

Chart 3



the coexistence of interconverting rotamers. Variable-temperature $^3J_{\text{HH}}$ measurements ruled out this hypothesis, in favor of the existence of a hydrogen bond interaction between the nitrogen at C2 (acceptor) and the C4-amino group (donor), thus forming a twist-like six-membered ring conformation. Both C2–C3 and C3–C4 fragments may still exist as staggered conformers, although with a reduced angular separation between substituents of only 20–30°.



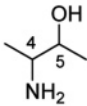
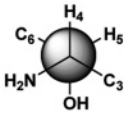
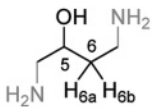
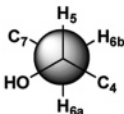
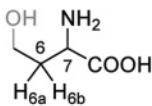
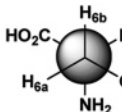
The reported cases opened the way to a more systematic application of the J -based configurational analysis to related systems.^{69–71}

Table 5. Comparison of the $^2J_{\text{HC}}$ Values in Mono-oxygenated 1,2-Dimethine Systems with the $^2J_{\text{HC}}$ Values in Monoaminated 1,2-Dimethine Systems

| rotamer ^a | $^2J_{\text{HC}}$ | heteroatom (Y) | | magnitude estimation ^b |
|----------------------|-------------------|----------------|------------|-----------------------------------|
| | | Nitrogen | Oxygen | |
| <p>gauche</p> | $^2J_{\text{HC}}$ | ca. –4 Hz | –4 → –6 Hz | large |
| <p>anti</p> | $^2J_{\text{HC}}$ | ca. –1 Hz | +2 → –1 Hz | small |

^a Stereorelation between nuclei refers to H2 and Y, the electronegative atom on C3 stereocenter. ^b The absolute value of the measured $^2J_{\text{HC}}$ is estimated.

Table 6. *J*-Based Configurational Analyses of C4–C5, C5–C6, and C6–C7 Segments of Ascaulitoxin

| segment | $^{2,3}J_{\text{HX}}$ | nuclei | value (Hz) | magnitude estimation | rotamer | configuration |
|--|-----------------------|----------------------|-------------------------|----------------------|--|---------------|
|  C4-C5 | $^3J_{\text{HH}}$ | H4-H5 | 2.5 | small |  | <i>syn</i> |
| | $^3J_{\text{HC}}$ | H4-C6 | < 3 | small | | |
| | | H5-C3 | 2.9 | small | | |
| | $^2J_{\text{HC}}$ | H4-C5 | 1.1 | small | | |
| | | H5-C4 | -1.9 | small | | |
|  C5-C6 | $^3J_{\text{HH}}$ | H5-H6a | 8.0, 9.2 ^a | large |  | <i>anti</i> |
| | | H5-H6b | 3.0, 3.3 ^a | small | | |
| | $^3J_{\text{HC}}$ | H5-C7 | 2.1 | small | | |
| | | H6a ^b -C4 | 1.8 | small | | |
| | $^2J_{\text{HC}}$ | H6a-C5 | -5.9 | large | | |
| | H6b ^b -C5 | -2.1 | small | | | |
|  C6-C7 | $^3J_{\text{HH}}$ | H7-H6a | 7.2, 8.6 ^a | medium |  | <i>anti</i> |
| | | H7-H6b | 7.6, 5.1 ^a | medium | | |
| | $^3J_{\text{HC}}$ | H7-C5 | 2.4, 2.7 ^a | small | | |
| | | H6a-C8 | 2.8, 2.2 ^a | small | | |
| | | H6b-C8 | < 3, < 3 ^a | small | | |
| | $^2J_{\text{HC}}$ | H6a-C7 | -5.4, -4.7 ^a | large | | |
| | | H6b-C7 | -4.3, -2.8 ^a | large | | |

^a Spectra recorded at 290 K in DMSO-*d*₆/D₂O (80:20). ^b H6a, high field; H6b, low field.

2.4.3. 1,2-Dichlorinated and 1-Chloro-2-hydroxy Dimethines

$^{2,3}J_{\text{HX}}$ values of polychlorinated compounds display a pattern of values qualitatively similar to those of polyoxygenated fragments (see Table 1). Their qualitative classification was corroborated by the concomitant application of molecular mechanics calculations in the stereochemical study of this class of compounds.^{72–75}

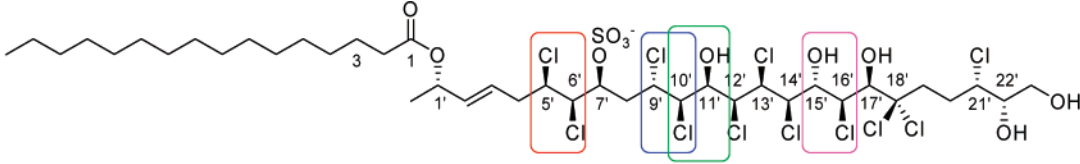
A relevant example of many adjacent or alternate hydroxychlorinated and dichlorinated stereopairs comes from the realm of marine natural products. Isolated from Adriatic toxic mussels, the cytotoxic sulfolipid **13** (Table 7) was fully characterized through the extensive use of *J*-based configurational analysis and NOE/ROE measurements.⁷²

Along these lines, a systematic *J*-based analysis on α -chloro- β -hydroxy diastereomers was also reported.⁷⁶

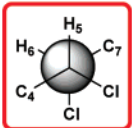
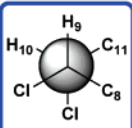
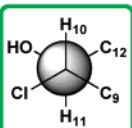
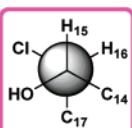
2.4.4. Heterosubstituted Methine-Quaternary Adjacent Stereocenters: 2'-Substituted Taxane Side Chains

Another type of complication comes from the case of adjacent methine-quaternary heterosubstituted stereocenters. The expected magnitudes of *J* values for *threo* stereoisomers of 1,2-dimethine and 1-methine-2-quaternary systems are comparatively analyzed in Figure 11. As stated earlier, the loss of one proton is followed by the loss of the whole corresponding set of *J* values which, in turn, implies the lack of the required parameters to unambiguously select the major

Table 7. *J*-Based Configurational Analyses of C5'–C6', C9'–C10', C10'–C11', and C15'–C16' Segments of Cytotoxic Sulfolipid 13



13

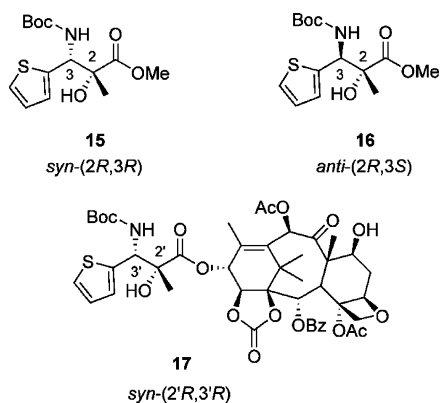
| segment | $^{2,3}J_{\text{HX}}$ | nuclei | value (Hz) | magnitude estimation | rotamer | configuration |
|-----------|-----------------------|---------|------------|----------------------|--|---------------|
| C5'–C6' | $^3J_{\text{HH}}$ | H5–H6 | 2.8 | small |  <i>syn</i> | |
| | $^3J_{\text{HC}}$ | H5–C7 | 0 | small | | |
| | | H6–C4 | 0 | small | | |
| | $^2J_{\text{HC}}$ | H6–C5 | -1.2 | small | | |
| H5–C6 | | -0.8 | small | | | |
| C9'–C10' | $^3J_{\text{HH}}$ | H9–H10 | 2.0 | small |  <i>anti</i> | |
| | $^3J_{\text{HC}}$ | H9–C11 | 0 | small | | |
| | | H8–C10 | 6.1 | large | | |
| | $^2J_{\text{HC}}$ | H10–C9 | -5.3 | large | | |
| H9–C10 | | -1.9 | small | | | |
| C10'–C11' | $^3J_{\text{HH}}$ | H10–H11 | 9.7 | large |  <i>syn</i> ^a | |
| | $^3J_{\text{HC}}$ | H10–C12 | 0 | small | | |
| | | H11–C9 | 0 | small | | |
| | $^2J_{\text{HC}}$ | H11–C10 | -5.9 | large | | |
| H10–C11 | | -5.2 | large | | | |
| C15'–C16' | $^3J_{\text{HH}}$ | H15–H16 | 1.8 | small |  <i>anti</i> | |
| | $^3J_{\text{HC}}$ | H15–C17 | 7.0 | large | | |
| | | H16–C14 | 3.0 | small | | |
| | $^2J_{\text{HC}}$ | H16–C15 | -2.1 | small | | |
| H15–C16 | | -4.8 | large | | | |

^a NOE experiments were also needed to accomplish this configuration assignment.

conformer and, consequently, to assign the relative configuration. Nevertheless, as reported in the case of the con-

figurational assignment of the C2'–C3' segment of 2'-substituted taxanes of general formula **14**,⁷⁷ the parallel

Chart 4



1-hydroxy-2-methyl dimethine frameworks need to be considered. Finally, in the C8–C9 segment of subunit B, a 1-hemiaminal-2-oxy framework, values reported in Table 5 can be used as reference. In addition, two 1,3-dioxygenated systems, the C9–C11 segment of the tetrahydropyran ring and C13–C15, are also present. The cases of subunit A and of the C8–C9 segment of subunit B are discussed with the aim of providing a significant overview on this NMR approach.

Table 8 and Figure 15 display the analysis of subunit A, which points to the *gauche*⁺/*gauche*[−] equilibrating rotamers of both *erythro* and *threo* series (Figure 14).

As previously observed (sections 2 and 2.3), in this case the stereoisomers are spectroscopically indistinguishable and the relative configuration cannot be assigned.

Conversely, the configuration of the C8–C9 segment of subunit B is unequivocally assigned by a combined analysis of *J* values and NOE data.

As it can be seen from Figure 16, even if the sole ^{2,3}*J*_{HX} values reported in Table 9 would not allow for discrimination between the two diastereomeric *anti* rotamers, thus leaving the case unresolved, a crucial dipolar effect between H10 and C8–OMe points to the *anti* conformer of the *erythro* series.

2.6. Sapinofuranone A: Toward the Computational Methods

A particularly difficult problem lies in the case of coexistence of two rotamers that account for less than 90% of the global population. The stereochemical assignment of the C4–C5 stereopair of sapinofuranone A **19**³⁹ serves as an example. Experimental ^{2,3}*J*_{HX} values, reported in Table 10, do not allow the selection of a unique rotamer among the six depicted in Figure 17.

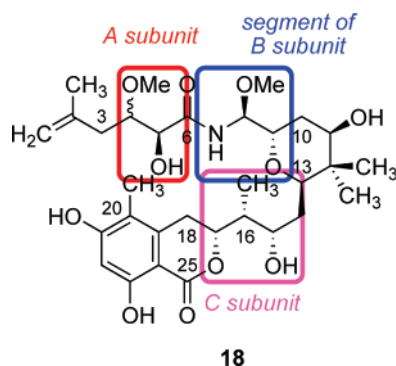
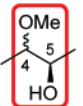


Figure 13. Relevant subunits in the psymberin skeleton.

Table 8. Measured ³*J*_{HH} and ²*J*_{HC} Relative to the C4–C5 Segment (Subunit A) in Compound 18

| segment | ^{2,3} <i>J</i> _{HX} | nuclei | value (Hz) | magnitude estimation |
|--|---------------------------------------|--------|------------|----------------------|
|  A subunit | ³ <i>J</i> _{HH} | H4-H5 | 2.5 | small |
| | ² <i>J</i> _{HC} | H4-C5 | 3 | medium |
| H5-C4 | | 3 | medium | |

As shown, the ³*J*_{H4–H5} *small* value is compatible with four of six rotamers (green circle), among which only two (dark violet circle and cross) are in agreement with the ³*J*_{H4–C6} *small* and the ²*J*_{H4–C5} *small* values (blue circle). However, the two remaining rotamers are both incompatible with the other ^{2,3}*J*_{HC} values. Indeed, the ³*J*_{H5–C3} *small* value would rule out the *gauche*⁺ rotamer of the *erythro* series, pointing to a *threo gauche*⁺ rotamer, whereas the ²*J*_{H5–C4} *medium/large* value is in agreement with the opposite scenario. The absence of key NOEs leaves unassigned the relative configuration. Conceivably, these apparently conflicting NMR data suggest conformational averaging, with rapid interconversion between two or more conformers on the NMR time scale. To solve the stereochemical problem the authors performed a molecular dynamics conformational search on both *erythro* and *threo* diastereoisomers followed by energy minimizations. The final ab initio geometry optimization at Hartree–Fock (HF) level performed on all of the significant minimum energy conformers pointed to five optimized rotamers for each diastereoisomer. Finally, the authors proposed a computational approach taking into account the Boltzmann averaged values of empirically³ computed homonuclear and heteronuclear coupling constant values, in which the energy differences associated with the weighting factors were computed at HF level. The comparison of the experimentally measured *J* values with their counterparts calculated as above unambiguously points to the *erythro* stereoisomer (Table 11). In particular, whereas the errors for the *erythro* stereoisomers were all below 1.0 Hz, a large error of 2.9 Hz relative to the ²*J*_{HC} H5–C4 suggested the exclusion of the *threo* isomer.

Besides the stereochemical analysis in itself, this mixed empirical–ab initio computational approach paved the way to more recent hybrid computational/experimental approaches, taking full advantage of state of the art ab initio

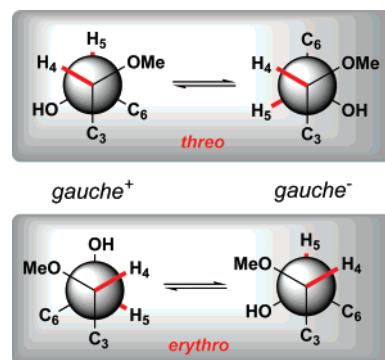


Figure 14. *gauche*⁺/*gauche*[−] equilibrated rotamers of both *threo* and *erythro* relative configurations of subunit A of psymberin.

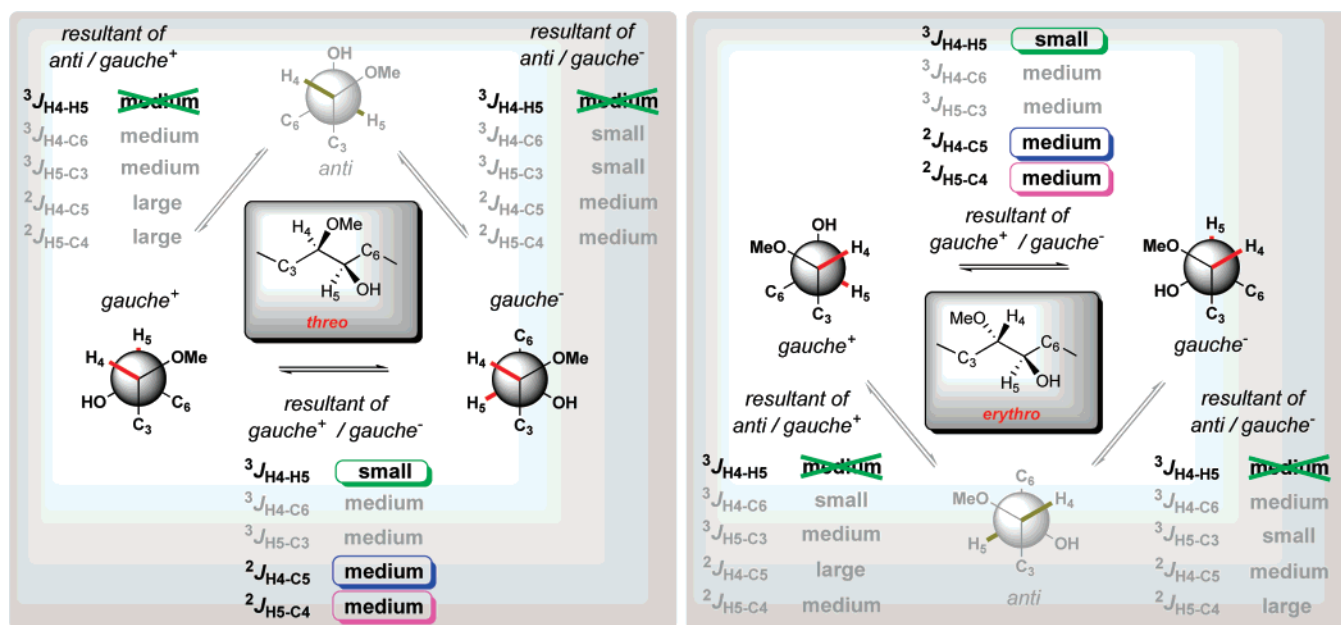


Figure 15. Conformational analysis for determining the relative configuration of the C4–C5 segment (subunit A) in compound 18. On the sole basis of J -based analysis the configurational assignment cannot be reached.

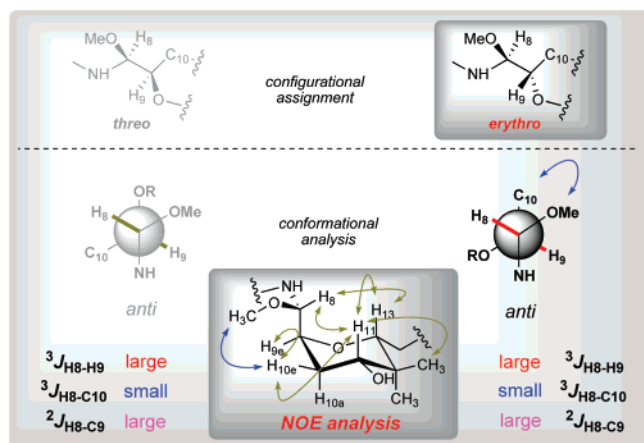


Figure 16. Combined analysis of J values and NOE data in the stereochemical assignment of C8–C9 segment (segment of subunit B) in compound 18.

Table 9. Measured $^3J_{\text{HH}}$ and $^{2,3}J_{\text{HC}}$ Relative to the C8–C9 Segment (Segment of Subunit B) in Compound 18

| segment | $^{2,3}J_{\text{HX}}$ | nuclei | value (Hz) | magnitude estimation |
|--------------------------|-----------------------|--------|------------|----------------------|
| segment of B subunit | $^3J_{\text{HH}}$ | H8-H9 | 8.0 | large |
| | $^3J_{\text{HC}}$ | H8-C10 | 3 | small |
| | $^2J_{\text{HC}}$ | H8-C9 | 6 | large |

methods, including prediction of NMR parameters from first principles (see section 4 and following subsections).

2.7. Survey of $^3J_{\text{HH}}$ and $^{2,3}J_{\text{HC}}$ Values

The aforementioned methodological extensions and validations allow the confident application of J -based analysis to the solution of a variety of stereochemical problems concerning highly functionalized molecules. To close this

Table 10. Measured $^3J_{\text{HH}}$ and $^{2,3}J_{\text{HC}}$ Relative to the C4–C5 Segment in Compound 19

| segment | $^{2,3}J_{\text{HX}}$ | nuclei | value (Hz) | magnitude estimation |
|---------|-----------------------|--------|------------|----------------------|
| C4-C5 | $^3J_{\text{HH}}$ | H4-H5 | 3.1 | small |
| | $^3J_{\text{HC}}$ | H4-C6 | < 1.0 | small |
| C4-C5 | $^2J_{\text{HC}}$ | H4-C5 | 1.0 | small |
| | $^3J_{\text{HC}}$ | H5-C3 | 2.6 | small |
| C4-C5 | $^2J_{\text{HC}}$ | H5-C4 | -3.3 | medium/large |

section, and for the benefit of the reader, in Table 12 are summarized the ranges of $^3J_{\text{HH}}$ and $^{2,3}J_{\text{HC}}$ of the most important disubstituted 1,2-dimethine systems.

3. Universal NMR Database in Achiral Solvents: Concept and Proof

Along with the methods previously discussed, other approaches suggest the comparison of the chemical shifts of the compounds with unknown configuration with libraries of model compounds with known stereostructures, as described in the pioneering paper of Hoyer regarding the stereochemical assignment of the bistetrahydrofuran moiety of uvaricin.⁸⁰ Among these approaches, the universal NMR database (UDB)⁸¹ has recently emerged as another useful

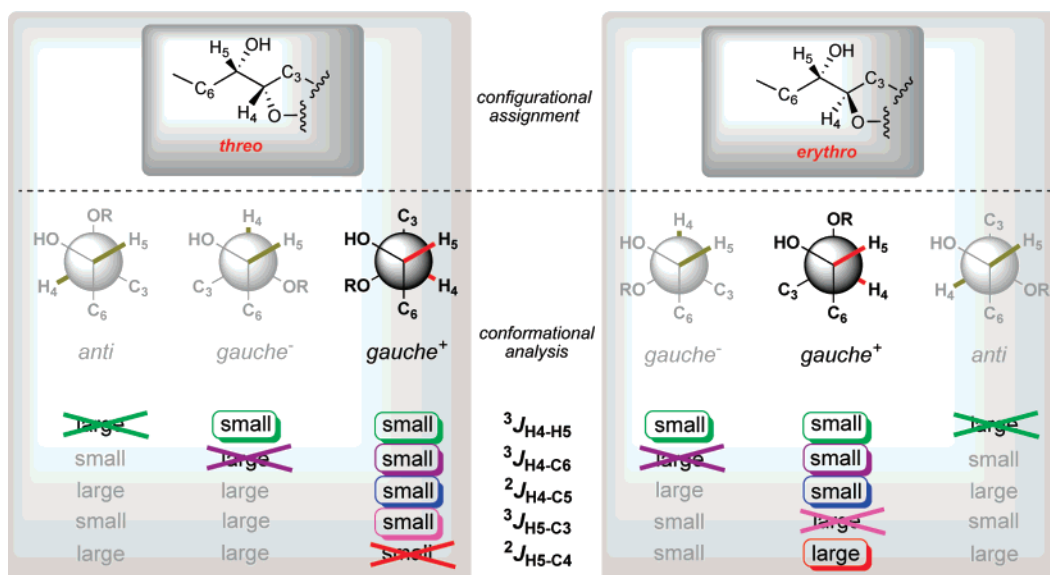
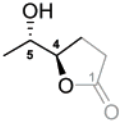


Figure 17. Conformational analysis for determining the relative configuration of the C4–C5 segment (subunit A) in compound **19**. On the sole basis of *J*-based analysis the configurational assignment cannot be reached.

Table 11. Comparison of Measured and Calculated *J* Values in the Determination of the Relative Configuration of the C4–C5 Segment in Compound **19**

| segment | $^{2,3}J_{\text{HX}}$ | nuclei | measured value (Hz) | magnitude estimation | calculated value (Hz) | |
|--|-----------------------|--------|---------------------|----------------------|-----------------------|-------------|
| | | | | | threo | erythro |
|  C4-C5 | $^3J_{\text{HH}}$ | H4-H5 | 3.1 | small | 3.3 | 3.9 |
| | $^3J_{\text{HC}}$ | H4-C6 | < 1.0 | small | 2.4 | 0.9 |
| | $^2J_{\text{HC}}$ | H5-C4 | -3.3 | medium/large | -0.4 | -3.4 |
| | $^2J_{\text{HC}}$ | H4-C5 | 1.0 | small | -0.3 | 0.2 |
| | $^3J_{\text{HC}}$ | H5-C3 | 2.6 | small | 2.1 | 2.9 |

tool to tackle the problem of configurational analysis. As a natural evolution of the monumental work of Kishi's group in the field of chemical synthesis of complex natural products,⁸² the UDB approach is rooted in the following assumption, as phrased by Kishi himself: "the structural properties of a compound in question are (1) inherent to the specific stereochemical arrangements of (small) substituents on its carbon backbone and (2) independent from the rest of the molecule."^{81a}

The arithmetical elaboration of both carbon (Figure 18) and proton (Figure 19) chemical shifts shown as NMR histogram plots⁸³ relative to the eight diastereoisomers **20a–h** (Table 13), expressing individual deviations from mean values,⁸⁴ testify to the validity of such a hypothesis.

In this way, the full chemical shift (cs) data set of compounds **20a–h** represent the UDB of the general structure **20**, which, once made available, may be successfully used to determine the relative configuration of an unknown compound having a structure that encompasses a fragment like **20**, provided that such fragment is conformationally unconstrained, that is, acyclic or embedded in a sufficiently large ring. Indeed, a highly complex and func-

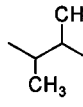
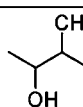
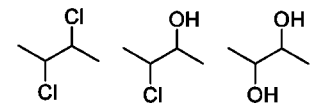
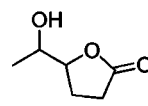
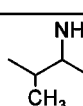
tionalized molecule can be considered, from a structural viewpoint, as the sum of independent subunits (stereoclusters) linked together. This second assumption, referred to as a self-contained box,⁸² constitutes one of the key foundations for this approach. Hence, the relative configuration of each subunit can be related to that of a model diastereoisomer having the same connectivity of the undetermined subunit. By simply comparing the proton and carbon cs of the unknown stereocluster with those of an appropriate cs database, a configurational assignment is made. The structural elucidation of the desertomicin/oasomicin class of natural products represents the first example of the application of the UDB approach, also used to prove its validity.^{81b,85}

3.1. Desertomicin/Oasomicin Class of Natural Products: Databases

The molecular skeleton of the desertomicin/oasomicin class of natural products can be considered as the sum of the following stereoclusters (rectangles in color of Figure 20).

Each subunit can be represented by the simplified structures of Chart 5, the proton and carbon cs databases (of all

Table 12. Summary of $^3J_{\text{HH}}$ and $^{2,3}J_{\text{HC}}$ Values and Estimations of the Most Important Disubstituted 1,2-Dimethine Systems

| 1,2- dimethine systems | $^3J_{\text{HH}}$ (Hz) | | $^3J_{\text{HC}}$ (Hz) | | $^2J_{\text{HC}}$ (Hz) ^a | |
|---|------------------------|---------------|------------------------|---------------|-------------------------------------|--------------------|
| | rotamer | | | | | |
| | <i>anti</i> | <i>gauche</i> | <i>anti</i> | <i>gauche</i> | <i>anti</i> | <i>gauche</i> |
| | magnitude estimation | | | | | |
| | large | small | large | small | small ^a | large ^a |
|  | 9-12 | 2-4 | 6-8 | 1-3 | / | / |
|  | 8-11 | 1-4 | 6-8 | 1-3 | 0 to -2 | -5 to -7 |
|  | 7-10 | 0-4 | 5-7 | 1-3 | 2-0 | -4 to -6 |
|  | | / | | / | +3 to -5 | |
|  | | / | | / | ca -1 | ca -4 |

^a The signed value of the measured J has to be considered.

their diastereoisomers) being required to correctly predict the relative configuration of the above stereoclusters.

As an example, the structural elucidation of the C5–C10 stereocluster of oasomycin B **21b** will be reviewed. Working on this fragment, represented by the generic structure **20**, demands the full set of diastereoisomers **20a–h** to build the database. To account for connectivity differences between the stereocluster to be defined and the (simplified) models constituting the database, the authors suggested correcting all stereocluster cs by a suitable factor,⁸¹ the latter being derived from empirically predicted cs. The Schaller program delivered with the ChemDraw software package⁸⁶ has been used for this purpose. The differences between adjusted carbon chemical shifts of oasomycin B and those of the database elements **20a–h** were computed and plotted as histograms (Figure 21). Even at first glance, it can be appreciated that **20e** matches to the greatest extent the cs of the natural product fragment.

By extending the same kind of analysis to all other stereoclusters and databases,⁸⁵ the relative configuration of all the stereocenters of the desertomycin/oasomycin class of natural products could be assigned.⁸⁷ A combined UDB analysis on both proton and carbon cs puts the final assignment on a firmer ground, as the case of the C29–C32

segment seems to imply.^{85a} Empirical rules and specific patterns also emerge from these cs comparative analyses and come as an added bonus. For instance, in the case of 3,5,7-triol systems **22a–d**^{85c,88} in Figure 22, the carbon cs of the central C5 depends upon the configurational pattern of the C3–C5 and C5–C7 stereopairs: using as a starting point the C5 cs value when both pairs display *anti* arrangements, a $\Delta\delta_{\text{C5}}$ of 2 ppm is observed for oppositely configured pairs (*syn/anti* or *anti/syn*), whereas an additional $\Delta\delta_{\text{C5}}$ of 2 ppm correlates with a *syn/syn* configurational pattern (left side of Figure 22). This empirical rule was termed the “plus-two increments” of the triol systems.^{85a,c} Increments of similar magnitude, although in the opposite direction, have also been correlated with other specific stereopatterns falling within the general structure **23a–d** (right side of Figure 22).^{85d,89}

After its disclosure to the scientific community, the UDB approach was eventually applied to solve a variety of other structural problems.

3.2. Applications of the UDB Approach: Caylobolide A, Scyphostatin, and Ritterazine M

An intrinsic feature of the UDB method is that, upon its application to a structural problem, a new database is made

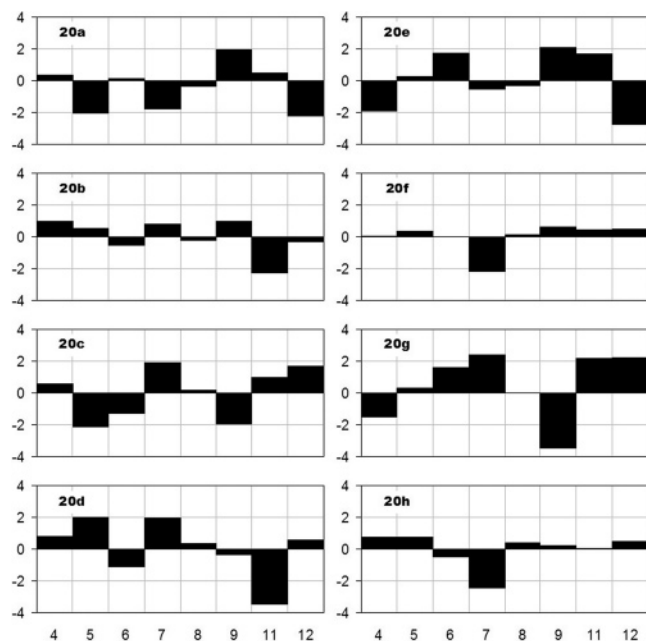


Figure 18. Deviations from the average of the carbon chemical shifts of compounds **20a–h**. The *x* and *y* axes represent position number and $\Delta\delta$ in parts per million, respectively, for all graphs in this paper.

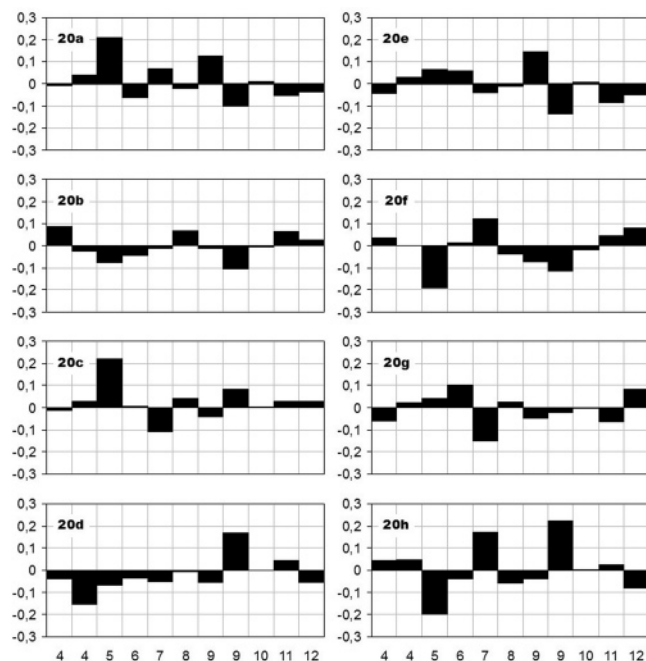


Figure 19. Deviations from the average of the proton chemical shifts of compounds **20a–h**.

available to the chemical community, allowing for other meaningful stereochemical correlations and assignments. Likewise, Kishi's work on 1,3,5-triol systems opened the way to further stereochemical analysis by the Molinski group aimed, this time, at solving the relative configuration of the C25–C29 segment of the marine product caylobolide **24** (Chart 6).⁹⁰ Typically, however, the stereocontrolled synthesis of all the constitutive elements of the database is a necessary step and has to be considered a prerequisite. This was indeed the case for the study of the C1'–C20' trienoyl fragment of scyphostatin **25**,⁹¹ previously isolated but not completely characterized⁹² (the configuration at C8' and C10' still awaited definition) until the Sankyo group⁹³ deduced it.

Table 13. General Structure and Relative Orientation of the Substituents in the Eight Diastereoisomers **20a–h**

20

| | C5 | C6 | C7 | C8 |
|------------|----------|----------|----------|----------|
| 20a | α | α | β | β |
| 20b | α | α | α | α |
| 20c | α | α | β | α |
| 20d | α | α | α | β |
| 20e | β | α | β | β |
| 20f | β | α | α | α |
| 20g | β | α | β | α |
| 20h | β | α | α | β |

Also, the structural revision⁹⁴ of the north spiroketal moiety of ritterazine M **26**⁹⁵ (Chart 7) required the synthesis of model compounds **27–31** (Chart 8).

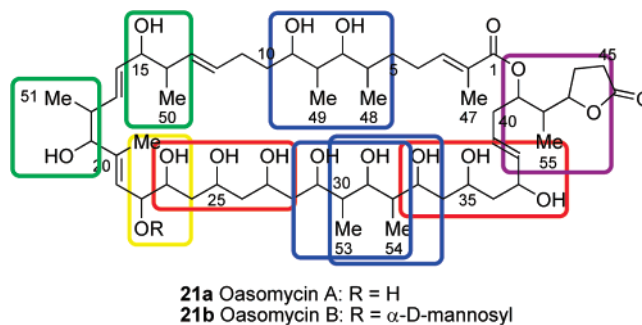
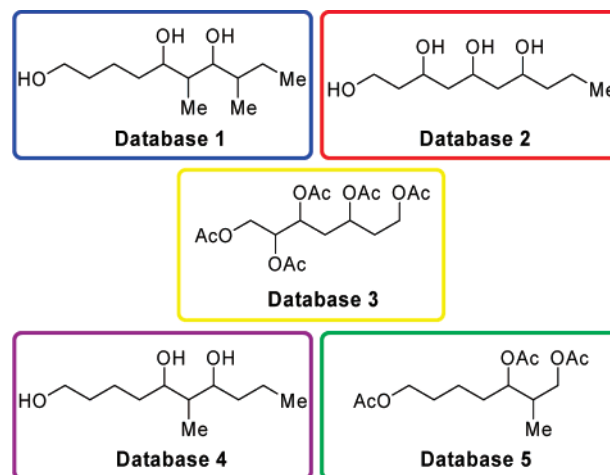


Figure 20. Molecular skeleton of oasomycins A and B in which different stereoclusters are evidenced by colored rectangles.

Chart 5



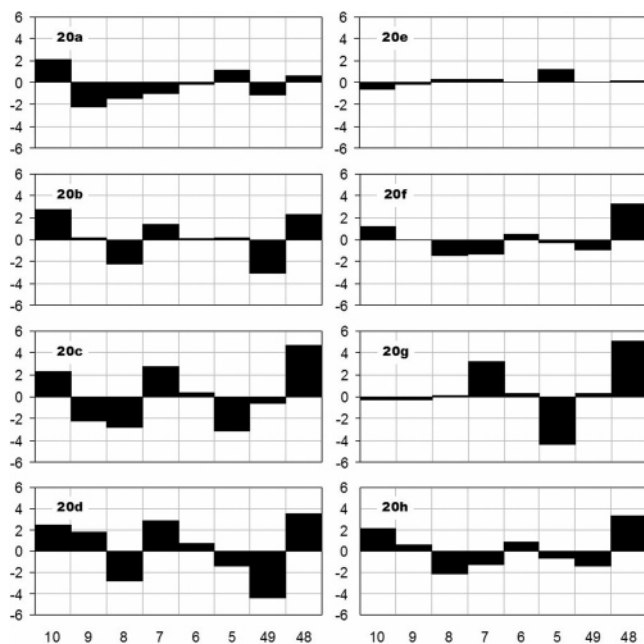


Figure 21. Difference between adjusted carbon chemical shifts of oasomycin B (**21b**) and those of compounds **20a–h** (100 MHz, ppm, DMSO-*d*₆).

Comparison of carbon (black bars) and proton (violet bars) cs of the synthetic models **27–31** with their ritterazine M counterparts led to the unequivocally revised structure of this intriguing marine dimeric steroid as **26b**.

3.3. Extension of the Method: Universal NMR Database in Chiral Solvents

As a useful extension to this kind of analysis, the UDB method was eventually implemented in chiral deuterated solvents.^{96–98} The solvent of choice was deuterated *N*, α -dimethylbenzylamine (DMBA), available in both pure enantiomeric forms. The NMR profiles of the eight **20'a–h** diastereoisomers (Table 14) in both (*R*)- and (*S*)-DMBA are displayed in Figure 24 by histogram plots.

The advantage gained by performing a UDB analysis in chiral solvents is the unique possibility to assign both the relative and the absolute configurations of a given stereo-cluster at the same time, which is like catching two birds with one stone. To prove the feasibility of such an extended approach, first the relative configuration of the oasomycin A (**21a**) C5–C10 stereo-cluster was reassigned in a 9.1% v/v mixture of (*R*)-DMBA-*d*₁₃/DMSO-*d*₆. Following the same rules and procedures established in achiral solvents, the analysis pointed to the same relative configuration previously found in DMSO-*d*₆ (Figure 25).

Then, by exploiting the $\Delta\delta$ values between (*R*)- and (*S*)-DMBA cs measured for each enantiopure diastereoisomer **20'a–h**, the feasibility of the determination of the absolute configuration was proved (Figure 26). Indeed, the absolute configurations at the stereocenters within C5–C10⁹⁶ and C21–C38⁹⁷ moieties of oasomycin A were assigned. In Figure 27 are comparatively reported the chemical shift differences ($\delta_R - \delta_S$) observed for **20'e** (violet bars) and oasomycin A (black bars) in a 9.1% v/v mixture of DMBA-*d*₁₃/DMSO-*d*₆ [(*R*)- and (*S*)-DMBA were alternatively used]. Figure 27 shows that both compounds give rise to the same pattern, allowing the assignment of the absolute configuration of the stereocenters belonging to the C5–C10 segment of

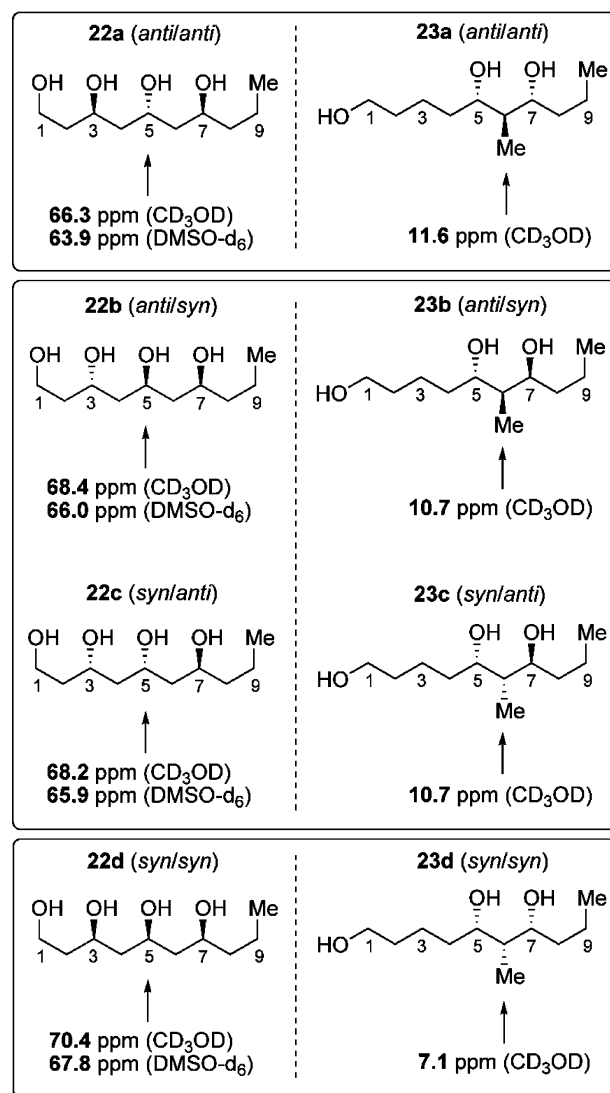
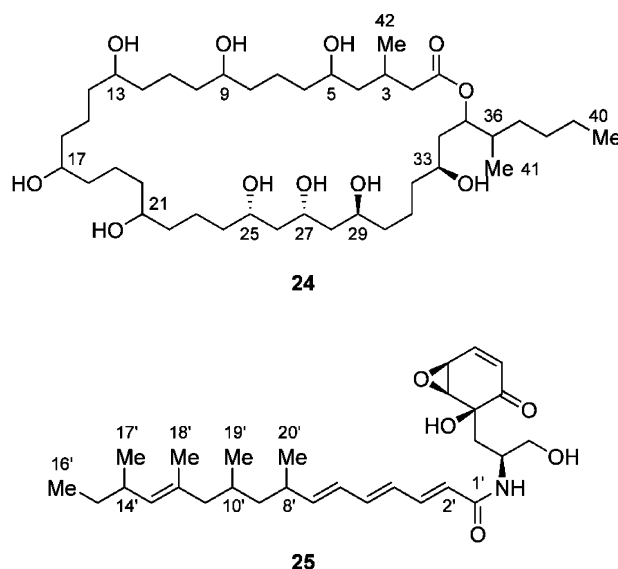


Figure 22. Effect of relative configuration on the chemical shift of the central carbon in 1,3,5-triol and 1,3-diol-2-methyl systems.

Chart 6



oasomycin A as those of compound **20'e**. After this successful case, other NMR databases in chiral solvents soon followed.⁹⁹

Chart 7

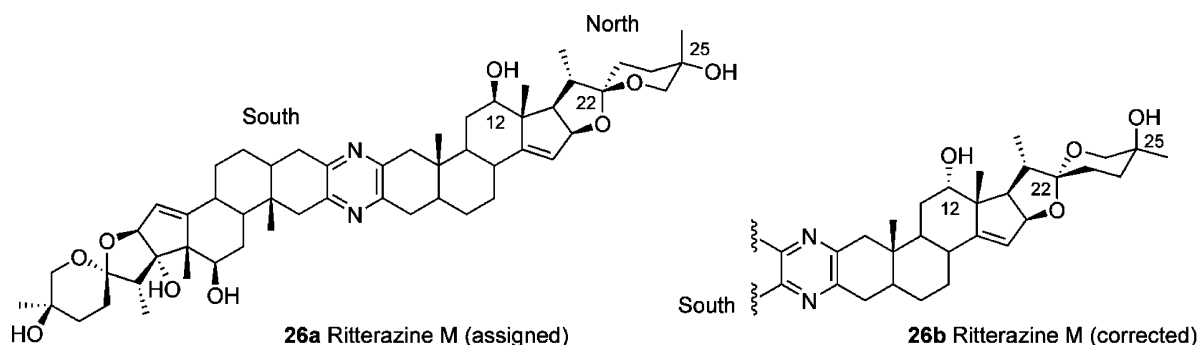
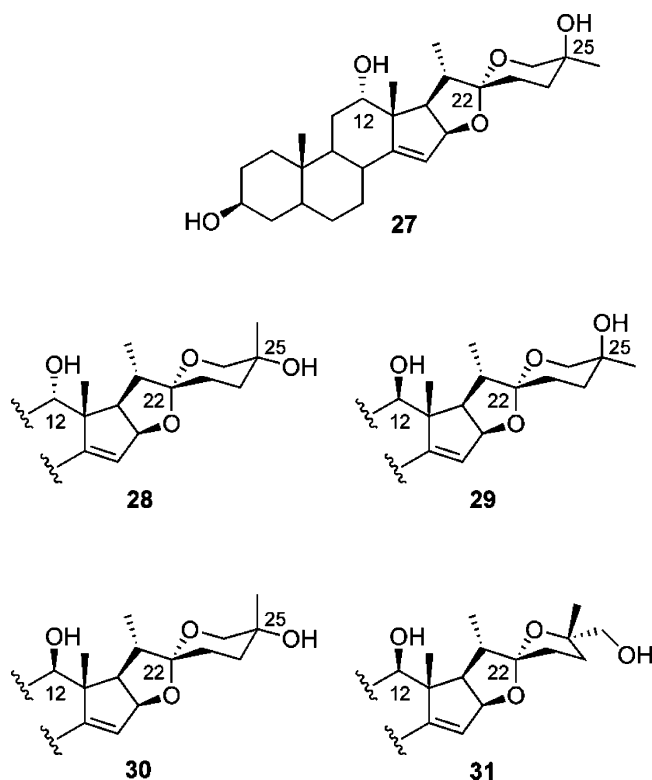


Chart 8



However, the most common NMR methods for the assignment of absolute configuration are, by far, those based on the use of chiral derivatizing reagents, the legacy of the original Mosher work¹⁰⁰ and the subject of a recent excellent review by Riguera and co-workers.¹ Chiral lanthanide shift reagents may offer a valid alternative.¹⁰¹

3.4. Application of the "Extended" UDB Method: Mycolactones and Tetrafibricin

Two successful applications of combined UDB analyses, in both achiral and chiral solvents, are represented by the full stereochemical elucidation of mycolactones **32a,b**¹⁰² and tetrafibricin **33**.⁸⁹

The case of mycolactones can be instructive, as the self-contained box principle was claimed to be applicable for the C16–C19 and C12'–C15' stereoclusters (simplified as **34** and **35**, respectively, in Figure 28), but not for the two C5–C6 and C11–C12 stereopairs, due to the difficulty of selecting appropriate models. Hence, two new NMR databases were first prepared, corresponding to the general structures **34** (studied in achiral solvent)^{102a} and **35** (studied in both achiral and chiral solvents)^{102b} (Figure 28), allowing

stereoassignments within the northern and southern side chains.

The relative configurations at C5, C6, C11, and C12 stereocenters had to be addressed by preparing the full diastereomeric ensemble of C1–C25 synthetic models and their NMR study in achiral and chiral solvents. By crossing the information gathered by this last UDB analysis with the outcome of Mosher's esters analysis of the core structure, all stereocenters of mycolactones A and B could be finally assigned.

3.5. UDB Scope and Limitation: Altromycin B and 2'-Substituted Taxanes

To date, there have been only two papers highlighting possible limitations in the applicability of the UDB method. A first case has to do with a stereoassignment in the northwestern quadrant of altromycin B **36**¹⁰³ (Figure 29).

The authors claimed that no conclusive results could be obtained by simple application of the UDB strategy if the NMR database was built from the two epimeric model compounds **37** and **38**. Table 15 and Figure 30 show the details of this comparison.

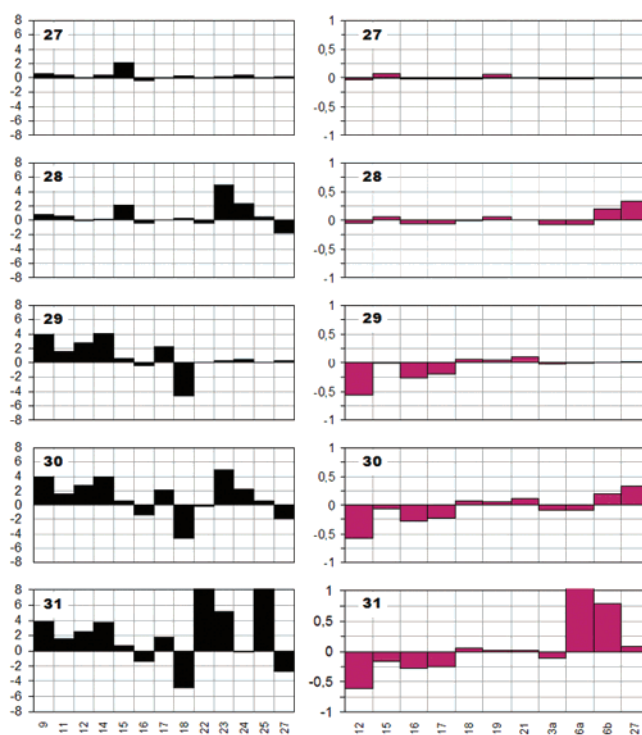
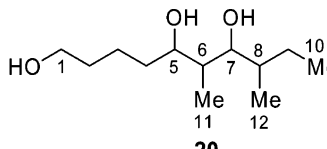


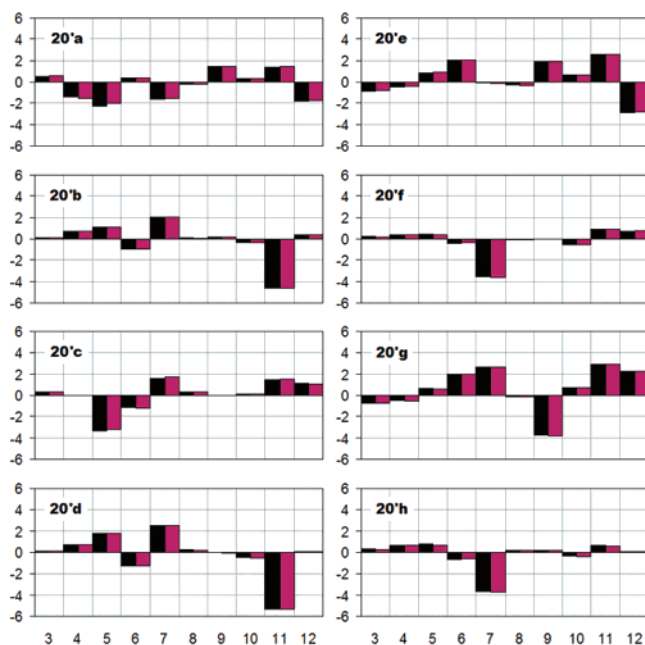
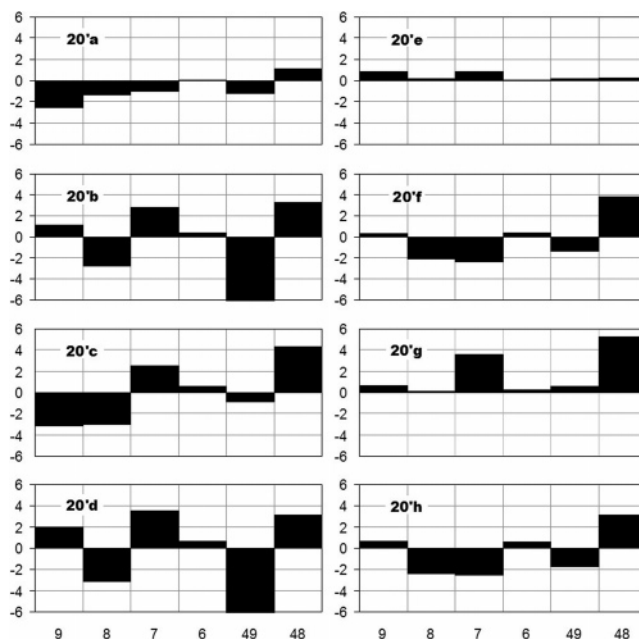
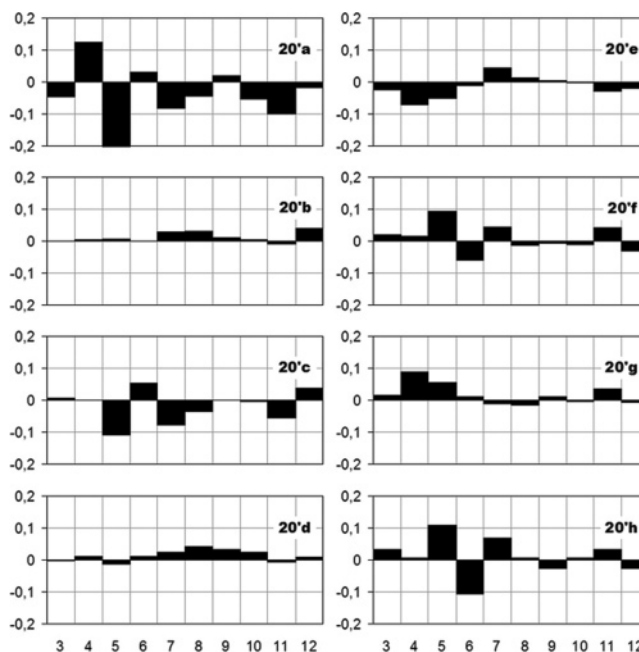
Figure 23. Differences in carbon (black bars) and proton (violet bars) chemical shifts of ritterazine M and compounds **27**–**31**.

Table 14. General Structure and Absolute Configurations of the Eight Diastereoisomers 20a–h


| | C5 | C6 | C7 | C8 |
|-------------|----------|----------|----------|----------|
| 20'a | <i>S</i> | <i>R</i> | <i>S</i> | <i>R</i> |
| 20'b | <i>S</i> | <i>R</i> | <i>R</i> | <i>S</i> |
| 20'c | <i>S</i> | <i>R</i> | <i>S</i> | <i>S</i> |
| 20'd | <i>S</i> | <i>R</i> | <i>R</i> | <i>R</i> |
| 20'e | <i>S</i> | <i>S</i> | <i>R</i> | <i>S</i> |
| 20'f | <i>R</i> | <i>R</i> | <i>R</i> | <i>S</i> |
| 20'g | <i>R</i> | <i>R</i> | <i>S</i> | <i>S</i> |
| 20'h | <i>R</i> | <i>R</i> | <i>R</i> | <i>R</i> |

The lesson to be learned is that, evidently, the method is sensitive to the nature of the models chosen to represent the “real” structure. One would like to faithfully reproduce all stereoelectronic and conformational properties of the real system by using tailored models, but this comes at a price. For selected systems, this may even translate into the synthesis of models so close to the stereo-undefined molecule that the cost/benefit ratio becomes unfavorable.

Provisionally, one would conclude that the method tends to be particularly handy when dealing with a chain (or

**Figure 24.** Difference in carbon chemical shifts between the average and the values for **20'a–h** (100 MHz): black bar, (*R*)-DMBA; violet bar, (*S*)-DMBA.**Figure 25.** Difference between adjusted carbon chemical shifts of oasomycin A and those for **20'a–h** [$\Delta\delta = \delta_{20'a-h} - \delta_{\text{oasomycin A}}$, 100 MHz, (*R*)-DMBA-*d*₁₃/DMSO-*d*₆ (9.1% v/v)].**Figure 26.** Difference between (*R*)- and (*S*)-DMBA carbon chemical shifts of compounds **20'a–h** (100 MHz).

unstrained macrocycle) hosting an array of two to four stereogenic centers, even better if the chain is not intimately connected to other functionalities of the molecule. On the other hand, compact, polycyclic, functionally dense natural products appear to be much harder to manage. However, this may well change as the collective experience and knowledge in this specific area advance.

Difficulties were also encountered upon the application of UDB analysis on side chains of 2'-alkylated taxanes, in the attempt to address their relative configuration at the C2'–C3' stereopair.⁷⁷

In this case, side-chain model methyl esters **39** and **40**^{77b} (Chart 10) failed to reproduce the NMR properties of the epimeric 2'-methyl taxanes **41** and **42** so that it was

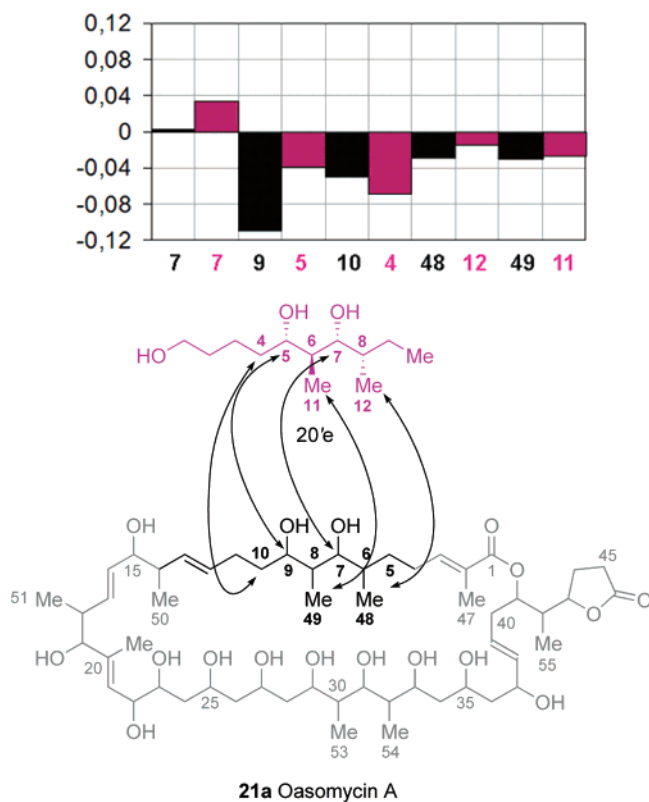


Figure 27. Comparative UDB analysis of the chemical shift differences ($\delta_R - \delta_S$) observed for **20'e** (violet bars and structure) and oasomycin A (black bars and structure) in a 9.1% v/v mixture of DMBA- d_{13} /DMSO- d_6 [(*R*)- and (*S*)-DMBA were alternatively used]. Arrows connect homologous carbons in reference structure (**20'e**) and in compound to be assigned (**21a**).

impossible to unambiguously reach a configurational assignment (Figure 31).

Notably, a satisfactory NMR stereodifferentiation within each (diastereomeric) pair of the 2'-alkyltaxanes' collection was not easily achieved, even using 2'-methyltaxanes as elements for the NMR database.

The authors envisaged the reason of this failure in the absence of conformational information in the classical UDB approach.^{77a} To overcome the problem and to achieve a suitable diastereomeric differentiation in the collection of differently 2'-substituted taxanes (**43a/b**–**47a/b** in Table 16), an improved version of UDB analysis was proposed.

The authors considered both 2'-epimeric taxanes **41** and **42** as constitutive elements of the database and hypothesized that the *syn* diastereoisomer of database element and the *syn* diastereoisomer of unassigned compound were homoconformers. The same hypothesis was assumed for *anti* diastereoisomers as well. For each carbon a correcting factor was computed as the difference of the mean value of *syn/anti* diastereoisomers of unknown compound and the mean value of *syn/anti* diastereoisomers of database elements. In this way, the effect of configuration and conformation on the cs value of each carbon was averaged. The adjusted cs value of the unknown compound was obtained as the difference between the experimental values and the aforementioned correcting factors. With these data in hand, the classical UDB analysis was performed separately on the complete set of homologues taxanes, which were easily differentiated to allow for the stereochemical assignment (Figure 32).

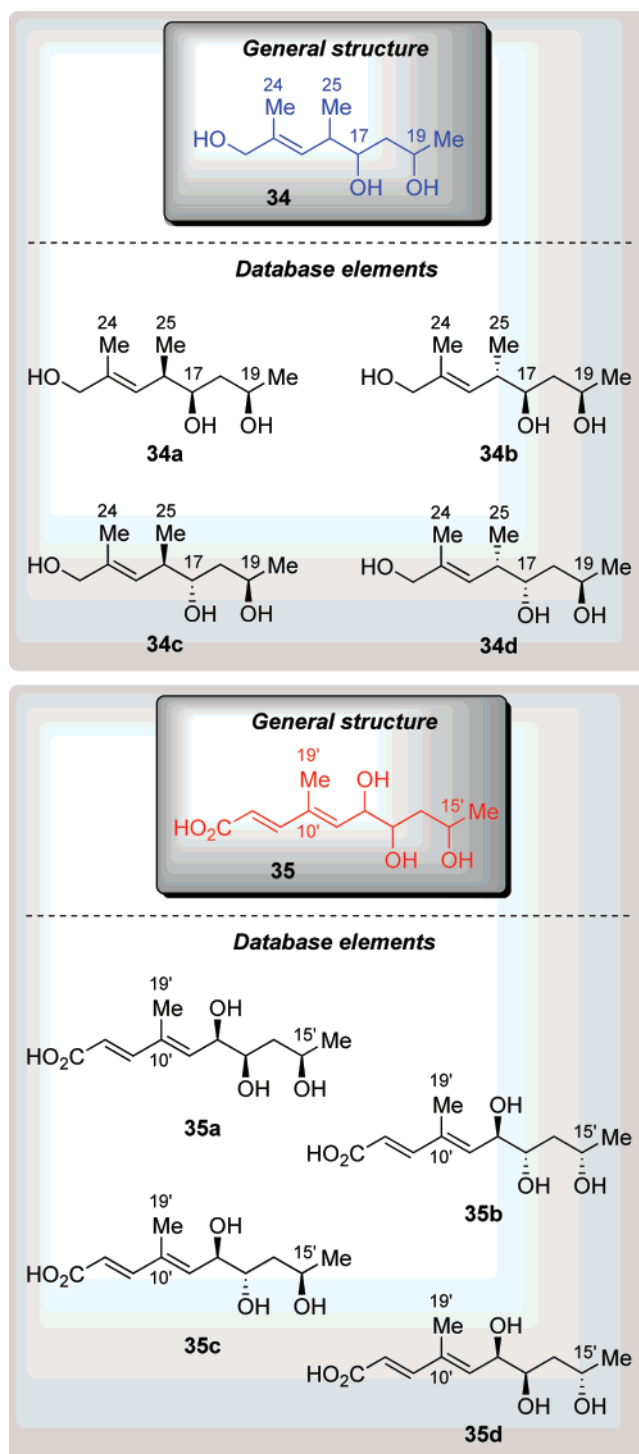


Figure 28. Two independent stereoclusters (**34**, **35**) of mycolactones A and B (**32a**, **32b**) along with the employed database elements (**34a**–**d** and **35a**–**d**).

The hypothesis of a homoconformational relationship between the same diastereoisomers of database elements and unassigned compounds is a necessary requirement of this modified UDB approach. It was experimentally tested using the *J*-based configurational analysis which, at the same time, assigned the major rotamer of each diastereoisomer and confirmed the UDB configurational analysis. When the homoconformational relationship is missing, as in the case of heteroconformers of 2'-tertbutyl taxanes, the modified UDB approach also failed.

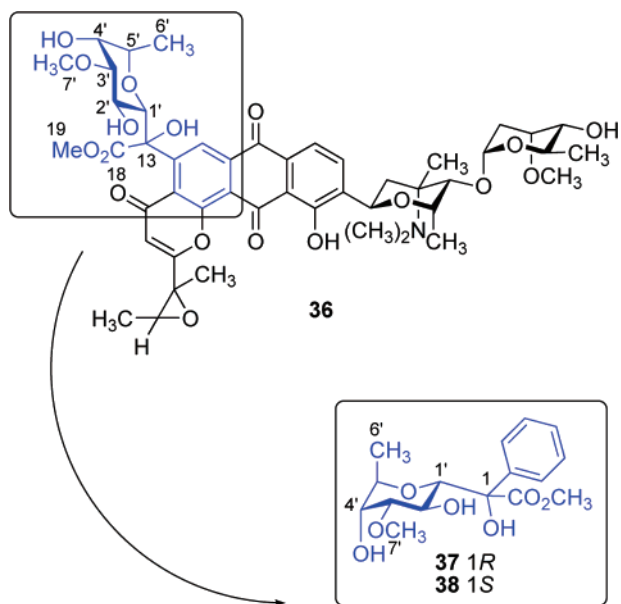


Figure 29. Structures of altromycin B (36) and of both C1-epimers (37 and 38) of its northwestern quadrant.

Table 15. Comparison of ^{13}C Chemical Shift Values of Altromycin B with Those of the Two Models 37 and 38

| | Altromycin B | 37 | 38 |
|--------------|--------------|--------|--------|
| δ C13 | 81.16 | 79.96 | 78.56 |
| δ C18 | 170.80 | 173.68 | 173.27 |
| δ C19 | 52.85 | 53.40 | 53.16 |
| δ C1' | 73.88 | 77.05 | 75.59 |
| δ C2' | 68.18 | 67.39 | 67.09 |
| δ C3' | 80.43 | 80.84 | 81.61 |
| δ C4' | 69.15 | 69.16 | 69.85 |
| δ C5' | 74.02 | 73.48 | 73.43 |
| δ C6' | 14.29 | 15.14 | 14.54 |
| δ C7' | 58.14 | 58.12 | 58.10 |

Even though a major limitation of this modified UDB analysis is the need to have all diastereoisomers of unas-

Chart 9

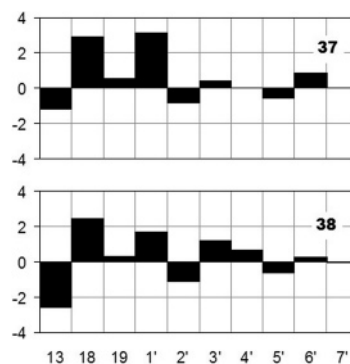
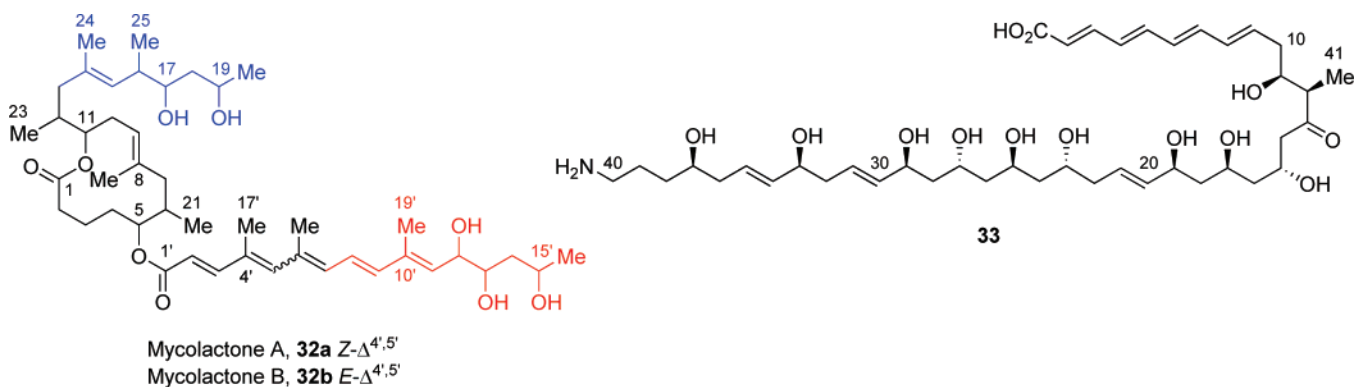


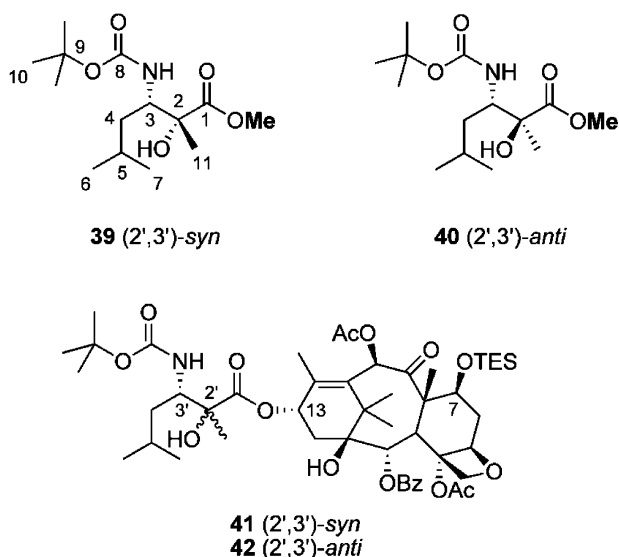
Figure 30. Graphical representation of the differences in ^{13}C NMR shift values between altromycin B and the two models 37 and 38 (merged with Table 13).

signed compounds, making it unsuitable for natural products stereochemical analysis, this modification may be the most promising method to assign large collections of similar compounds, such as those afforded by a combichem synthetic approach.

4. Quantum Mechanical Calculation of NMR Properties in the Configurational Assignment of Organic Molecules

In structure elucidation, a learned analysis of NMR spectra of a new organic compound drives to the correct solution through the ability of the researcher in finding correlations and analogies between the new spectra and her/his baggage of accumulated experience and literature data. To facilitate the process, a number of empirical methods for obtaining the prediction of ^1H and ^{13}C chemical shift values of organic molecules have been devised; some of them are based on additivity rules, and, usually, a dedicated software is employed for faster predictions.^{104,105} More recently, the growing number of ^1H and ^{13}C NMR data of natural and synthetic organic molecules has allowed the compilation of various NMR databases, which in turn have been exploited by artificial neural network technologies¹⁰⁶ or have been rendered available to the community through the Internet.¹⁰⁷ It has to be mentioned that NMR databases have been used not only for the characterization of the planar structure but also for the assignment of the configuration, as is documented in section 3 (and references cited therein) of this review. Besides database approaches, computational chemistry is also contributing to the field of organic spectroscopy. In the past decade we have witnessed an amazing burst in computational power, along with a notable progress in the development of QM methods of chemical interest. This has opened new

Chart 10



avenues in the area of prediction of molecular properties based on first principles. Recent examples include, but are not limited to, the reproduction of ORD and/or CD spectra, which proved to be particularly useful in the configurational assignment of some organic molecules.^{108–110}

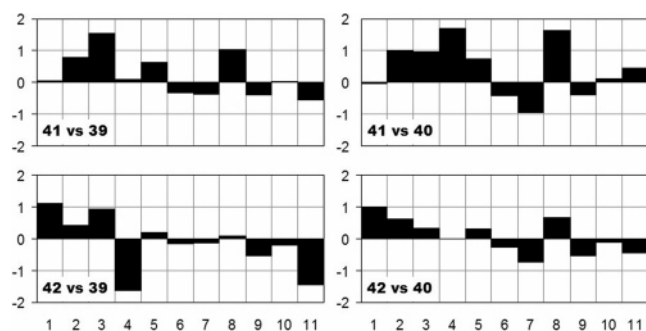
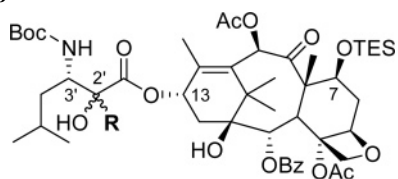


Figure 31. Differences in carbon chemical shifts between both 2'-epimers of 2'-methyltaxanes (**41** and **42**) and database elements **39** and **40**.

Table 16. General Structure of 2'-Alkylated Taxanes **43a/b–47a/b**



| <i>syn/anti</i> mixture | |
|-------------------------|-------|
| taxane | R |
| 43a/b | Et |
| 44a/b | i-Pr |
| 45a/b | t-Bu |
| 46a/b | Ph |
| 47a/b | Vinyl |

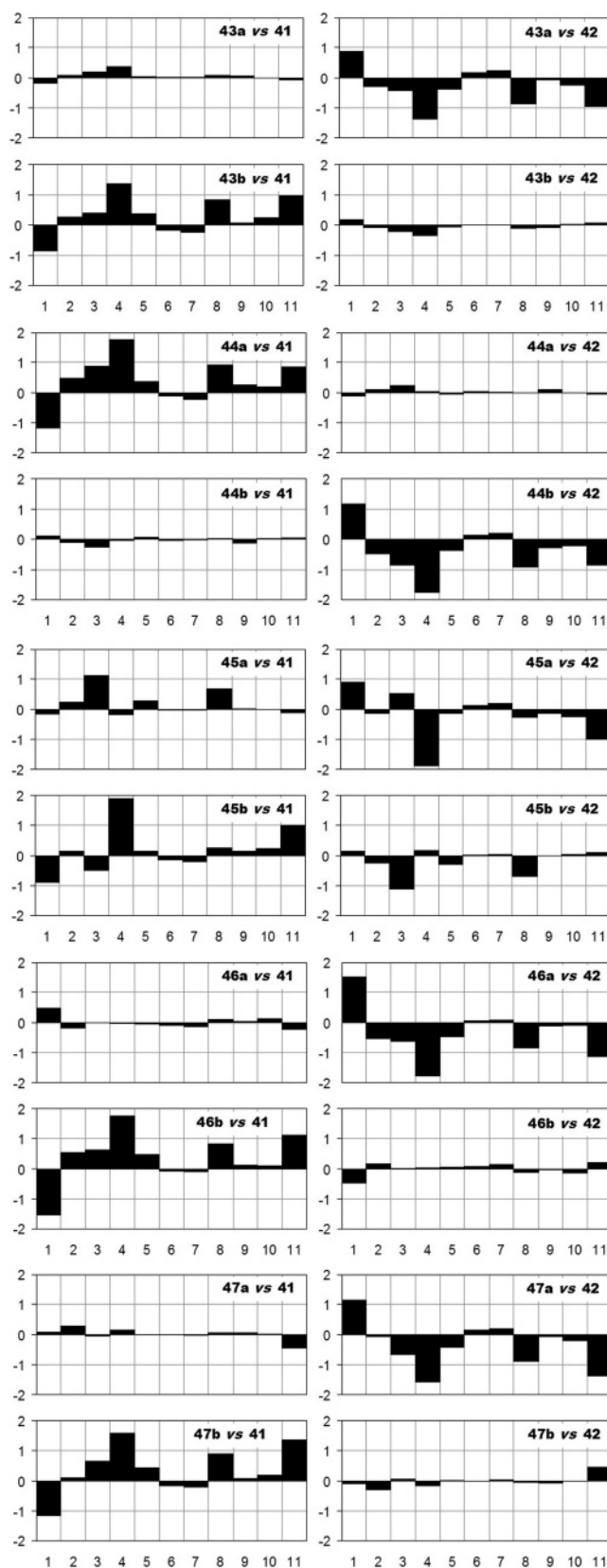
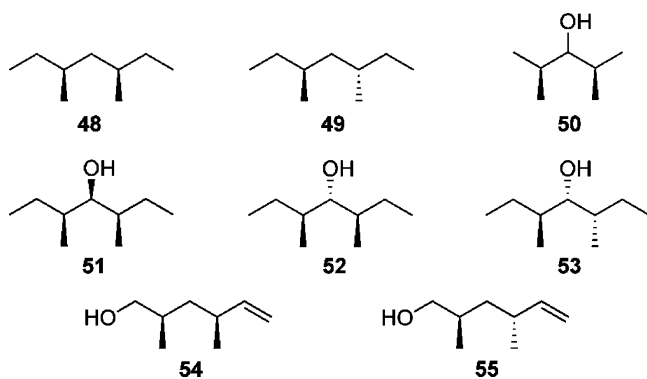


Figure 32. Differences in carbon chemical shifts between both 2'-epimers of all the 2'-alkylated taxanes (**43a/b–47a/b**) and database elements **41** and **42**.

4.1. Quantum Chemical Calculation of NMR Parameters

NMR chemical shift calculation by quantum chemistry methods represents a powerful strategy for the interpretation

Chart 11



of the experimental spectra^{111–116} Among the four most common approaches for calculating nuclear magnetic shielding tensors, namely, IGLO, LORG, GIAO, and CSGT, the GIAO (gauge including atomic orbital) method^{117,118} is probably the most widely used, and it has shown to provide results that are more accurate than those achieved by other approaches at the same basis set size.¹¹⁹ An important point concerns the level of theory to be applied for computing nuclear magnetic properties of organic molecules. In fact, it has been pointed out that Hartree–Fock calculations may not be accurate enough in cases when electron correlation effects become important, whereas Moeller–Plesset perturbation methods may provide much better results,¹¹⁹ even if at much higher computational cost. However, recent developments in new DFT functionals such as B3LYP^{120,121} have offered new opportunities at a more reasonable computational cost, and as a consequence such methods have often been preferred in the study of medium and large systems.¹²²

4.2. QM–NMR in Structural and Conformational Analysis

A literature search undeniably shows that QM calculations are about to become standard tools in the armory of organic chemistry laboratories. Accordingly, QM methods are gaining increasing popularity in the structural study of medium- to large-sized molecules, including natural products.

Structure validation protocols of new natural products by QM GIAO calculation of ¹³C NMR chemical shifts may supply a new way to sort out difficult cases in the elucidation process. Along these lines, this approach was tested on three examples of natural products having structures that had been revised, considering the fitting of the theoretical ¹³C cs of both correct and wrong structures with the experimental data.¹²³ For instance, the above methodology was exploited in the structural revision of halipeptins **9** and **10**,⁶⁶ in reassigning the structure of the fungal metabolite TAEMC161 as the phytotoxin viridiol,¹²⁴ and in the structural assignment of isomeric quinozalines.¹²⁵ More recently, theoretical predictions of ¹³C NMR chemical shifts have also been proposed as a tool to facilitate interpretation of polymers spectra.¹²⁶

The high accuracy in the prediction of ¹H and ¹³C chemical shifts and the satisfactory results achieved at a low demanding level of theory^{119,127} have also led researchers to focus on problems inherent to the determination of the three-dimensional structure of organic compounds. In particular, calculated ¹³C spectra have been used in the study of multiple conformer equilibria.^{128–130} In addition, a combined analysis of GIAO/DFT ¹H, ¹³C, and ¹⁵N shieldings has been proposed for the conformational analysis of amines,¹³¹ and three-

Chart 12

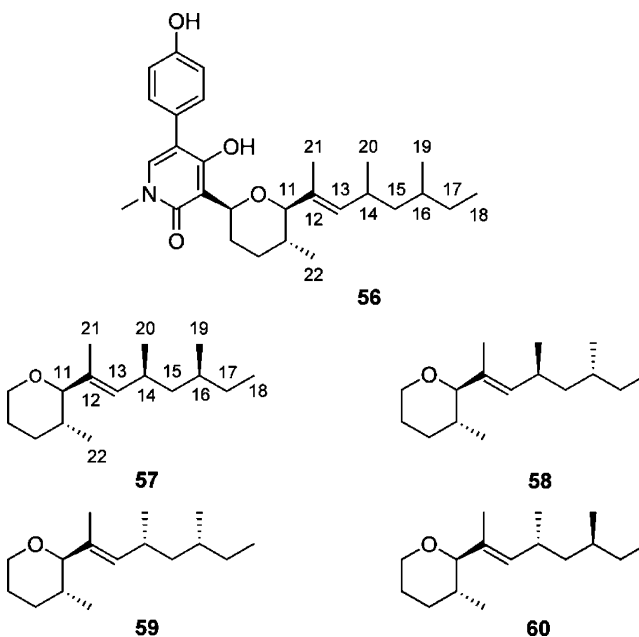


Table 17. Selected Experimental ¹³C NMR Chemical Shifts of the Side Chain of Sambutoxin **56** and Calculated (SOS-DFPT/IGLO) Shifts of the Corresponding Carbon Atoms in Model Compounds **57–60**^a

| | 56 | 57 | 58 | 59 | 60 |
|-------|-----------|---------------------|----------------------|---------------------|---------------------|
| n (%) | - | 9 (80) ^b | 12 (82) ^b | 7 (82) ^b | 8 (81) ^b |
| δ C17 | 28.9 | 31.3 | 28.3 | 31.5 | 27.7 |
| δ C19 | 19.5 | 18.4 | 19.4 | 18.1 | 19.8 |
| δ C20 | 20.6 | 21.3 | 20.9 | 21.0 | 20.5 |
| δ C21 | 11.6 | 13.1 | 12.8 | 11.4 | 11.6 |

^a Shifts were calculated for the number *n* of MM3 conformers and Boltzmann averaged, covering the percentage of the conformer population given in parentheses. To account for systematic errors, the authors subtracted from the calculated values increments of 7.8 ppm for methylene groups and 5.7 ppm for methyl groups. ^b The total number of conformers for each of the stereoisomers **56–60** was around 150 using a cutoff of 30 kJ/mol in the conformational analysis. Nine conformers for **57**, 12 for **58**, 7 for **59**, and 8 for **60** granted a representation of at least 80% of the population in all diastereomers.

dimensional ¹³C cs surfaces have been calculated as a function of the φ, ψ, and χ dihedral angles of peptides^{132–134} and as a function of glycosidic bond φ,ψ dihedral angles in oligosaccharide and glycopeptide model compounds.¹³⁵ Moreover, coupling constant calculations in the conformational analysis of open-chain organic compounds were first proposed in 1997, using molecular mechanics (MM3) for geometry optimization and a density functional (SOS-DFPT/IGLO) method for computing NMR parameters.¹³⁶

However, the most challenging task in the specific area of QM-calculated NMR parameters is the determination of the relative configuration, because it necessarily includes the assessment of the covalent structure of the new compound, and, in cases when multiple conformer equilibria are present, it also requires a preliminary conformational space sampling.

Chart 13

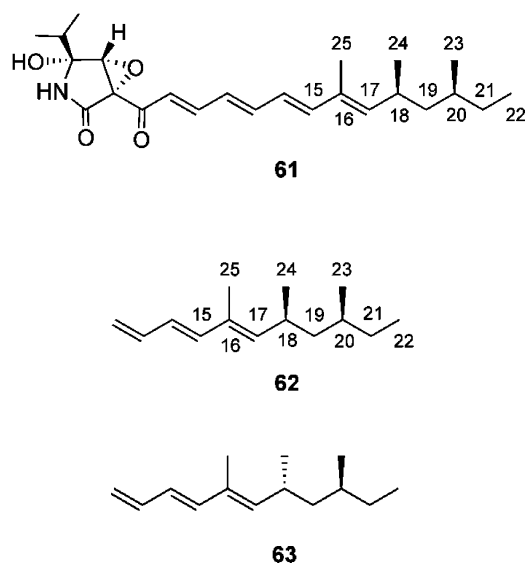


Table 18. Selected Experimental ^{13}C NMR Chemical Shifts of the Side Chain of Bradykinin Inhibitor **61 and Calculated (SOS-DFPT/IGLO) Shifts of the Corresponding Carbon Atoms in Model Compounds **62** and **63**^a**

| | 61 | 62 | 63 |
|--------------|-----------|-----------|-----------|
| n (%) | - | 20 (91) | 20 (88) |
| δ C21 | 30.4 | 30.9 | 29.3 |
| δ C23 | 19.2 | 19.2 | 19.6 |
| δ C24 | 21.4 | 20.4 | 19.7 |

^a Shifts were calculated for the number n of MM3 conformers and Boltzmann averaged. The choice of 20 of ca. 250 conformers (cutoff of 30 kJ/mol in the conformational search) for both stereoisomers **62** and **63** allowed coverage of the percent of the conformer population given in parentheses. To account for systematic errors, the authors subtracted from the calculated values increments of 7.8 ppm for methylene groups and 5.7 ppm for methyl groups.

4.3. Relative Configuration Assignments by Combined MM/QM Approaches

One of the first examples of stereostructural assignment of natural products by means of QM calculation regards the

prediction of the relative configuration of sambutoxin **56** and the bradykinin inhibitor L-755,897 **61**.¹³⁷ In their study, Hoffmann and co-workers preliminarily investigated the performance of a combination of molecular mechanics (MM3) and SOS-DFPT/IGLO calculation for the prediction of the ^{13}C chemical shifts of selected 1,3-dimethylated hydrocarbon segments **48**–**55** (Chart 11). Such compounds displayed a substitution pattern frequently seen in polyketide natural products and therefore could be conveniently employed as a benchmark for the chosen computational protocol.

Due to their mobility, a conformational search by means of the MCM3¹³⁸ method using the MM3* force field, as implemented in Macromodel 4.5,¹³⁹ was preliminarily run on these compounds, affording an MM3 energy based Boltzmann distribution for each of them. On this basis, the weighted averages of ^{13}C NMR chemical shifts were calculated. Even though the ^{13}C NMR chemical shifts were computed starting with MM3 geometries and energies, the observed agreement with the experimental data was fair, encouraging the authors to move on to the next task of addressing the relative configuration assignments of sambutoxin and L-755,897.

To this end, the possible stereoarrangements of the sambutoxin side chain were modeled by the four simplified compounds **57**–**60** depicted in Chart 12. Computed ^{13}C NMR chemical shifts were attained by MM3//SOS-DFPT/IGLO, as seen above.

Table 17 shows a comparison between theoretical and experimental values of key carbon atoms C17, C19, C20, and C21 of compounds **57**–**60**. On this ground, the authors proposed the relative configuration of sambutoxin as in **58**.

In analogy with the sambutoxin case, L-755,897 **61** was represented by two diastereomeric model compounds, **62** and **63** (Chart 13), considered to be suitable for describing the parent molecule side chain. As shown in Table 18, ^{13}C cs calculated values for the model **62** provided the best match, suggesting a *syn* relative configuration for C18 and C20 stereocenters of L-755,897.

4.4. Conformational and Configurational Analysis via ^{13}C NMR GIAO Chemical Shifts Prediction on MM Geometries

Contemporaneously with the paper of Hoffmann and co-workers described above, Forsyth and Sebag presented an approach based on the calculation of ^{13}C chemical shifts using GIAO theory with a small basis set and with geometries obtained from computationally inexpensive molecular me-

Table 19. Experimental and Predicted ^{13}C Chemical Shifts for (*E*)- and (*Z*)-2-Butenes

| compound | carbon | B3LYP/3-21G(X,6-31+G*)//MM3 | | B3LYP/6-31G(d)//B3LYP/6-31G(d) | | expt |
|-----------------------|--------|-------------------------------|----------------------|--------------------------------|----------------------|-------|
| | | δ_{preds} , ppm | $\Delta\delta$, ppm | δ_{preds} , ppm | $\Delta\delta$, ppm | |
| (<i>E</i>)-2-butene | C1 | 19.4 | 2.6 | 18.7 | 1.9 | 16.8 |
| | C2 | 128.9 | 3.5 | 128.2 | 2.8 | 125.4 |
| (<i>Z</i>)-2-butene | C1 | 12.9 | 1.5 | 12.5 | 1.1 | 11.4 |
| | C2 | 126.9 | 2.7 | 126.8 | 2.6 | 124.2 |

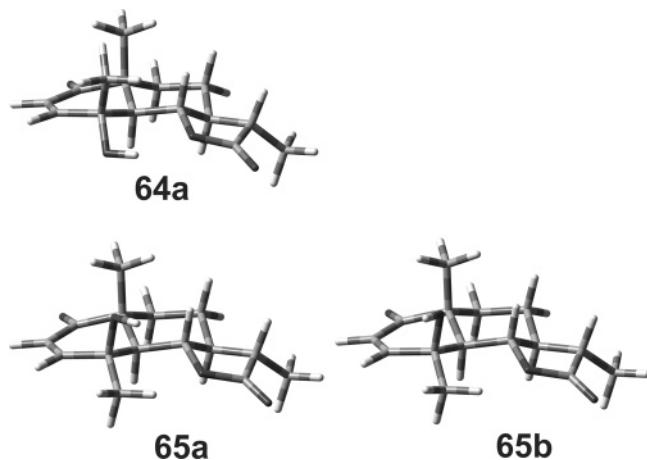


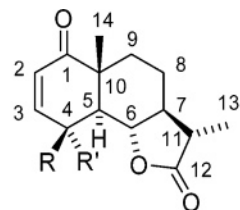
Figure 33. MM3-predicted geometries for the most stable conformers of **64** and **65** (adapted from ref 13).

chanics methods.¹¹⁵ They suggested that B3LYP and HF GIAO isotropic shielding results based on MMX and MM3 geometries had to be empirically scaled to obtain a satisfactory agreement with experimental values. In particular, the scaled GIAO B3LYP/3-21G(X,6-31+G*)/MM3 shieldings adequately accounted (rms error ~ 3 ppm) for the ^{13}C shifts of carbon nuclei that occur in a variety of common functional groups containing C, H, O, and N atoms and in simple alkyl groups. It is noteworthy that, even if the experimental data were obtained in a variety of solvents, the above-mentioned theory level offered a fair agreement with the experimental.¹¹⁵ It is not unusual for chemical shifts to differ by several parts per million between the gas phase and solution or to differ by 1–2 ppm in different solutions. To limit complications arising from these deviations, the authors proposed to empirically scale the calculated shieldings.

Because in the literature many conformational and configurational effects are inferred from γ -substituent effects on ^{13}C chemical shifts,¹⁴⁰ Forsyth and Sebag investigated the ability of their proposed QM/MM method in assigning the configuration of (*E*)- and (*Z*)-2-butenes, of axial and equatorial methylcyclohexanes, of *exo*- and *endo*-2-norbornanols, and of vulgarin **64** and epivulgarin **65**. Three criteria were proposed to judge the quality in the reproduction of experimental ^{13}C chemical shift values, that is, (a) the individual deviations, $\Delta\delta$, between experimental and predicted ($\delta_{\text{C}} - \delta_{\text{pred}}$) ^{13}C chemical shifts; (b) the mean absolute deviation, $|\Delta\delta|_{\text{av}}$; and (c) the rms error from a linear regression analysis of the correlation between δ_{C} and δ_{pred} .

In the simple case of (*E*)- and (*Z*)-2-butenes, calculation at the B3LYP/3-21G(X,6-31+G*)/MM3 level correctly reproduced the ^{13}C chemical shift trends (Table 19). In particular, both the methyl and alkene carbons of (*Z*)-2-butene were correctly predicted to be more shielded than the corresponding nuclei in (*E*)-2-butene, as expected on the basis of the well-documented empirical rules regarding the γ -substituent effect.¹⁴⁰ The authors showed that if the *Z* isomer were the only available isomer, it would be readily identified as such by comparison of the measured δ_{C} of 11.4 and 124.2 ppm with the δ_{pred} of 12.9 and 126.9 ppm (*Z* isomer) versus δ_{pred} of 19.4 and 128.9 (*E* isomer). However, if only the *E* isomer were available, the wrong identification would be made as suggested by a higher $\Delta\delta_{\text{av}}$ of 3.0 ppm for the correct match (*E* isomer) with respect to the lower $\Delta\delta_{\text{av}}$ of 2.7 ppm for the incorrect one (*Z* isomer). When the same tests were run at the B3LYP/6-31G(d)/B3LYP/

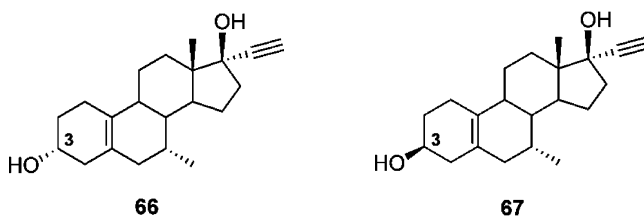
Table 20. Experimental ^{13}C NMR Chemical Shifts for **64** and **65** and Predicted ^{13}C Chemical Shifts for Conformers **64a**, **65a**, and **65b**



64 R=CH₃ R'=OH
65 R=OH R'=CH₃

| | 64a , δ_{pred} | 64 , δ_{C} | (65a + 65b)/2 δ_{pred} | 65 , δ_{C} |
|-----------------------|-------------------------------------|---------------------------------|--|---------------------------------|
| δ_{C1} | 200.5 | 201.6 | 203.8 | 203.1 |
| δ_{C2} | 130.5 | 125.7 | 131.3 | 125.3 |
| δ_{C3} | 156.0 | 151.7 | 152.1 | 150.2 |
| δ_{C4} | 70.5 | 70.1 | 67.8 | 68.2 |
| δ_{C5} | 55.7 | 54.7 | 52.1 | 51.0 |
| δ_{C6} | 79.5 | 79.6 | 78.2 | 79.2 |
| δ_{C7} | 53.0 | 52.5 | 53.4 | 52.3 |
| δ_{C8} | 24.9 | 22.7 | 25.1 | 22.8 |
| δ_{C9} | 35.7 | 34.3 | 34.3 | 32.5 |
| δ_{C10} | 45.6 | 46.2 | 47.0 | 45.9 |
| δ_{C11} | 39.5 | 40.6 | 39.8 | 40.1 |
| δ_{C12} | 178.6 | 178.1 | 179.3 | 179.0 |
| δ_{C13} | 14.3 | 12.4 | 14.4 | 12.5 |
| δ_{C14} | 21.1 | 19.7 | 22.9 | 20.6 |
| δ_{C15} | 24.1 | 23.8 | 30.6 | 31.7 |

Chart 14

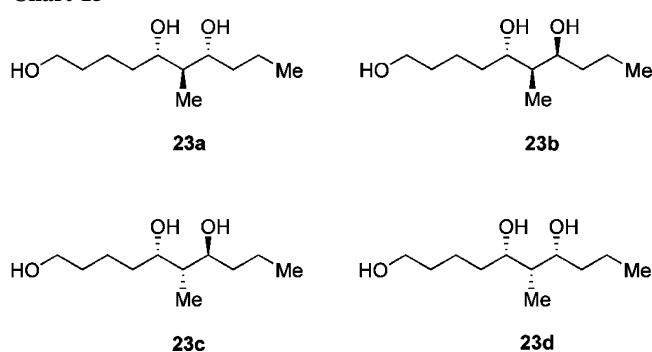


6-31G(d) level, $\Delta\delta_{\text{av}}$ values for both *E* and *Z* isomers always pointed to the right set of experimental data (Table 19), raising the question whether empirical geometries are sufficiently refined for the task.

The same rationale was followed for assigning the configuration of axial and equatorial methylcyclohexanes *exo*- and *endo*-2-norbornanols, again predicting the ^{13}C chemical shifts values by calculation at the B3LYP/3-21G(X,6-31+G*) level on MM3 geometries.¹¹⁵

Table 21. Comparison of the Different Methods for Prediction of ^1H and ^{13}C Chemical Shifts by RMS Errors (in Parts per Million)

| Compound | HF/ | | B3LYP/ | | B3PW91/ | | |
|-----------|---|------------|----------|------------|----------|------------|------|
| | 6-31G(d) | 6-31G(d,p) | 6-31G(d) | 6-31G(d,p) | 6-31G(d) | 6-31G(d,p) | |
| 66 | All ^{13}C | 5.3 | 4.6 | 3.2 | 3.1 | 2.6 | 2.5 |
| | sp^2 and sp^3 ^{13}C | 4.9 | 4.2 | 1.7 | 2.3 | 1.5 | 2.0 |
| | All ^1H | 0.29 | 0.39 | 0.26 | 0.26 | 0.25 | 0.25 |
| | sp^3 ^1H | 0.30 | 0.40 | 0.19 | 0.20 | 0.19 | 0.20 |
| 67 | All ^{13}C | 5.3 | 4.6 | 3.2 | 3.1 | 2.6 | 2.5 |
| | sp^2 and sp^3 ^{13}C | 4.9 | 4.3 | 1.7 | 2.3 | 1.5 | 2.0 |
| | All ^1H | 0.29 | 0.38 | 0.23 | 0.22 | 0.22 | 0.21 |
| | sp^3 ^1H | 0.30 | 0.39 | 0.15 | 0.16 | 0.16 | 0.15 |

Chart 15

Finally, the authors tested their method on the C4-epimeric sesquiterpenes vulgarin, **64**, and epivulgarin, **65**, the configurations of which were previously established through comparative NOE studies.^{141–143}

First of all, MM3 calculations indicated that **64** presented only one significantly populated conformer **64a**, whereas for **65** two hydroxyl rotamers, **65a** and **65b**, were found to be energetically very similar (Figure 33). In Table 20 are reported the δ_{pred} for **64a** and for the average of **65a** and **65b**, along with the experimental ^{13}C chemical shift values for the natural products **64** and **65**. Also in this case the trend of the calculated values is in good accordance with the experimental trend of **64** and **65**, despite the MM3-based averaging of **65a** and **65b**. In detail, the $|\Delta\delta|_{\text{av}}$ value regarding the matching of the δ_{C} (**64**) with δ_{pred} (**64a**) is 1.4 ppm, whereas the same parameter is higher than 2.2 ppm if the average of **65a** and **65b** is considered instead. In the same way, the $|\Delta\delta|_{\text{av}}$ value observed considering the matching of δ_{C} (**65**) with δ_{pred} (**65a** and **65b**) is 1.5 ppm, whereas the same figure is 2.2 ppm for the opposite scheme (δ_{C} of **65** compared with δ_{pred} of **64a**).

4.5. Stereochemical Analysis of the 3α - and 3β -Hydroxy Metabolites of Tibolone through NMR and Quantum Chemical Investigations

The stereochemical analysis of the 3α - and 3β -hydroxy metabolites (**66** and **67**, respectively, in Chart 14) of tibolone

Table 22. Sum of $|\Delta\delta|$ Values (Parts per Million) of Theoretical versus Experimental Chemical Shifts for Stereoisomers 23a–d^a

| | 23a calc. | 23b calc. | 23c calc. | 23d calc. |
|-----------------|------------|------------|-------------|------------|
| 23a exp. | 8.0 | 12.7 | 12.4 | 23.4 |
| 23b exp. | 15.1 | 9.9 | 18.5 | 26.5 |
| 23c exp. | 16.1 | 15.9 | 10.9 | 26.7 |
| 23d exp. | 20.0 | 17.3 | 18.0 | 6.8 |

^a In bold are reported the calculated values that are in good agreement with the experimental.

(the corresponding C3 ketone) through NMR and quantum chemical investigations is one of the first applications in which the GIAO method is tested for two organic compounds of biological interest.¹⁴⁴ In particular, Colombo et al. first determined the configuration at C3 of the 3α - and 3β -hydroxy metabolites of tibolone, a synthetic steroid that is widely used in hormone replacement therapy (HRT) for menopausal complaints, by extensive use of one- and two-dimensional ^1H and ^{13}C NMR spectroscopy combined with a conformational study performed at the B3LYP/6–31G(d) level.

Subsequently, to test the efficiency of GIAO methods in discriminating two different stereoisomers, a set of shielding tensors of the two molecules was computed using HF and DFT approaches; the 6-31G(d), and the 6-31G(d,p) basis sets were tested for the Hartree Fock method and for two different DFT functionals, namely, B3LYP and B3PW91. A comparison of the calculated NMR chemical shifts with the experimental values revealed that the density functional methods produced the best results for the reproduction of both ^1H and ^{13}C spectra, even though the errors for the predicted proton resonances are relatively higher considering the smaller spectral window of the proton with respect to the carbon (Table 21). It is noteworthy that a more comprehensive study regarding the performance of different

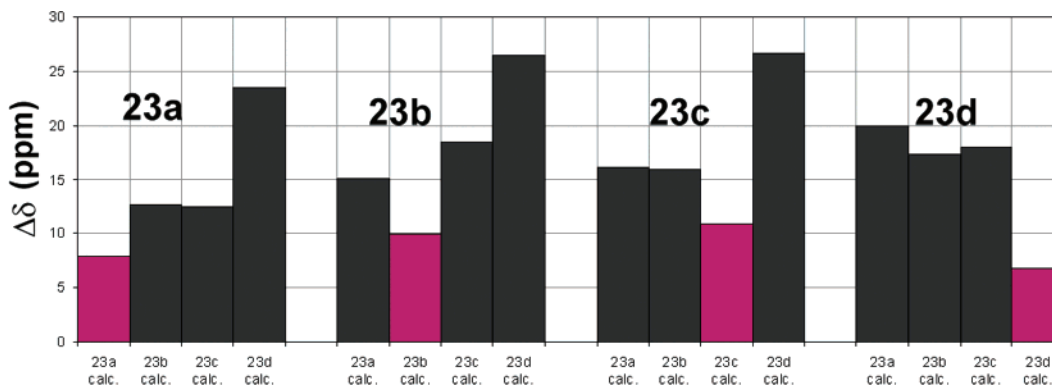


Figure 34. Sum of $|\Delta\delta|$ values (parts per million) of theoretical versus experimental chemical shifts for stereoisomers **23a–d**.

Table 23. Possible Staggered Rotamers for Each Relative Stereochemical Arrangement

| erythro | | |
|---------------------|------|---------------------|
| gauche ⁺ | anti | gauche ⁻ |
| | | |
| threo | | |
| gauche ⁺ | anti | gauche ⁻ |
| | | |

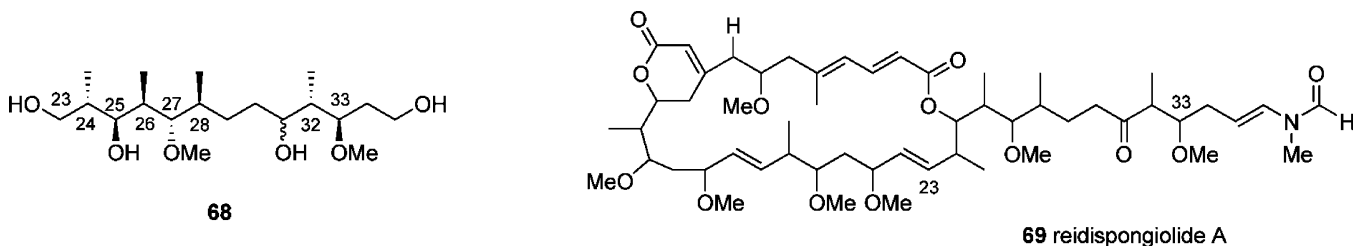
theory models and basis sets in the calculation of ^{13}C NMR chemical shifts of organic compounds has recently appeared in the literature.¹²⁷

4.6. Determination of the Relative Configuration of Flexible Organic Compounds through Boltzmann Weighted GIAO ^{13}C NMR Chemical Shift Calculations

The encouraging results obtained both by MM/QM hybrid approaches on flexible compounds, such as sambutoxin **56**, and by the full ab initio calculations, as in tibolone metabolites **66** and **67**, have propelled additional studies in this area. As a result, it has been possible to face both conformational and configurational problems by purely quantum mechanical methods. A general assumption is that only if the contributions of all significant conformers of a given flexible stereoisomer are taken in due account will its

physicochemical properties be correctly reproduced. Another key point is that the estimation of relative energies needs to be performed at a dependable and affordable theory level. In a recent study by Bifulco and co-workers, four sample diastereoisomeric compounds **23a–d** (Chart 15) were submitted to a protocol that was, according to the above considerations, specifically tailored to verify the quality of computed NMR properties in flexible systems.¹⁴⁵ The proposed protocol consists of four fundamental steps: (a) conformational search and a preliminary geometry optimization of all the significantly populated conformers of each stereoisomer (as defined below); (b) final geometry optimization of all the species at Hartree–Fock or post-HF level; (c) GIAO ^{13}C NMR calculations of all the so-obtained structures at HF or post-HF level; (d) comparison of the Boltzmann averaged ^{13}C cs calculated for each stereoisomer with those measured for the compound under examination. It has to be noted that while the conformational search (step a) may be performed by means of empirical, systematic, or statistical methods, it is during step b that the conformers generated in the previous step undergo the final geometry and energy optimization at QM level. In this pilot paper, the preliminary conformational search was performed by empirical force field molecular dynamics (CVFF force field, Discover module of InsightII, version 2000.2, Accelrys, San Diego, CA); subsequently, all of the conformers found were optimized at HF level using the 6-31G(d) basis set, and thermochemical calculations, in the harmonic approximation of the vibration modes, allowed the evaluation of the standard Gibbs free energy of the conformers at 298.15 K. By discarding all of the conformations higher in energy than a threshold of 10 kcal/mol from the most stable species, 10 major conformers were found for compound **23a**, 13 for **23b**, and 8 for **23c** and **23d**. Finally, GIAO ^{13}C cs calculations were performed at the HF/6-31G(d) level on each set of conformers relative to compounds **23a–d**. All of the calculations were carried out using the Gaussian 98W program package. For each stereoisomer, the ^{13}C NMR chemical shift of a given carbon atom was obtained as the

Chart 16



weighted average chemical shift value of the same atom in all of the conformers sampled by the initial conformational search. The cs averages of stereoisomers **23a–d**, obtained by applying a Boltzmann distribution using the relative standard free energies as weighting factors, were compared with the corresponding ^{13}C NMR data reported for **23a–d**.

Given the intrinsically small chemical shift differences among the four compounds and to facilitate a comprehensive analysis of the data, the experimental versus calculated chemical shift differences, in absolute value, were summed and are listed in Table 22 and reported as a histogram in Figure 34. A careful analysis shows that calculated chemical shift data fit unequivocally the corresponding experimental data. In particular, it is clear that the differences are small for stereochemically homogeneous pairs, whereas larger discrepancies are observed for the “wrong” matches. It is interesting that, even at a level of theory which, in these days, may be already considered primitive, calculation of ^{13}C chemical shifts has proven to be a powerful tool in the configurational analysis of flexible compounds, suggesting that, with increasing level of theory, the differences between calculated and experimental data will tend to zero, allowing determination of the relative configuration of unknown compounds with increasing levels of confidence.

4.7 Quantum Mechanical Calculations of NMR J -Coupling Values: Toward the Automatic Determination of Relative Configuration in Organic Compounds

Besides the reported application of GIAO-calculated ^{13}C NMR chemical shifts for the stereochemical analysis of molecular systems endowed with conformational mobility, the quantum mechanical calculation of spin–spin coupling constants may be considered as a new and interesting tool, due to the close connection of such parameters to both the conformation and the configuration of organic compounds.¹⁴⁶

As we have pointed out in section 2 (see ref 5 and references cited therein), the use of (experimental) heteronuclear J values in configurational assignments of organic compounds has lately been shown to have great potential, and, accordingly, it has been used to tackle a number of stereochemical problems. Nevertheless, although homonuclear $^3J_{\text{HH}}$ values are widely described in the literature and efficient empirical rules allow one to derive from them fairly accurate dihedral angles,^{2,3,22,23} the use of heteronuclear $^{2,3}J_{\text{HC}}$ couplings in the analysis of the relative configuration has been limited because of the difficulties arising from the need to make reliable judgments on the size (*large* or *small*) of a given value in the absence of the desirable wealth of literature data.

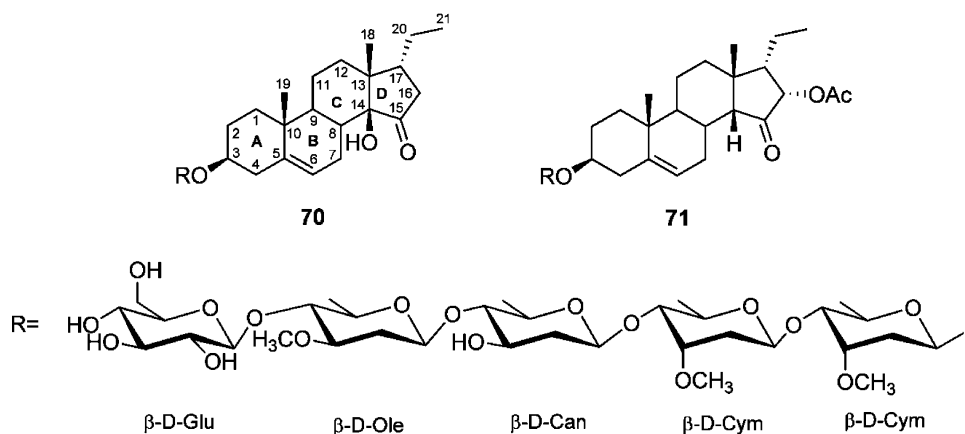
4.7.1. Quantum Mechanical Calculations of NMR J -Coupling Values: Relative Configuration Assignment of the C23–C33 Reidspongiolide Fragment

To address the above drawback, a recent advance in this field has been pursued by DFT calculation of the J -coupling values and subsequent comparison against the corresponding experimental counterparts.²⁴ The strategy is based on the calculation of homo- and heteronuclear coupling constant values for each of the six staggered rotamers (three for each relative stereochemical arrangement) in which any given two-carbon (chiral) fragment of a molecule can be ideally represented (see Table 23). In detail, each compound undergoes a full geometry optimization using the mPW1PW91

Table 24. Calculated Data Sets of J Values for the Various Conformational and Configurational Arrangements of **69** in Comparison with the Experimental Values

| | Calculated | | | | | | Exp |
|--|------------|------------|------------|------------|------|-------|------|
| | erythro | | | threo | | | |
| | g^+ | anti | g^- | g^+ | anti | g^- | |
| C32-C33 | | | | | | | |
| $^3J_{\text{H32-H33}}$ | 2.4 | 3.1 | 2.9 | 0.7 | 9.1 | 6.0 | 2.6 |
| $^2J_{\text{H32-C33}}$ | -4.7 | -1.5 | 0.9 | 0.4 | -3.4 | -3.5 | -5.4 |
| $^3J_{\text{H32-C34}}$ | 4.4 | 5.2 | 1.1 | 2.9 | 1.4 | 5.1 | 4.8 |
| $^3J_{\text{H33-C31}}$ | 1.9 | 1.0 | 6.1 | 3.7 | 0.8 | 5.6 | 0.5 |
| $^3J_{\text{H33-Me32}}$ | 4.8 | 7.5 | 3.6 | 3.7 | 3.1 | 1.0 | 4.4 |
| $\Sigma J_{\text{calc}}-J_{\text{exp}} $ | 3.1 | 8.5 | 16.7 | 13.5 | 13.5 | 14.1 | |
| C27-C28 | | | | | | | |
| $^3J_{\text{H27-H28}}$ | 3.2 | 8.6 | 3.4 | 2.4 | 9.0 | 3.5 | 8.9 |
| $^2J_{\text{H28-C27}}$ | 1.5 | -3.5 | -3.8 | 1.5 | -4.0 | -4.0 | -3.6 |
| $^3J_{\text{H28-CH26}}$ | 0.8 | 1.6 | 5.0 | 1.0 | 1.3 | 5.1 | 1.0 |
| $^3J_{\text{H27-CH29}}$ | 6.1 | 2.7 | 1.2 | 3.1 | 0.6 | 5.1 | 2.2 |
| $^3J_{\text{H27-Me28}}$ | 2.7 | 1.9 | 5.7 | 5.5 | 3.5 | 2.0 | 1.4 |
| $\Sigma J_{\text{calc}}-J_{\text{exp}} $ | 16.2 | 2.0 | 15.0 | 16.8 | 4.5 | 13.4 | |
| C26-C27 | | | | | | | |
| $^3J_{\text{H26-H27}}$ | 0.6 | 7.5 | 1.9 | 2.8 | 8.7 | 3.0 | 2.4 |
| $^2J_{\text{H26-C27}}$ | -5.8 | -3.1 | 0.9 | 0.7 | -4.2 | -5.0 | -1.5 |
| $^3J_{\text{H26-C28}}$ | 1.8 | 4.9 | 0.4 | 0.2 | 1.3 | 5.6 | 0.5 |
| $^3J_{\text{H27-C25}}$ | 5.4 | 0.3 | 5.0 | 2.7 | 5.9 | 4.6 | 6.7 |
| $^3J_{\text{H27-Me26}}$ | 3.2 | 5.4 | 3.3 | 6.0 | 3.4 | 1.9 | 3.1 |
| $\Sigma J_{\text{calc}}-J_{\text{exp}} $ | 8.8 | 19.8 | 4.9 | 9.8 | 10.9 | 12.5 | |
| C25-C26 | | | | | | | |
| $^3J_{\text{H25-H26}}$ | 2.6 | 8.6 | 3.4 | 3.6 | 8.4 | 9.6 | 1.2 |
| $^2J_{\text{H26-C25}}$ | 0.7 | -3.4 | -3.7 | 0.8 | -3.7 | -1.9 | -0.5 |
| $^3J_{\text{H26-C24}}$ | 0.9 | 0.8 | 4.5 | 0.7 | 0.7 | 3.8 | 0.5 |
| $^3J_{\text{H25-C27}}$ | 6.6 | 3.0 | 1.5 | 1.3 | 0.4 | 2.8 | 0.9 |
| $^3J_{\text{H25-Me26}}$ | 3.5 | 0.8 | 5.5 | 5.7 | 3.6 | 1.2 | 6.7 |
| $\Sigma J_{\text{calc}}-J_{\text{exp}} $ | 11.9 | 18.6 | 11.2 | 5.3 | 14.2 | 20.5 | |
| C24-C25 | | | | | | | |
| $^3J_{\text{H24-H25}}$ | 2.8 | 8.6 | 0.1 | 0.3 | 8.2 | 4.2 | 9.9 |
| $^2J_{\text{H24-C25}}$ | -4.2 | -3.7 | -0.9 | -0.6 | -3.0 | -3.8 | -2.4 |
| $^3J_{\text{H24-C26}}$ | 5.1 | 1.3 | 2.3 | 3.3 | 1.0 | 5.7 | 1.1 |
| $^3J_{\text{H25-C23}}$ | 1.0 | 3.4 | 4.1 | 7.5 | 0.8 | 6.2 | 3.3 |
| $^3J_{\text{H25-Me24}}$ | 4.6 | 1.2 | 6.2 | 3.0 | 3.5 | 1.8 | 1.4 |
| $\Sigma J_{\text{calc}}-J_{\text{exp}} $ | 18.4 | 3.1 | 18.1 | 19.4 | 7.0 | 15.0 | |

Chart 17



functional and the 6-31G(d) basis set. Then, on the obtained geometries, the calculation of the J couplings is performed using the same functional and the 6-31G(d,p) basis set, taking into account the contributions of the following interactions: Fermi contact (FC), paramagnetic spin-orbit (PSO), diamagnetic spin-orbit (DSO), and spin-dipole (SD).

Once the six data sets of J -coupling values are obtained, they can be compared to the experimental set, allowing one to draw a conclusion on the relative configuration of the examined 2-C molecular fragment. In particular, as we will see below, it is only one of the six calculated data sets that displays a satisfactory agreement with the experimental data set.

For large molecular systems, such as the C23–C33 reidispongiolid fragment **68** proposed by the authors,²⁴ it is suggested that, given the prohibitive computational requirement for a simultaneous consideration of all combinations of the possible conformations and configurations, the molecule be dissected into appropriately reduced subsystems prior to the J -coupling calculations.

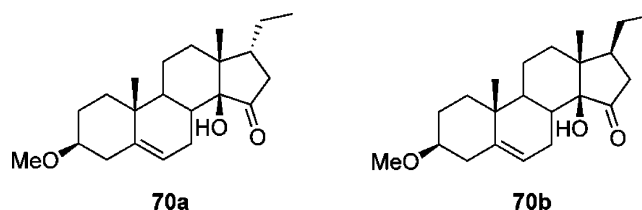
The side-chain **68** of the marine macrolide reidispongiolid A **69** depicted in Chart 16 obtained by chemical degradation of the parent natural product features seven stereogenic centers previously determined by combined degradative and synthetic studies.¹⁴⁷ Analysis of Table 24, in which are reported the experimental data sets of J values of **69** and all of the calculated coupling constants for the various conformational and configurational arrangements of each of the five 2-C fragments, shows an excellent agreement between calculated and experimental data for the most populated rotamers with correct configuration. On the contrary, in the wrong alignments calculated data match poorly with the experimental ones.

Moreover, the accuracy with which experimental values are theoretically reproduced is sufficiently high to permit the distinction of the two different *anti* arrangements. It is noteworthy that such a differentiation would be impossible if one had to rely on only a semiquantitative classification (*small*, *medium*, and *large*) of the heteronuclear J values without resorting to interpretation of dipolar effects (see section 2 and Figure 16).

4.7.2. New Combined NMR–Quantum Mechanical Strategy in the Determination of the Relative Configuration of Steroids: Application to Stemmosides C and D

On the basis of the powerful potential offered by the GIAO ¹³C NMR chemical shift in the determination of the relative

Chart 18



configuration of flexible organic compounds, and thanks to the recent advances in the QM calculations of NMR J -coupling values, a straightforward combined NMR–QM strategy has been recently applied for the determination of the relative configuration of stemmosides C, **70**, and D, **71** (Chart 17), two novel pregnane glycosides characterized by an unusual C17 α side chain isolated from the pericarps of *Solenostemma argel*.¹⁴⁸ Structure elucidation was complicated by the fact that stemmoside D, **71**, displays an uncommon 14 β proton configuration, apparently being the first pregnane isolated from plants having a 15-keto-*cis* CD ring junction. It has to be pointed out that the NMR determination of configurational patterns in steroidal side chains and ring junctions usually relies on comparison with literature data.^{149–151} Alternatively, analysis of NMR 2D-NOESY and ROESY spectra^{151–153} and analysis of their biosynthetic pathways may offer insightful stereochemical information.¹⁵⁴ In this regard, the stereostructure determination of stemmosides C and D may represent an important case study for other configurational analyses of steroids.

For compound **70**, the two possible stereoisomers differing at C17 (**70a** and **70b** in Chart 18) were built, simplified by the substitution of the sugar moiety with a methyl group. Subsequently, a conformational search, performed by molecular mechanics and dynamics calculations, provided a minimum energy conformer for each stereoisomer.

The two structures were further optimized at the MPW1-PW91 level, using the 6-31G(d) basis set. Single-point GIAO calculations using the same functional and the 6-31G(d,p) basis set provided the ¹³C and ¹H theoretical values, whereas ONIOM calculations using the MPW1PW91 functional and the 3-21G (low level, rings A–B) and 6-31G(d,p) (high level, ring C–D) basis sets were executed on the two stereoisomers, providing theoretical J values for ring D. The obtained calculated ¹H and ¹³C chemical shifts were then compared with the experimental NMR data of compound **70** to discriminate between the two stereoisomers. In particular, concerning ¹³C shifts, preliminary considerations based on $\Delta\delta = \delta_{\text{exptl}} - \delta_{\text{calcd}}$ values, and the MAE parameter (mean

Table 25. Crucial ^{13}C NMR Values for Stemmoside C (70), GIAO ^{13}C NMR Chemical Shifts (δ) for the Stereoisomers 70a and 70b, and $\Delta\delta^a$ Values for 70a and 70b

| atom | 70 | 70a | 70b | $\Delta\delta$ 70a | $\Delta\delta$ 70b |
|--------------|------|------|------|--------------------|--------------------|
| δ C8 | 38.0 | 36.1 | 35.4 | 1.9 | 2.6 |
| δ C11 | 21.9 | 22.9 | 23.1 | -1.0 | -1.3 |
| δ C12 | 29.3 | 29.5 | 38.0 | -0.2 | -8.7 |
| δ C13 | 45.7 | 46.2 | 45.1 | -0.5 | 0.6 |
| δ C14 | 82.5 | 79.9 | 80.0 | 2.6 | 2.5 |
| δ C16 | 40.0 | 39.6 | 39.0 | 0.4 | 1.0 |
| δ C17 | 43.5 | 42.1 | 44.6 | 1.4 | -1.1 |
| δ C18 | 15.3 | 15.4 | 15.3 | -0.1 | 0.0 |
| δ C20 | 22.4 | 24.2 | 31.1 | -1.8 | -8.7 |
| δ C21 | 13.4 | 15.1 | 15.4 | -1.7 | -2.0 |

^a $\Delta\delta = \delta_{\text{exptl}} - \delta_{\text{calcd}}$, differences for experimental versus calculated ^{13}C NMR cs.

Table 26. Significant ^1H NMR Chemical Shifts for 70, Corresponding GIAO ^1H NMR Chemical Shifts Calculated for Stereoisomers 70a and 70b, and $\Delta\delta^a$ Values for 70a and 70b

| atom | 70 | 70a | 70b | $\Delta\delta$ 70a | $\Delta\delta$ 70b |
|-----------------------|------|------|------|--------------------|--------------------|
| δ H16 α | 1.77 | 1.74 | 2.33 | 0.03 | -0.56 |
| δ H16 β | 2.62 | 2.60 | 2.09 | 0.02 | 0.53 |
| δ H17 | 2.17 | 2.28 | 1.33 | -0.11 | 0.84 |

^a $\Delta\delta = \delta_{\text{exptl}} - \delta_{\text{calcd}}$, differences for experimental versus calculated ^1H NMR cs.

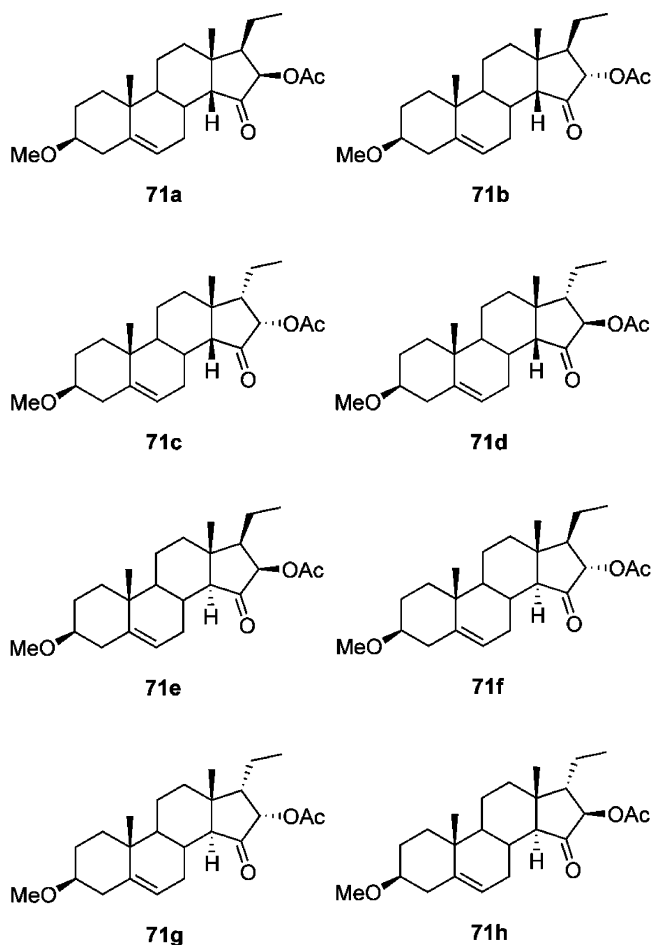
absolute error, $\text{MAE} = \sum[|(\delta_{\text{exptl}} - \delta_{\text{calcd}})|]/n$, pointed to stereoisomer **70a**, displaying a MAE of 1.63 versus 2.48 for **70b**. Moreover, a careful analysis was done on individually calculated ^{13}C chemical shifts for rings C and D, which were expected to experience larger variations upon inversion of configuration at C17. As shown in Table 25, very large differences in the $\Delta\delta$ ^{13}C cs values of **70a** and **70b** were observed for C12 and C20 (-0.2 vs -8.7 and -1.8 vs -8.7, respectively), suggesting again the exclusion of stereoisomer **70b**.

The same observations resulted from the analysis of the calculated ^1H chemical shifts for **70a** and **70b**. In Table 26 are shown the calculated and experimental ^1H values for the protons of ring D. Analysis of the $\Delta\delta$ values shows that the chemical shift values for H16 α , H16 β , and H17 of **70a** faithfully reproduce the experimental ones, whereas the corresponding results obtained for compound **70b** display relatively large differences with respect to the experimental.

Finally, coupling constant $^3J_{\text{HH}}$ values reported in Table 27 for compound **70a** fitted very well the experimental values, both unusually large. On the other hand, a small (3.3

Table 27. Comparison between Experimental (70) and Calculated (Stereoisomers 70a,b) $^3J_{\text{HH}}$ Values of Ring D, in Hertz

| atom | 70 | 70a | 70b | $\Delta\delta$ 70a | $\Delta\delta$ 70b |
|-----------------------|------|------|------|--------------------|--------------------|
| δ H16 α | 1.77 | 1.74 | 2.33 | 0.03 | -0.56 |
| δ H16 β | 2.62 | 2.60 | 2.09 | 0.02 | 0.53 |
| δ H17 | 2.17 | 2.28 | 1.33 | -0.11 | 0.84 |

Chart 19**Table 28. ^{13}C and ^1H MAE^a Values for 71a–h**

| | 71a | 71b | 71c | 71d | 71e | 71f | 71g | 71h |
|---------------------|------|------|------|------|------|------|------|------|
| MAE ^{13}C | 2.64 | 2.66 | 1.81 | 2.14 | 2.87 | 3.20 | 2.59 | 2.56 |
| MAE ^1H | 0.16 | 0.14 | 0.13 | 0.15 | 0.15 | 0.15 | 0.16 | 0.15 |

^a Mean average error, $\text{MAE } ^{13}\text{C} = \sum[|(\delta_{\text{exptl}} - \delta_{\text{calcd}})|]/n$; $\text{MAE } ^1\text{H} = \sum[|(\delta_{\text{exptl}} - \delta_{\text{calcd}})|]/n$.

Hz) and a large J coupling (9.0 Hz) calculated for stereoisomer **70b** reproduced a pattern previously described in the literature for other steroids,^{155,156} but allowed exclusion of the stereostructure of **70b** for stemmoside C **70**.

The same strategy was applied to stemmoside D, **71**. All of the possible stereoisomers differing at C14, C16, and C17 (**71a–h**, Chart 19) were taken into account.

MAE values for ^{13}C and ^1H chemical shifts were obtained for each of the eight models and, as outlined in Table 28, the lowest values (best matches) were observed for stereoisomer **71c**.

Table 29. Comparison between Experimental (71) and Calculated (Stereoisomers 71a–h) $^3J_{\text{HH}}$ Values of Ring D, in Hertz

| $^3J_{\text{HH}}$ | 71 | 71a | 71b | 71c | 71d | 71e | 71f | 71g | 71h |
|-------------------|------|-----|-----|-----|-----|-----|-----|-----|-----|
| H16–H17 | 10.1 | 5.4 | 2.6 | 9.7 | 8.4 | 9.1 | 3.3 | 8.9 | 1.9 |

Moreover, the calculated $^3J_{\text{HH}}$ values for ring D considering each of the eight possible stereoisomer **71a–h** were compared to the corresponding experimental values. As shown in Table 29, the value of 9.7 Hz, corresponding to the $^3J_{\text{HH}}$ value of H16–H17 of stereoisomer **71c**, displays the best agreement with the experimental value of 10.1 Hz.

Finally, it is noteworthy that a retrospective analysis of the NMR data of stemmoside D was performed to corroborate the unusual 14β proton configuration and relative configuration of H16 and H17 obtained from the QM calculations.

5. Conclusion and Future Perspectives

The scenario emerging from the critical review of all recently published work in the field of stereochemical analysis of organic compounds by NMR-based methods is undoubtedly optimistic. Not only have molecules, deemed just a decade ago to be too complex to be elucidated in every aspect, been fully characterized by simply resorting to purely NMR spectroscopic methods, but the practitioner of NMR structure elucidation may count nowadays on a variety of approaches, in many cases with a high degree of complementarity.

One cannot help but note that computational methods in support of NMR assignment are becoming increasingly important to undertake difficult problems, so it is likely that the relevance of hybrid experimental/theoretical approaches will continue to grow. However, new avenues are still being opened also in the area of novel experimental approaches. The best example is the very recent work on the use of residue dipolar couplings in the conformational and configurational assignment of organic compounds in oriented media,¹⁵⁷ another example of the fruitful transfer of knowledge from the field of NMR spectroscopy applied to macromolecular systems to the realm of organic chemistry.

6. Addendum

Several significant papers regarding the use of the *J*-based configurational analysis,¹⁵⁸ the UDB,¹⁵⁹ and the quantum chemical calculation of NMR parameters¹⁶⁰ for the determination of relative configuration in organic compounds have appeared in the literature during the review acceptance processes of this review.

7. Notes and References

- Seco, J. M.; Quiñoá, E.; Riguera, R. *Chem. Rev.* **2004**, *104*, 17.
- Karplus, M. *J. Chem. Phys.* **1959**, *30*, 11.
- Haasnoot, C. A. G.; De Leeuw, F. A. A. M.; Altona, C. *Tetrahedron* **1980**, *36*, 2783.
- Hansen, P. E. *Prog. NMR Spectrosc.* **1981**, *14*, 175.
- Matsumori, N.; Kaneno, D.; Murata, M.; Nakamura, H.; Tachibana, K. *J. Org. Chem.* **1999**, *64*, 866.
- Matsumori, N.; Murata, M.; Tachibana, K. *Tetrahedron* **1995**, *51*, 12229.
- Sasaki, M.; Matsumori, N.; Maruyama, T.; Nonomura, T.; Murata, M.; Tachibana, K.; Yasumoto, T. *Angew. Chem., Int. Ed. Engl.* **1996**, *35*, 1672.
- Nonomura, T.; Sasaki, M.; Matsumori, N.; Murata, M.; Tachibana, K.; Yasumoto, T. *Angew. Chem., Int. Ed. Engl.* **1996**, *35*, 1675.
- Matsumori, N.; Nonomura, T.; Sasaki, M.; Murata, M.; Tachibana, K.; Satake, M.; Yasumoto, T. *Tetrahedron Lett.* **1996**, *37*, 1269.
- Sakai, R.; Kamiya, H.; Murata, M.; Shimamoto, K. *J. Am. Chem. Soc.* **1997**, *119*, 4112.
- Murata, M.; Matsuoka, S.; Matsumori, N.; Paul, G. K.; Tachibana, K. *J. Am. Chem. Soc.* **1999**, *121*, 870.
- Kobayashi, J.; Tsuda, M. *Nat. Prod. Rep.* **2004**, *21*, 77.
- Costantino, V.; Fattorusso, E.; Menna, M.; Tagliatalata-Scafati, O. *Curr. Med. Chem.* **2004**, *11*, 1671.
- Ciminiello, P.; Fattorusso, E. *Eur. J. Org. Chem.* **2004**, 2533.
- Riccio, R.; Bifulco, G.; Cimino, P.; Bassarello, C.; Gomez-Paloma, L. *Pure Appl. Chem.* **2003**, *75*, 295.
- Okino, T. *Kagaku to Seibutsu* **2003**, *41*, 517.
- Bassarello, C.; Cimino, P.; Gomez-Paloma, L.; Riccio, R.; Bifulco, G. *Recent Res. Dev. Org. Chem.* **2003**, *7*, 219.
- Ciminiello, P.; Dell'Aversano, C.; Fattorusso, E.; Forino, M.; Magno, S. *Pure Appl. Chem.* **2003**, *75*, 325.
- Gomez-Paloma, L.; Bifulco, G.; Bassarello, C.; Cimino, P. In *Seminars in Organic Synthesis, Summer School "A. Corbella"*, 26th, Gargnano, Italy, June 18–22, 2001; Società Chimica Italiana: Rome, Italy, 2001; pp 145–171.
- Murata, M.; Yasumoto, T. *Nat. Prod. Rep.* **2000**, *17*, 293.
- Contreras, R. H.; Peralta, J. E. *Prog. Nucl. Magn. Reson. Spectrosc.* **2000**, *37*, 321.
- Karplus, M. *J. Phys. Chem.* **1960**, *64*, 1793.
- Karplus, M. *J. Am. Chem. Soc.* **1963**, *85*, 2870.
- Bifulco, G.; Bassarello, C.; Riccio, R.; Gomez-Paloma, L. *Org. Lett.* **2004**, *6*, 1025.
- (a) Hoye, R. T.; Hanson, P. R.; Vyvyan, J. R. *J. Org. Chem.* **1994**, *59*, 4096. (b) Hoye, R. T.; Zhao, H. *J. Org. Chem.* **2002**, *67*, 4014.
- (a) Biamonti, C.; Rios, C. B.; Lyons, B. A.; Montelione, G. T. *Adv. Biophys. Chem.* **1994**, *4*, 51. (b) For a survey on NMR experiments for the determination of $^2,3J_{\text{HC}}$ see: Marquez, B. L.; Gerwick, W. H.; Williamson, R. T. *Magn. Reson. Chem.* **2001**, *39*, 499.
- (a) Kurz, M.; Schmieder, P.; Kessler, H. *Angew. Chem., Int. Ed. Engl.* **1991**, *30*, 1329. (b) Wollborn, U.; Leibfritz, D. *J. Magn. Reson.* **1992**, *98*, 142.
- Zhu, G.; Live, D.; Bax, A. *J. Am. Chem. Soc.* **1994**, *116*, 8370.
- Zhu, G.; Bax, A. *J. Magn. Reson. Ser. A* **1993**, *104*, 353.
- Boyd, J.; Soffe, N.; John, B.; Plant, D.; Hurd, R. *J. Magn. Res.* **1992**, *98*, 660.
- Davis, A. L.; Keeler, J.; Lane, E. D.; Moskau, D. *J. Magn. Reson.* **1992**, *98*, 207.
- Bassarello, C.; Bifulco, G.; Zampella, A.; D'Auria, M. V.; Riccio, R.; Gomez-Paloma, L. *Eur. J. Org. Chem.* **2001**, 39.
- Uhrin, D.; Batta, G.; Hruby, V. J.; Barlow, P. N.; Kovér, K. E. *J. Magn. Reson.* **1998**, *130*, 155.
- Williamson, R. T.; Marquez, B. L.; Gerwick, W. H.; Köver, K. E. *Magn. Reson. Chem.* **2000**, *38*, 265.
- Meissner, A.; Sørensen, O. W. *Magn. Reson. Chem.* **2001**, *39*, 49.
- Achkar, J.; Sanchez-Larraza, I.; Johnson, C. A.; Wei, A. *J. Org. Chem.* **2005**, *70*, 214.
- Bugni, T. S.; Janso, E. J.; Williamson, R. T.; Feng, X.; Bernan, V. S.; Greenstein, M.; Carter, G. T.; Maiese, W. M.; Ireland, C. M. *J. Nat. Prod.* **2004**, *67*, 1396.
- Campagnuolo, C.; Fattorusso, C.; Fattorusso, E.; Ianaro, A.; Pisano, B.; Tagliatalata-Scafati, O. *Org. Lett.* **2003**, *5*, 673.
- Cimino, P.; Bifulco, G.; Evidente, A.; Abouzeid, M.; Riccio, R.; Gomez-Paloma, L. *Org. Lett.* **2002**, *4*, 2779.
- Espelt, L.; Parella, T.; Bujons, J.; Solans, C.; Joglar, J.; Delgado, A.; Clapes, P. *Chem. Eur. J.* **2003**, *9*, 4887.
- Grassia, A.; Bruno, I.; Debitus, C.; Marzocco, S.; Pinto, A.; Gomez-Paloma, L.; Riccio, R. *Tetrahedron* **2001**, *57*, 6257.
- Ikeda, H.; Matsumori, N.; Ono, M.; Suzuki, A.; Isogai, A.; Nagasawa, H.; Sakuda, S. *J. Org. Chem.* **2000**, *65*, 438.
- Jadulco, R.; Edrada, R. A.; Ebel, R.; Berg, A.; Schumann, K.; Wray, V.; Steube, K.; Proksch, P. *J. Nat. Prod.* **2004**, *67*, 78.
- Knust, H.; Hoffmann, R. W. *Helv. Chim. Acta* **2003**, *86*, 1871.
- Kobayashi, J.; Shimbo, K.; Sato, M.; Tsuda, M. *J. Org. Chem.* **2002**, *67*, 6585.
- Kubota, T.; Tsuda, M.; Kobayashi, J. *Org. Lett.* **2001**, *3*, 1363.
- Kubota, T.; Tsuda, M.; Kobayashi, J. *J. Org. Chem.* **2002**, *67*, 1651.
- Luesch, H.; Yoshida, W. Y.; Moore, R. E.; Paul, V. J.; Corbett, T. H. *J. Am. Chem. Soc.* **2001**, *123*, 5418.
- Nakamura, H.; Maruyama, K.; Fujimaki, K.; Murai, A. *Tetrahedron Lett.* **2000**, *41*, 1927.
- Paterson, I.; Britton, R.; Delgado, O.; Wright, A. E. *Chem. Commun.* **2004**, 632.
- Ratnayake, A. S.; Yoshida, W. Y.; Mooberry, S. L.; Hemscheidt, T. *Org. Lett.* **2001**, *3*, 3479.

- (52) (a) Shimbo, K.; Tsuda, M.; Izui, N.; Kobayashi, J. *J. Org. Chem.* **2002**, *67*, 1020. (b) Ghosh, A. K.; Gong, G. *J. Am. Chem. Soc.* **2004**, *126*, 3704. (c) Ghosh, A. K.; Gong, G. *J. Org. Chem.* **2006**, *71*, 1085.
- (53) Tan, L. T.; Marquez, B. L.; Gerwick, W. H. *J. Nat. Prod.* **2002**, *65*, 925.
- (54) Tsuda, M.; Izui, N.; Shimbo, K.; Sato, M.; Fukushi, E.; Kawabata, J.; Katsumata, K.; Horiguchi, T.; Kobayashi, J. *J. Org. Chem.* **2003**, *68*, 5339.
- (55) Tsuda, M.; Izui, N.; Shimbo, K.; Sato, M.; Fukushi, E.; Kawabata, J.; Kobayashi, J. *J. Org. Chem.* **2003**, *68*, 9109.
- (56) Tsuda, M.; Nozawa, K.; Shimbo, K.; Ishiyama, H.; Fukushi, E.; Kawabata, J.; Kobayashi, J. *Tetrahedron Lett.* **2003**, *44*, 1395.
- (57) Williams, P. G.; Yoshida, W. Y.; Moore, R. E.; Paul, V. J. *J. Nat. Prod.* **2003**, *66*, 1006.
- (58) Williams, P. G.; Yoshida, W. Y.; Quon, M. K.; Moore, R. E.; Paul, V. J. *J. Nat. Prod.* **2003**, *66*, 1545.
- (59) Williamson, R. T.; Boulanger, A.; Vulpanovici, A.; Roberts, M. A.; Gerwick, W. H. *J. Org. Chem.* **2002**, *67*, 7927.
- (60) Williamson, R. T.; Marquez, B. L.; Sosa, A. C. B.; Koehn, F. E. *Magn. Reson. Chem.* **2003**, *41*, 379.
- (61) Oikawa, M.; Adachi, S.; Kusumoto, S. *Org. Lett.* **2005**, *7*, 661.
- (62) Wu, M.; Okino, T.; Nogle, L. M.; Marquez, B. L.; Williamson, R. T.; Sitachitta, N.; Berman, F. W.; Murray, T. F.; McGough, K.; Jacobs, R.; Colson, K.; Asano, T.; Yokokawa, F.; Shioiri, T.; Gerwick, W. H. *J. Am. Chem. Soc.* **2000**, *122*, 12041.
- (63) Yokokawa, F.; Asano, T.; Okino, T.; Gerwick, W. H.; Shioiri, T. *Tetrahedron* **2004**, *60*, 6859.
- (64) Chen, J.; Forsyth, C. *J. Angew. Chem. Int. Ed.* **2004**, *43*, 2148.
- (65) Randazzo, A.; Bifulco, G.; Giannini, C.; Bucci, M.; Debitus, C.; Cirino, G.; Gomez-Paloma, L. *J. Am. Chem. Soc.* **2001**, *123*, 10870.
- (66) Della Monica, C.; Randazzo, A.; Bifulco, G.; Cimino, P.; Aquino, M.; Izzo, I.; De Riccardis, F.; Gomez-Paloma, L. *Tetrahedron Lett.* **2002**, *43*, 5707.
- (67) Williamson, R. T.; Singh, I. P.; Gerwick, W. H. *Tetrahedron* **2004**, *60*, 7025.
- (68) Bassarello, C.; Bifulco, G.; Evidente, A.; Riccio, R.; Gomez-Paloma, L. *Tetrahedron Lett.* **2001**, *42*, 8611.
- (69) He, H.; Williamson, R. T.; Shen, B.; Graziani, E. I.; Yang, H. Y.; Sakya, S. M.; Petersen, P. J.; Carter, G. T. *J. Am. Chem. Soc.* **2002**, *124*, 9729.
- (70) McDonald, L. A.; Barbieri, L. R.; Carter, G. T.; Lenoy, E.; Lotvin, J.; Petersen, P. J.; Siegel, M. M.; Singh, G.; Williamson, R. T. *J. Am. Chem. Soc.* **2002**, *124*, 10260.
- (71) Yamashita, A.; Norton, E. B.; Williamson, R. T.; Ho, D. M.; Sinishtaj, S.; Mansour, T. S. *Org. Lett.* **2003**, *5*, 3305.
- (72) Ciminiello, P.; Dell'Aversano, C.; Fattorusso, E.; Forino, M.; Magno, S.; Di Rosa, M.; Ianaro, A.; Poletti, R. *J. Am. Chem. Soc.* **2002**, *124*, 13114.
- (73) Campagnuolo, C.; Fattorusso, E.; Tagliatalata-Scafati, O.; Ianaro, A.; Pisano, B. *Eur. J. Org. Chem.* **2002**, *61*.
- (74) Ciminiello, P.; Fattorusso, E.; Forino, M.; Di Rosa, M.; Ianaro, A.; Poletti, R. *J. Org. Chem.* **2001**, *66*, 578.
- (75) Ciminiello, P.; Dell'Aversano, C.; Fattorusso, E.; Forino, M.; Magno, S.; Di Meglio, P.; Ianaro, A.; Poletti, R. *Tetrahedron* **2004**, *60*, 7093.
- (76) Kaluzna, I. A.; Feske, B. D.; Wittayanan, W.; Ghiviriga, I.; Stewart, J. D. *J. Org. Chem.* **2005**, *70*, 342.
- (77) (a) Dambrooso, P.; Bassarello, C.; Bifulco, G.; Appendino, G.; Battaglia, A.; Fontana, G.; Gomez-Paloma, L. *Org. Lett.* **2005**, *7*, 983. (b) Dambrooso, P.; Bassarello, C.; Bifulco, G.; Appendino, G.; Battaglia, A.; Guerrini, A.; Fontana, G.; Gomez-Paloma, L. *Tetrahedron Lett.* **2005**, *46*, 3411.
- (78) Battaglia, A.; Guerrini, A.; Bertucci, C. *J. Org. Chem.* **2004**, *69*, 9055.
- (79) Cichewicz, R. H.; Valeriote, F. A.; Crews, P. *Org. Lett.* **2004**, *6*, 1951.
- (80) Hoye, T. R.; Suhadolnik, J. C. *J. Am. Chem. Soc.* **1987**, *109*, 4402.
- (81) (a) Kobayashi, Y.; Lee, J.; Tezuka, K.; Kishi, Y. *Org. Lett.* **1999**, *1*, 2177. (b) Lee, J.; Kobayashi, Y.; Tezuka, K.; Kishi, Y. *Org. Lett.* **1999**, *1*, 2181. The UDB acronym was purposefully created by the authors of this review and used throughout the paper.
- (82) For a review on Palitoxin, see: Kishi, Y. *Tetrahedron* **2002**, *58*, 6239.
- (83) For each nucleus (proton or carbon) of each diastereoisomer, the differences of the experimentally measured *c*s from the computed mean values were plotted as histograms.
- (84) For each nucleus (proton or carbon) of each diastereoisomer, the mean value of the experimentally measured *c*s was computed.
- (85) (a) Kobayashi, Y.; Tan, C. H.; Kishi, Y. *Angew. Chem. Int. Ed.* **2000**, *39*, 4279. (b) Tan, C. H.; Kobayashi, Y.; Kishi, Y. *Angew. Chem. Int. Ed.* **2000**, *39*, 4282. (c) Kobayashi, Y.; Tan, C. H.; Kishi, Y. *Helv. Chim. Acta* **2000**, *83*, 2562. (d) Kobayashi, Y.; Tan, C. H.; Kishi, Y. *J. Am. Chem. Soc.* **2001**, *123*, 2076.
- (86) CambridgeSoft.
- (87) The absolute configurations of the stereocenters were assigned by comparing the optical rotation of the synthesized fragments and the degradation products (for C21–C38 segment) or synthesizing the Mosher esters of both synthesized or degraded products (C5–C10, C41–C43, C14–C15, and C18–C19 segments). See ref 85d.
- (88) For a complete survey on the UDB of contiguous polyols see: Higashibayashi, S.; Czechtizky, W.; Kobayashi, Y.; Kishi, Y. *J. Am. Chem. Soc.* **2003**, *125*, 14379.
- (89) Kobayashi, Y.; Czechtizky, W.; Kishi, Y. *Org. Lett.* **2003**, *5*, 93.
- (90) MacMillan, J. B.; Molinski, T. F. *Org. Lett.* **2002**, *4*, 1535.
- (91) Hoye, T. R.; Tennakoon, M. A. *Org. Lett.* **2000**, *2*, 1481.
- (92) Tanaka, M.; Nara, F.; Suzuki-Konagai, K.; Hosoya, T.; Ogita, T. *J. Am. Chem. Soc.* **1997**, *119*, 7871.
- (93) Saito, S.; Tanaka, N.; Fujimoto, K.; Kogen, H. *Org. Lett.* **2000**, *2*, 505.
- (94) Lee, S.; LaCour, T. G.; Lantrip, D.; Fuchs, P. L. *Org. Lett.* **2002**, *4*, 313.
- (95) Fukuzawa, S.; Matsunaga, S.; Fusetani, N. *Tetrahedron* **1995**, *51*, 6707.
- (96) Kobayashi, Y.; Hayashi, N.; Tan, C. H.; Kishi, Y. *Org. Lett.* **2001**, *3*, 2245.
- (97) Hayashi, N.; Kobayashi, Y.; Kishi, Y. *Org. Lett.* **2001**, *3*, 2249.
- (98) Kobayashi, Y.; Hayashi, N.; Kishi, Y. *Org. Lett.* **2001**, *3*, 2253.
- (99) (a) Kobayashi, Y.; Hayashi, N.; Kishi, Y. *Org. Lett.* **2002**, *4*, 411. (b) Kobayashi, Y.; Hayashi, N.; Kishi, Y. *Tetrahedron Lett.* **2003**, *44*, 7489. (c) Higashibayashi, S.; Kishi, Y. *Tetrahedron* **2004**, *60*, 11977.
- (100) Dale, J. A.; Mosher, H. S. *J. Am. Chem. Soc.* **1973**, *95*, 512.
- (101) (a) Ghosh, I.; Zeng, H.; Kishi, Y. *Org. Lett.* **2004**, *6*, 4715. (b) Ghosh, I.; Kishi, Y.; Tomoda, H.; Omura, S. *Org. Lett.* **2004**, *6*, 4719.
- (102) (a) Benowitz, A. B.; Fidanze, S.; Small, P. L. C.; Kishi, Y. *J. Am. Chem. Soc.* **2001**, *123*, 5128. (b) Fidanze, S.; Song, F.; Szlosek-Pinaud, M.; Small, P. L. C.; Kishi, Y. *J. Am. Chem. Soc.* **2001**, *123*, 10117. (c) Judd, T. C.; Bischoff, A.; Kishi, Y.; Adusumilli, S.; Small, P. L. C. *Org. Lett.* **2004**, *6*, 4901.
- (103) Pasetto, P.; Franck, R. W. *J. Org. Chem.* **2003**, *68*, 8042.
- (104) Clerc, J.-T.; Sommerauer, H. A. *Anal. Chim. Acta* **1977**, *95*, 33.
- (105) Fürst, A.; Pretsch, E. *Anal. Chim. Acta* **1990**, *229*, 17.
- (106) Meiler, J.; Will, M.; Meusinger, R. *J. Chem. Inf. Comput. Sci.* **2000**, *40*, 1169.
- (107) (a) <http://www.nmrshiftdb.org>. (b) Steinbeck, C.; Krause, S.; Kuhn, S. *J. Chem. Inf. Comput. Sci.* **2003**, *43*, 1733.
- (108) Specht, K. M.; Nam, J.; Ho, D. M.; Berova, N.; Kondru, R. K.; Beratan, D. N.; Wipf, P.; Pascal, R. A., Jr.; Kahne, D. *J. Am. Chem. Soc.* **2001**, *123*, 8961.
- (109) Stephens, P. J.; Devlin, F. J.; Cheeseman, J. R.; Frisch, M. J.; Mennucci, B.; Tomasi, J. *Tetrahedron: Asymmetry* **2000**, *11*, 2443.
- (110) Donnoli, M. I.; Giorgio, E.; Superchi, S.; Rosini, C. *Org. Biomol. Chem.* **2003**, *1*, 3444.
- (111) Casanovas, J.; Namba, A. M.; Leon, S.; Aquino, G. L. B.; da Silva, G. V. J.; Aleman, C. *J. Org. Chem.* **2001**, *66*, 3775.
- (112) Sebag, A. B.; Forsyth, D. A.; Plante, M. A. *J. Org. Chem.* **2001**, *66*, 7967.
- (113) Chesnut, D. B. In *Reviews in Computational Chemistry*; Lipkowitz, K. B., Boyd, D. B., Eds.; VCH: New York, 1996; Vol. 8, Chapter 5, pp 245–297.
- (114) de Dios, A. C. *J. Prog. Nucl. Magn. Reson. Spectrosc.* **1996**, *29*, 229.
- (115) Forsyth, D. A.; Sebag, A. B. *J. Am. Chem. Soc.* **1997**, *119*, 9483.
- (116) Helgaker, T.; Jaszunski, M.; Ruud, K. *Chem. Rev.* **1999**, *99*, 293.
- (117) Ditchfield, R. *J. Chem. Phys.* **1972**, *56*, 5688.
- (118) Wolinski, K.; Hinton, J. F.; Pulay, P. *J. Am. Chem. Soc.* **1990**, *112*, 8251.
- (119) Cheeseman, J. R.; Trucks, G. W.; Keith, T. A.; Frisch, M. J. *J. Chem. Phys.* **1996**, *104*, 5497.
- (120) Adamo, C.; Barone, V. *J. Chem. Phys.* **1998**, *108*, 664.
- (121) Adamo, C.; Barone, V. *J. Chem. Phys.* **1999**, *110*, 6158.
- (122) Friesner, R. A.; Murphy, R. B.; Beachy, M. D.; Ringnalda, M. N.; Pollard, W. T.; Dunietz, B. D.; Cao, Y. *J. Phys. Chem. A* **1999**, *103*, 1913.
- (123) Barone, G.; Gomez-Paloma, L.; Duca, D.; Silvestri, A.; Riccio, R.; Bifulco, G. *Chem. Eur. J.* **2002**, *8*, 3233.
- (124) Wipf, P.; Kerekes, A. D. *J. Nat. Prod.* **2003**, *66*, 716.
- (125) Balandina, A.; Mamedov, V.; Franck, X.; Figadere, B.; Latypov, S. *Tetrahedron Lett.* **2004**, *45*, 4003.
- (126) Asirvatham, P. S.; Subramanian, V.; Balakrishnan, R.; Ramasami, T. *Macromolecules* **2003**, *36*, 921.
- (127) Cimino, P.; Duca, D.; Gomez-Paloma, L.; Riccio, R.; Bifulco, G. *Magn. Reson. Chem.* **2004**, *42*, S26–S33.
- (128) Stahl, M.; Schopfer, U. *J. Chem. Soc., Perkin Trans. 2* **1997**, *5*, 905.
- (129) Duca, D.; Bifulco, G.; Barone, G.; Casapullo, A.; Fontana, A. *J. Chem. Inf. Comput. Sci.* **2004**, *44*, 1024.

- (130) Bausch, J. W.; Rizzo, R. C.; Sneddon, L. G.; Wille, A. E.; Williams, R. E. *Inorg. Chem.* **1996**, *35*, 131.
- (131) Akorta, I.; Elguero, J. *Magn. Reson. Chem.* **2004**, *42*, 955.
- (132) de Dios, A. C. *Prog. NMR Spectrosc.* **1996**, *29*, 229.
- (133) de Dios, A. C.; Oldfield, E. *J. Am. Chem. Soc.* **1994**, *116*, 5307.
- (134) Oldfield, E. *J. Biomol. NMR.* **1995**, *5*, 217.
- (135) Swalina, C. W.; Zauhar, R. J.; DeGrazia, M. J.; Moyna, G. *J. Biomol. NMR* **2001**, *21*, 49.
- (136) Stahl, M.; Schopfer, U.; Frenking, G.; Hoffmann, R. W. *J. Org. Chem.* **1997**, *62*, 3702.
- (137) Stahl, M.; Schopfer, U.; Frenking, G.; Hoffmann, R. W. *J. Org. Chem.* **1996**, *61*, 8083.
- (138) Chang, G.; Guida, W. C.; Still, W. C. *J. Am. Chem. Soc.* **1989**, *111*, 4379.
- (139) MACROMODEL 4.5, Department of Chemistry, Columbia University, New York, NY.
- (140) (a) Grant, D. M.; Paul, E. G. *J. Am. Chem. Soc.* **1964**, *86*, 2984. (b) Paul, E. G.; Grant, D. M. *J. Am. Chem. Soc.* **1963**, *85*, 1701.
- (141) Ando, M.; Tajima, K.; Takase, K. *Bull. Chem. Soc. Jpn.* **1979**, *52*, 2737.
- (142) Villar, A.; Zafra-Polo, M. C.; Nicoletti, M.; Galeffi, C. *Phytochemistry* **1983**, *22*, 777.
- (143) Metwally, M. A.; Jakupovic, J.; Youns, M. I.; Bohlmann, F. *Phytochemistry* **1985**, *24*, 1103.
- (144) Colombo, D.; Ferraboschi, P.; Ronchetti, F.; Toma, L. *Magn. Reson. Chem.* **2002**, *40*, 581.
- (145) Barone, G.; Duca, D.; Silvestri, A.; Gomez-Paloma, L.; Riccio, R.; Bifulco, G. *Chem. Eur. J.* **2002**, *8*, 3240.
- (146) (a) Tahtinen, P.; Bagno, A.; Klika, K. D.; Pihlaja, K. *J. Am. Chem. Soc.* **2003**, *125*, 4609. (b) Cloran, F.; Carmichael, I.; Serianni, A. S. *J. Am. Chem. Soc.* **2001**, *123*, 4781. (c) Bagno, A. *Chem. Eur. J.* **2001**, *7*, 1652.
- (147) Zampella, A.; Sepe, V.; D'Orsi, R.; Bifulco, G.; Bassarello, C.; D'Auria, M. V. *Tetrahedron Asymmetry* **2003**, *14*, 1787.
- (148) Plaza, A.; Piacente, S.; Perrone, A.; Hamed, A.; Pizza, C.; Bifulco, G. *Tetrahedron* **2004**, *60*, 12201.
- (149) Luo, S.-Q.; Lin, L.-Z.; Cordell, G. A.; Xue, L.; Johnson, M. *Phytochemistry* **1993**, *34*, 1615.
- (150) Lin, L.-J.; Lin, L.-Z.; Gil, R.; Cordell, G. A.; Ramesh, M.; Srilatha, B.; Reddy, B.; Rao, A. V. N. A. *Phytochemistry* **1994**, *35*, 1549.
- (151) Jung, M. E.; Johnson, T. W. *Tetrahedron* **2001**, *57*, 1449.
- (152) Yin, J.; Kouda, K.; Tezuka, Y.; Tran, Q. L.; Miyahara, T.; Chen, Y.; Kadota, S. *J. Nat. Prod.* **2003**, *66*, 646.
- (153) Panda, N.; Mondal, N. P.; Banerjee, S.; Sahu, N. P.; Koike, K.; Nikaido, T.; Weber, M.; Luger, P. *Tetrahedron* **2003**, *59*, 8399.
- (154) Braca, A.; Bader, A.; Morelli, L.; Scarpato, R.; Turchi, G.; Pizza, C.; De Tommasi, N. *Tetrahedron* **2002**, *58*, 5837.
- (155) Yoshimura, S. I.; Narita, H.; Hayashi, K.; Mitsushashi, H. *Chem. Pharm. Bull.* **1983**, *31*, 3971.
- (156) Deepak, D.; Srivastav, S.; Khare, A. *Fort. Chem. Org. Nat.* **1997**, *71*, 169.
- (157) The reader interested in this specific area may consult recent reviews on the subject: (a) Gschwind, R. M. *Angew. Chem. Int. Ed.* **2005**, *44*, 4666. (b) Yan, J.; Zartler, E. R. *Magn. Reson. Chem.* **2005**, *43*, 53.
- (158) (a) Bunyajetpong, S.; Yoshida, W. Y.; Sitachitta, N.; Kaya, K. *J. Nat. Prod.* **2006**, *69*, 1539. (b) Hassfeld, J.; Fares, C.; Steinmetz, H.; Carlomagno, T.; Menche, D. *Org. Lett.* **2006**, *8*, 4751. (c) Plaza, A.; Bewley, C. A. *J. Org. Chem.* **2006**, *71*, 6898. (d) Sharman, G. J. *Magn. Reson. Chem.* **2007**, *45*, 317. (e) Williams, P. G.; Asolkar, R. N.; Kondratyuk, T.; Pezzuto, J. M.; Jensen, P. R.; Fenical, W. *J. Nat. Prod.* **2007**, *70*, 83. (f) Iranshahi, M.; Arfa, P.; Ramezani, M.; Jaafari, M. R.; Sadeghian, H.; Bassarello, C.; Piacente, S.; Pizza, C. *Phytochemistry* **2007**, *68*, 554. (g) Suntornchashwej, S.; Suwanborirux, K.; Koga, K.; Isobe, M. *Chem. Asian J.* **2007**, *2*, 114.
- (159) (a) Morsy, N.; Houdai, T.; Matsuoka, S.; Matsumori, N.; Adachi, S.; Oishi, T.; Murata, M.; Iwashita, T.; Fujita, T. *Bioorg. Med. Chem.* **2006**, *14*, 6548. (b) Lievens, S. C.; Molinski, T. F. *J. Am. Chem. Soc.* **2006**, *128*, 11764. (c) Seike, H.; Ghosh, I.; Kishi, Y. *Org. Lett.* **2006**, *8*, 3861. Seike, H.; Ghosh, I.; Kishi, Y. *Org. Lett.* **2006**, *8*, 3865.
- (160) (a) Arda, A.; Rodriguez, J.; Nieto, R. M.; Bassarello, C.; Gomez-Paloma, L.; Bifulco, G.; Jimenez, C. *Tetrahedron* **2005**, *61*, 10093. (b) Rychnovsky, S. D. *Org. Lett.* **2006**, *8*, 2895. (c) Arda, A.; Jimenez, C.; Rodriguez, J. *Eur. J. Org. Chem.* **2006**, *16*, 3645. (d) Bercion, S.; Buffeteau, T.; Lespade, L.; Coupe de K. Martin, M. *J. Mol. Struct.* **2006**, *791*, 186. (e) Bassarello, C.; Zampella, A.; Monti, M. C.; Gomez-Paloma, L.; D'Auria, M. V.; Riccio, R.; Bifulco, G. *Eur. J. Org. Chem.* **2006**, *3*, 604. (f) Chevallier, C.; Bugni, T. S.; Feng, X.; Harper, M. K.; Orendt, A. M.; Ireland, C. M. *J. Org. Chem.* **2006**, *71*, 2510. (g) Bassarello, C.; Bifulco, G.; Montoro, P.; Skhirtladze, A.; Kemertelidze, E.; Pizza, C.; Piacente, S. *Tetrahedron* **2007**, *63*, 148.

CR030733C